

# CHEMICAL BASIS OF DIESEL FUEL STABILIZATION BY TERTIARY ALKYL PRIMARY AMINES

Rajiv Banavali and Bharati Chheda,  
Rohm and Haas Company,  
Deer Park, Texas 77536

## ABSTRACT

The oxidative degradation products, formed under both the prolonged storage and thermal stress, are a problem in the utilization of diesel fuels. There is a continued challenge in developing fuel stabilizers that are increasingly cost-effective, do not degrade the performance of fuel, and are environmentally acceptable. Our interest in highly branched tertiary alkyl primary amines (TAPA) has led to evidence that they are excellent stabilizers for diesel fuels. TAPA possess unique chemical and physical properties. We will present the results of stability experiments for thermal and oxidative degradation of several diesel fuels. The TAPA are evaluated in these stability tests in comparison with other well-known stabilizers. Chemical factors preventing formation of color, insoluble sediments and gums were studied by modeling generally accepted degradation mechanisms. In this paper we will report our mechanistic investigation into the chemical details of the stabilization and effect of the TAPA chemical structure on the activity. Data for acid scavenging, reduction of hydroperoxides, and solubilization/dispersancy mechanisms of stabilization is presented

## INTRODUCTION

The oxidative degradation products, formed under both the prolonged storage and thermal stress, continue to be a problem in the utilization of diesel fuels. Fuel-instability reactions are defined in terms of the formation of deleterious products, such as filterable sediment, adherent gums, and peroxides. Sediments and gums which result from the oxidation reactions act to block filters and deposit on surfaces. There may be a relationship between the chemistry of deposit formation during normal long term storage and the deposits obtained by thermal stressing. Fuels containing higher amounts of olefins, certain nitrogen and sulfur compounds, organic acids, or dissolved metals are likely to degrade more and faster. Insolubles in diesel fuels are known to occur through several generally agreed mechanisms<sup>1</sup>. The sediment and gum formation mechanisms have been studied in great details<sup>2,3</sup> and can be summarized as: acid-base reactions involving N, O, and S species, free radical induced polymerization reactions involving unsaturated hydrocarbons, and esterification reactions involving aromatic and heterocyclic species. Previous studies have indicated that certain sulfonic acids<sup>4</sup>, organic nitrogen compounds<sup>5</sup>, and olefins<sup>6</sup>, when added to fuels that are then subjected to thermal or oxidative stress, tend to produce insoluble sediments.

Stabilizing additives are often used to counteract the above mechanisms<sup>7</sup>. Several chemistries may contribute to fuel stabilization. Antioxidants act to inhibit the reactions that form sediment. Most additives control peroxide formation, but do not curb formation of polymerized gum products. Dispersants act to suspend any sediment particles that form and prevent them from agglomerating and becoming a problem. The stability enhancing additives for middle distillate fuels include hindered phenols, alkylated diphenylamines, phenylenediamines, tertiary amines, metal deactivators and dispersants. Amine additives are generally considered as antioxidants (aromatic amines) and to neutralize acidic impurities/by-products (tertiary amines). Tertiary amines are generally considered<sup>2</sup> better than secondary or primary amines as fuel antioxidants. Phenylenediamine type antioxidants are more effective than hindered phenols in neutralizing peroxides. It was found that traditional amine stabilizers fail to control peroxide formation adequately. Also, these amines, while being more effective than hindered phenols in gasoline, are not being used in diesel because they degrade distillate fuel stability<sup>2b</sup>. Recent work has implicated that widely used fuel stabilizers such as hindered phenols are ineffective in reducing sediment formation. Phenylenediamines have been shown to be detrimental in both high and low sulfur diesels, as they participate in side reactions forming sediments<sup>2a</sup> and increasing color body formation<sup>2c</sup>. Thus, a search for better stabilizers continues.

Primary amines are not considered as good radical or peroxide quenchers as secondary or tertiary amines. This is true for typical straight-chain fatty amines. However, we are mainly interested<sup>7</sup> in a special class of primary amines that possess branched alkyl chains with the primary amino group attached to a tertiary carbon<sup>8</sup>. We will refer to these as tertiary alkyl primary amines (TAPA). Branched tertiary alkyl primary amines possess excellent oil solubility<sup>7</sup>, superior

thermal and oxidative stability<sup>10</sup>, strong basicity, and fluidity over a wide temperature range (See Table I). These benefits find usage in lubricant applications<sup>11</sup> also. We have previously shown<sup>12</sup> that TAPA can be used as fuel stabilizers, and are better than several other common stabilizers. We will describe here the work carried out recently at Rohm and Haas research laboratories with TAPA for their ability to stabilize diesel fuels. An attempt is made to form an interpretation of stabilization mechanisms of TAPA by using stability test methods under various conditions.

## EXPERIMENTAL

**I. Fuel Samples And Additives:** Fresh test samples of diesel fuel without any additives were obtained from commercial sources. The fuel samples were analyzed to ensure conformance with specifications and stored under ambient temperature, in dark, and under nitrogen atmosphere. All tests were started within a month of obtaining the fresh samples. All commercial additives used were as received without further purification. All the C<sub>9</sub>, C<sub>12</sub>, and C<sub>18</sub> TAPA samples were commercial products sold under the trademark Primene by Rohm and Haas company. Chemicals used for the experimental studies were purchased from Aldrich Chemical Company. The antioxidants used for the experiments included N,N-dimethylcyclohexylamine, 2,6-di-t-butyl-4-methylphenol, N,N'-di-sec-butyl-p-phenylenediamine, and dinonyl diphenylamine. Organic acid co-dopants included dodecylbenzene sulfonic acid. Classes of nitrogen compounds employed included N,N-di-methylaniline, 4-dimethylaminopyridine, and 2,5-dimethylpyrrole. Co-dopants such as metals and t-butylhydroperoxide were also used.

**II. Diesel Thermal Stability Tests:** A modified Octel/Du Pont F21 test was used as follows. A 50 mL sample of fuel oil in a test tube is stored in a 300°F bath for 90 minutes (or 180 Min.). After removal from the bath it is allowed to cool to room temperature (about 2 hr.). The aged fuel is then filtered through 4.25 cm Whatman No 1 filter paper. The paper is then washed with heptane and the color of the filter paper is compared to a set of standards (1 = No color, 20 = dark brown). The data is given in Tables II and III. Thermal stability tests were also done by using pressurized differential scanning calorimetry.

**III. Diesel Oxidation Stability Tests:** A modified ASTM D2274 was used for oxidative stability tests as follows. A 350 mL sample of fuel is heated at 95°C for 16 hr. (or 40 hr.) while oxygen is bubbled through at the rate of 3 liters per hour. After aging, the sample is cooled to room temperature and filtered to obtain the filterable insoluble quantity. Adherent insolubles are then removed from the associated glassware with trisolvant (TAM). The TAM is then evaporated to obtain the adherent insolubles. The sum of filterable and adherent insolubles, expressed as milligrams per 100 mL, is reported as total insolubles. The data is given in Table V. In addition, oxidative stability was also measured by DSC experiments and by ASTM D942 test.

**IV. Doping Studies:** Various fuel samples were doped with precise amounts of additives (inhibitors, peroxides, acids, bases, etc.) The fuel stabilities were then measured as mentioned in the above experiments. In the case of hydroperoxide doping experiments, peroxide numbers were measured by the standard ASTM D3703 method. The results are calculated as milligrams per kilogram (ppm) of peroxide.

**V. Solubility:** Solubility experiments were carried out with salts of dodecylbenzenesulfonic acid with various basic nitrogen compounds such as 2,5-dimethylpyrrole, 4-dimethylaminopyridine, alkylated-phenylenediamines, and C<sub>12</sub> TAPA. Solubility of the pure salts was then studied in diesel. The Kauri-butanol value (KB Value, ASTM D1133) was used as a measure of solvent power of TAPA. The KB was calculated by standardization with toluene (assigned KB of 105) and heptane-toluene (assigned KB of 40) blend.

## RESULTS AND DISCUSSION

Oxidative and thermal stability of diesel fuels was studied on fuel samples collected from major regions around the world; namely, North America, Latin America, and Asia. The results of the various stability tests as measured by color, sediments and gum formation show clearly that addition of TAPA, at few ppm levels, significantly improves the stability of diesels. Tables II and III show that the thermal stability of both low and high sulfur diesel fuels can be improved by TAPA doping at 8-40 ppm range. It is noteworthy that both sedimentation and color are improved by TAPA. The results of oxidative stability of diesel showing the similar TAPA benefits were shown earlier<sup>12</sup>. Several commercial fuel stabilizers at the same dosage level show similar or worse performance. The data that TAPA are equal or better stabilizers is also seen in comparative experiments with several well-known fuel antioxidants. C<sub>9</sub> TAPA shows the best results for the low sulfur diesel when compared on equal weight basis with other stabilizers. Although diphenylamines improve the stability, hindered phenol was only slightly effective.

However, addition of phenylenediamine degraded both the filter pad rating and color. The fuel oil stability results using the C<sub>12</sub> TAPA in combination with a dispersant and/or a metal deactivator have shown that the performance over the TAPA alone is not significantly improved. The diesel data, in addition, shows the differences in activity of various TAPA additives. This data allows both dosage and structure-activity relationships establishment. The mechanism by which TAPA act as antioxidants is not completely understood, but an attempt is made here to form a general interpretation of their stabilization mechanisms. The mechanistic study here is done based on structure-activity relationship of TAPA coupled with results of stability tests under various conditions.

### STRUCTURAL ATTRIBUTES OF TAPA

The feature of having a tertiary carbon attached to nitrogen is very beneficial because it imparts important characteristics<sup>8</sup> to these amines. Table 1 lists some of the key TAPA properties of value in diesel stabilization. TAPA with branched alkyl groups have low viscosity and are liquids at room temperature whereas most long chain linear amines are solids<sup>9</sup> at room temperature. Compared to linear alkyl primary amines the branched TAPA are readily soluble in fuel oils. In addition, these amines are also ashless and completely combustible. They are virtually insoluble in water and are not leached from fuels by contact with water during storage and handling. The fact that there are no  $\alpha$ -hydrogens attached to nitrogen gives TAPA better oxidative stability because this weak C-H bond is most prone to oxidation. The lack of  $\alpha$ -hydrogens also ensures that unstable imines are not formed which can deaminate in the presence of water. This makes TAPA oxidatively more stable than their corresponding linear amines. The oxidative stability of selected TAPA and their linear analogs were comparatively evaluated by DSC measurements<sup>10</sup>. In all cases the corresponding *n*-alkylamines decomposed before the TAPA indicating that the TAPA are oxidatively more stable than corresponding linear primary amines. Oxidation is the most common form of degradation of fuels. Hindered phenols and amines are commonly used as oxidation inhibitors and work by interrupting radical chain reactions. The chain carrying peroxy radical is scavenged by the phenol or amine by hydrogen atom donation. The resulting radicals are resonance stabilized and are eventually destroyed by reaction with another peroxy radical. Hindered amines, such as TAPA, can also react with free radicals to form stable intermediates that do not readily take part in chain reactions. Although they are not as resonance stabilized, they can regenerate by scavenging another hydrogen radical. A common test used to evaluate the antioxidant properties of additives involves heating base fluid in the presence of 0.5 - 1.0 % inhibitor at 120°C in an oxygen pressurized bomb and measuring the oxygen pressure drop as a function of time. We found<sup>11</sup> both C<sub>12</sub> and C<sub>18</sub> TAPA inhibited the oxidation of petroleum fluids. These TAPA proved similar to some commercially used phenolic and aminic antioxidants.

### ACID SCAVENGING

Hazelett has shown<sup>13</sup> the correlation of carboxylic and sulfonic acids in increasing deposit formation. The reaction of certain acidic compounds, such as naphthalene sulfonic acid, with nitrogen compounds, such as indoles, quinolines, and carbazoles, appears to be one of the mechanisms for fuel insolubles formation. Dodecylbenzenesulfonic acid promotes<sup>4</sup> sediment formation and also may become incorporated into the sediment. Amine based stabilizers can react with acidic species preferentially. For weak acids, the amines exhibit more than 1:1 action and certain amines exert favorable behavior only if they are strong organic bases. TAPA are strong bases<sup>14</sup> and can readily react with acidic species, sacrificing themselves to form salts that are miscible in these liquids and thus do not precipitate. In salt formation, two TAPA attributes are very important. First, the high basicity exhibited by these amines, in non-polar media such as fuels, allows very efficient and complete scavenging of both strong and weak acids. Furthermore, the branched and hindered carbon chain of TAPA helps envelop the salt thereby better solvating it. We have recently done<sup>14</sup> pK<sub>a</sub> measurements on these amines using both reaction calorimetry and quantum chemical estimates and find that TAPA are stronger bases than corresponding linear primary amines in non-polar solvents.

### REDUCTION OF HYDROPEROXIDES

Sediments that form in diesel fuels are often the direct result of autoxidation reactions involving hydroperoxides<sup>3</sup>. Thus, increasing peroxide concentration is often an indicator of the instability. The peroxides can stimulate insolubles by two processes. One is by converting thiols and aldehydes to sulfonic and carboxylic acids which act as acid catalysts and sediment promoters. The second is by a free-radical mechanism, possibly by oligomerizing olefins and by addition of the thyl radical to olefins. Induced decomposition of hydroperoxides can be catalyzed by metals, acids, and amines. The catalytic efficiency of the amines generally correlates with their ionization potentials. This correlation supports the mechanistic interpretation that a charge

transfer complex between the amine and the peroxide weakens the O-O bond. Quenching by amines is also subject to steric effects. Tertiary amines have been well-studied as hydroperoxide scavengers, but not much is known about TAPAs. However, oxidation of mercaptans in sour fuels to disulfides by organic hydroperoxides has been shown<sup>15</sup> to be catalyzed efficiently by C<sub>12</sub> TAPA. We studied the effect of added hydroperoxide to the fuel by measuring both the oxidative stability and concentration of peroxides (See Table IV). As anticipated, addition of hydroperoxide greatly destabilizes the fuel by showing much higher amounts of gum and sediments than in the undoped sample. Also as expected, addition of 2, 5-dimethylpyrrole further increases the sediment formation. However, addition of TAPA greatly increases stability as measured by the reduction in sediment and also reduces the peroxide concentration. The effect of TAPA on reducing sediments is better than that shown by both the secondary and tertiary amines.

## SOLUBILIZATION AND DISPERSANCY

For a good stabilizer, it is important not only to mitigate the oxidative process, but also to help resolve problems caused by them. Not only are the TAPAs soluble in base oil but many salts of oil insoluble organic and inorganic acids of these TAPA are completely miscible in base oil. We have studied<sup>10</sup> the solubility of several inorganic and organic salts of TAPA in kerosene and white mineral oil. For example the TAPA salts of EDTA, trichloroacetic acid, molybdic acid, tungstic acid, and sulfuric acid are readily soluble (>20%) in mineral oil compared to their free acid. TAPA can act by forming fuel soluble salts with acidic by-products of oxidation. Furthermore, their complexation with metals and other species can allow suspension of gums and particles. By keeping the sediment particles from agglomerating they can be kept small enough to be dispersed through the fuel filters. Molecular modeling shows that the resulting complexes can effectively shield the metal atoms thereby reducing their ability to catalyze degradative reactions. The role of TAPA in minimizing gums and sediment formation by "solvating ability" of the branched alkyl chains of TAPA is also likely. The high Kauri Butanol values measured are indicative of that. For the C<sub>18</sub> TAPA the KB value of more than 119 compares well with that of only 30-35 seen for the diesel. The decreased sediment seen, in both the thermal and oxidative tests, is most likely in part due to better solvent properties<sup>16</sup>. To confirm this theory, we prepared salts of model acidic compounds(Dodecylbenzenesulfonic acid) with various amines. The pure salts were then tried to dissolve in diesel fuel at various levels. The results can be seen in Table V. It was noted that acid salts of TAPA were not solids, unlike other amine salts, and could be readily dissolved in the diesel. Furthermore, these salts had much lighter color than the salts prepared from phenylenediamines.

## CONCLUSIONS

We have shown that deterioration is delayed, color degradation is inhibited and sludge formation is reduced by addition of TAPA to the diesel fuels. The tertiary alkyl primary amines are highly effective stabilizers for the prevention of sludge and color formation under both thermal and oxidative stress. Their performance is equal or better than many other commonly used fuel stabilizers. They inhibit the reactions responsible for sludge formation and also disperse the gum and sediment from depositing. The additive concentration and structure effect suggest that the stabilization properties of TAPA result from factors such as acid scavenging, hydroperoxide decomposition, dispersing of gums and particulates, or any combination of these factors. The several established fuel degradation mechanisms pathways can be prevented or resolved by the use of these amines.

## ACKNOWLEDGMENTS

We would like to thank Rohm and Haas company for providing the support for this work and permission to publish the results.

## REFERENCES

- 1) Beaver, B.; *Fuel Science And Technology Intl.*, **1991**, 9(10), 1287 and **1992**, 10(1), 1.
- 2) a) Batt, R. J.; Henry, C. P.; Whitesmith, P. R.; *Proceedings of the 5th International Conference on Long Term Storage Stability of Liquid Fuels*, **1995**; Eds.: Giles, H. N.; National Technical Information Service, Springfield, Va, Vol. 2, 761. b) Hazlett, R. N.; Hardy, D. R.; *NRL Letter Report 6180-832*, Naval Research Laboratory, Washington, DC, **1984**. c) Henry, C.; *Proceedings of the 2nd Intl Conf on Long Term Storage Stabilities of Liquid Fuels*, Stavina, L.L.; Ed.; SWRI, San Antonio, TX; **1986**, p 807.

- 3) Mushrush, G. W.; Speight, J. G.; In "Petroleum Products: Instability and Incompatibility", Taylor and Francis, Washington, DC; 1995.
- 4) Wechter, M. A., Hardy, D. R., *Energy & Fuels*, 1996, 10, 117.
- 5) Pedley, J. F., Hiley, R. W., Hancock, R. A., *Fuel*, 1989, 68, 27.
- 6) Adiwari, Batts, B. D., *Proceedings of the 5th International Conference on Long Term Storage Stability of Liquid Fuels*, 1995; Eds.; Giles, H. N.; National Technical Information Service, Springfield, Va, Vol. 2, 649.
- 7) These TAPA are commercially available from Rohm and Haas Company as Primene® Amines. The C-9 is available as Primene® BC-9, C-12 as Primene® 81-R and C-18 as Primene® JM-T.
- 8) Banavali, R.; Ellis, M. J.; Piccolini, R. J.; *Resin Review*, Rohm and Haas, Philadelphia, Pa, 1993, XLIII, 1, 13.
- 9) Banavali, R.; Chheda, B.; In *International Symposium on Production and Application of Lube Base Stocks*, Singh, H.; Prasada Rao, T.S. R.; Eds., Tata McGraw-Hill, New Delhi, 1994; p 318.
- 10) Banavali, R.; Chheda, B.; Ufran, J.; In *2nd Brazilian Symposium on Lubricants*, Instituto Brasileiro de Petroleo, 1995, p 1.
- 11) Banavali, R.; Karki, S. B.; *Prepr. Pap.- Am. Chem. Soc. Div. Of Pet. Chem.*, 1997, 42(1), p 232.
- 12) Banavali, R., Chheda, B., *Prepr. Pap -Am. Chem. Soc., Div. Fuel Chem.*, 1997, 42(3), 784.
- 13) Hazlett, R. N.; *Fuel Science and Technology*, 6(2), 185, 1988.
- 14) Rohm and Haas Research Laboratory Unpublished Data.
- 15) S. Wang, G. L. Roof, B.W. Porlier, Nalco Chemical Company, U. S. Patent #4,514,286, 1985.
- 16) Westbrook, S. R., Stavinoha, L. L., Present, D. L., *Interim Report BFLRF No. 255*, Southwest Research Institute, San Antonio, TX, 1988,

**Table I. Tertiary Alkyl Primary Amine Properties**

Property	TAPA C <sub>9</sub>	TAPA C <sub>12</sub>	TAPA C <sub>18</sub>
Chemical name	t-nonylamines	t-dodecylamines	t-octadecylamines
Molecular Weight	143 (average)	185 (average)	269 (average)
Boiling Range (°C)	170-180	220-240	265-305
Pour point	-85°C/ -185°F	<-59°C/-74°F	<-40°C/-40°F
Base Strength (pKa)	11	11	11
Water solubility at 25°C	0.53%	1000 ppm maximum	900 ppm max
K <sub>p</sub> (Water/Heptane)	0.00772	0.0036	0.0031
Surface tension at 20°C (dynes/cm <sup>2</sup> , ASTM D-1331)	27	30	31
Interfacial Tension with water (dynes/cm <sup>2</sup> , ASTM D 971)	1.5	2	8
Kauri-Butanol Value (ASTM-1133)	20	35	>119
Thermal Stability by DSC	>500°C	>500°C	>500°C

**Table II. Thermal Stability Test Results Using Du Pont F-21 @ 150°C/90 Min.**

Additives (ppm)	Diesel #1		Diesel #2		Diesel #3		Diesel #4	
	Filter Pad Rating	ASTM Color						
Sulfur Content	0.24%		0.38%		0.56%		0.72%	
None	11	2.5	16	5	16	6	18	5
TAPA C <sub>12</sub> (8.5)	3	2	4	3.5	3	4	2	3
TAPA C <sub>12</sub> (17)	2	2	2	3.5	4	3.5	2	2.5
TAPA C <sub>12</sub> (35)	2	2	3	3	4	3	3	2.5
Commercial AO #1 (8.5)	5	2	2	3	6	4	4	3
Commercial AO #1 (17)	2	2	3	3.5	4	4	4	2.5
Commercial AO #1 (35)	2	2	2	3.5	2	3.5	5	2.5
Commercial AO #2 (8.5)	3	2	11	2	10	3.5	8	2
Commercial AO #2 (17)	3	2	10	2	7	3	8	2
Commercial AO #2 (35)	2	2	7	2	6	2.5	6	2

**Table III. Thermal Stability Test Results of Using Du Pont F-21 test @ 150°C /180 Min.**

Additives (ppm)	Diesel #5	
	Filter Pad Rating	ASTM Color
Sulfur Content	0.04%	
None	13	1.5
TAPA C <sub>12</sub> (20)	9	1.5
TAPA C <sub>9</sub> (20)	10	1.5
2,6-di-t-butyl-4-methylphenol (20)	11	1.5
2,6-di-t-butyl-4-methylphenol (40)	12	2
N,N'-di-sec-butyl-p-phenylenediamine (20)	14	2.5
N,N'-di-sec-butyl-p-phenylenediamine (40)	14	2.5
Dinonyl diphenylamine (20)	9	2.5

**Table IV Comparative Oxidation Stability (ASTM D2274 @ 40 hr) with Added Peroxide and Stabilizers**

Diesel + additives *	Total Insolubles (mg/100 ml)	Peroxide, ppm (before 2274)	Peroxide, ppm (after 2274)
Blank	0.1	0.1	4.5
+ t-BHP	1	99.8	25.6
Dimethylpyrrole + t-BHP	57.6	58.6	2.3
Dimethylcyclohexylamine + t-BHP	1.5	>118	2
Dinonyl diphenylamine + t-BHP	0.6	92.8	5.3
N,N'-di-sec-butyl-p-phenylenediamine + t-BHP	5.4	97.7	8.7
TAPA C <sub>9</sub> + t-BHP	0	97.9	10.9
TAPA C <sub>12</sub> + t-BHP	0.1	99.1	14
TAPA C <sub>18</sub> + t-BHP	0	90.8	19

\* For the doping experiments, following amounts were used: t-butylhydroperoxide at 100 ppm peroxide and stabilizer at 135 ppm Nitrogen concentration.

**Table V. Solubility of Dodecylbenzene Sulfonic Acid Salts of Aminic Bases\* in Diesel**

Aminic Bases	0.1% in diesel	0.2% in diesel	0.5% in diesel	0.7% in diesel	Comments
TAPA C <sub>12</sub>	Soluble	Soluble	Soluble	Soluble	The salt is a light colored gum
4-(dimethylamino)-pyridine (solid)	Soluble	Soluble	Soluble	Slightly soluble	The salt was made using diesel as a solvent, light colored paste, and foamy when mixed with diesel
2,5-Dimethylpyrrole	Not soluble	Not soluble	Not soluble	Not soluble	The salt was made using diesel as a solvent, dark colored gum
N,N'-di-sec-butyl-phenylenediamine	Not soluble	Not soluble	Not soluble	Not soluble	The salt was made using diesel, dark colored gum

\* Salt was prepared by reacting Dodecylbenzene sulfonic acid and aminic bases at 1:1 equivalent ratio

# EFFECT OF INCREASINGLY SEVERE HYDROTREATING ON STABILITY-RELATED PROPERTIES OF NO. 2 DIESEL FUEL

J. Andrew Waynick

Amoco Petroleum Products, 150 West Warrenville Road  
Naperville, Illinois 60563-1460, USA

## ABSTRACT

This paper reports the effect of increasingly severe hydrotreating on the compositional and stability-related properties of four No. 2 diesel fuels ranging in sulfur level from 222 ppm to 11 ppm. Denitrification was essentially complete when the fuel sulfur level had been reduced to 86 ppm. At 222 ppm sulfur (similar to current U.S. low sulfur diesel fuels), fewer multi-ring but similar total aromatics were present compared with the high sulfur feed. With further sulfur removal, total aromatics were reduced as well, due to removal of mono-ring aromatics. Storage stability was excellent for all four fuels. Hydroperoxide susceptibility appeared adequate to excellent under conditions similar to commercial transport and storage. Additional information concerning diesel fuel instability chemistry was also demonstrated.

## INTRODUCTION

Before October 1993, No. 2 distillate fuel sold in the United States contained 0.2-0.4%(wt) sulfur. As of October 1993, No. 2 distillate fuel used for on-highway vehicles was required to have a sulfur level no greater than 0.05%(wt), i.e. 500 ppm(wt). This sulfur level reduction has been achieved by increasing the severity by which diesel fuel feedstocks are hydrotreated.

Limited early data indicated that such low sulfur diesel fuels would have improved storage stability,<sup>1-3</sup> i.e. form less sediment and dark-colored fuel-soluble materials. A more recent study verified this conclusion.<sup>4</sup>

A few studies have been published to date concerning the effect of hydrotreating on No. 2 diesel fuel peroxidation tendency.<sup>7-8</sup> The most significant and most recent study indicated that commercial U.S. low sulfur diesel fuels did have increased hydroperoxide susceptibility compared with commercial U.S. high sulfur diesel fuels under sufficiently accelerated conditions. However, no such tendency was observed under ordinary field conditions of fuel transport and storage.<sup>4</sup>

The primary objective of the work reported in this paper was to evaluate an already available set of four hydrotreated No. 2 diesel fuels made from the same feedstock. Since finished fuel sulfur levels began at 222 ppm and went as low as 11 ppm, trends in fuel properties as a function of hydrotreating severity could be examined. Resulting data could provide useful insight not possible by looking only at commercial U.S. low sulfur (LS) and high sulfur (HS) diesel fuels. Also, the data could provide important information for future U.S. diesel fuel production, which might be required to attain even lower sulfur levels

## EXPERIMENTAL

### Fuel Samples

Each of the four No. 2 diesel fuel samples used in this work was obtained by a two-stage hydrotreating of a highly aromatic feedstock having the following gross compositional properties as measured by mass spectrometry:

Aromatics, %(wt)	
Total	46.5
Mono	17.6
Di	23.5
Tri	2.9

Stage	First	Second
Catalyst	Co/Mo	Pt/Pd on Mol Sieve
Psig H2	500	900
lhsv	2.1	1.0
Temperature, °F	650	500-550
H2-Circulation Rate, scf/bbl	1,500	5,000

The samples were about one year old when testing began. During that year, they had been stored in clear, sealed glass bottles at ambient laboratory temperature.

## Tests

The four additive-free fuel samples were tested for chemical composition and stability using the following procedures:

### Chemical Composition

Total Sulfur by Dispersive X-Ray  
Fluorescence (ASTM D4294)  
Total Nitrogen (ASTM D4629, modified)  
Basic Nitrogen (ASTM D2896)  
SMORS  
Phenalenones  
Aromatics by Mass Spectrometry

### Stability

Oxidative Stability (ASTM D2274)  
Nalco Pad Stability  
Storage Stability (ASTM D4625)  
40-Hour Stability  
Initial Peroxide Number  
(ASTM D3703)  
Peroxide Number after  
ASTM D4625 (ASTM D3703)  
Hydroperoxide Potential,  
CRC Procedure  
Hydroperoxide Potential, Oxygen  
Overpressure (OP) Procedure

The ASTM procedures are well documented and will not be described further here. The Nalco Pad stability procedure measures thermal stability and has been described elsewhere.<sup>5</sup> ASTM D2274 and the Nalco Pad test are known not to correlate with real storage stability. However, they were included since they continue to be used as specification tests by many diesel fuel marketers and customers. The 40-Hour Stability test is a procedure developed and used by Amoco Oil Company and has been shown to correlate well with the reliable ASTM D4625. During this test, a 350 ml sample of distillate fuel is stressed at 80°C for 40 hours in a mineral oil bath while oxygen is bubbled through the sample at a rate of 3 liters/hour. The sample is then removed from the oil bath and allowed to cool for two hours in the dark. After determining the final color, the sample is diluted to 1, 225 ml with N-pentane, mixed thoroughly, and filtered through a tared 0.8 micron filter. After rinsing with N-pentane, the filter is dried and weighed to determine the total insolubles. Initial Peroxide Number should actually be regarded as a Peroxide Potential (susceptibility) test with a one year, ambient temperature storage period. The CRC Hydroperoxide Potential procedure was originally developed for jet fuels<sup>6</sup> and involves heating a 100 ml fuel sample at 65°C and 1 atmosphere air for four weeks. Peroxide number is then determined as an indication of the fuel's hydroperoxide susceptibility. The OP procedure for hydroperoxide potential was adapted from previously documented work involving jet fuels.<sup>7</sup> The procedure involves heating a 50 ml fuel sample at 100°C and 690 kPa (100 psia O<sub>2</sub>) for 24 hours. The peroxide number is then determined. The modification to the total nitrogen procedure was that the fuel sample was delivered to the combustion tube by a platinum boat rather than by standard syringe injection. SMORS (soluble macromolecular oxidatively reactive species) are believed to be sediment precursors, and the procedure for measuring them has been previously documented.<sup>8</sup> Phenalenones are believed to be SMORS and sediment precursors, and the analytical method for measuring them was based on a previously reported procedure.<sup>9</sup>

## RESULTS AND DISCUSSION

### Chemical Composition

Chemical composition test results are given in Table I. Total and basic nitrogen levels dropped significantly as the fuel was hydrotreated from 222 ppm to 86 ppm sulfur. Further reductions in sulfur did not result in much further decrease in nitrogen levels. No phenalenones were detected in any of the four hydrotreated diesel fuels. Since phenalenones are formed by the facile oxidation of phenalene, this indicates that the hydrotreating process was probably severe enough to reduce all phenalenes that may have been present in the original feed. Only the 222 ppm sulfur fuel had a high level of SMORS. The other three fuels had SMORS that were similar to the mean values of both LS and HS commercial U.S. diesel fuels.<sup>4</sup> This indicates that by hydrotreating the feed to 86 ppm sulfur, SMORS precursors were nearly removed. Since phenalenones are believed to be SMORS precursors, the absence of phenalenones and the high SMORS level in the 222 ppm sulfur fuel is interesting. It implies that either phenalenones initially present in the feed were not removed by hydrotreating and then completely reacted to form SMORS during the one year storage, or else the SMORS formed in the 222 ppm sulfur fuel were formed from precursors other than phenalenones. As will be shown in the subsequent section on stability, the latter explanation is the more likely one.

Gross hydrocarbon analysis indicated that the main change in going from the feed to the 222 ppm sulfur fuel was to reduce polycyclic aromatics to monocyclic aromatics, with no overall reduction in aromatic content. This is consistent with earlier U.S. commercial diesel fuel survey data.<sup>4</sup> However, as hydrotreating became progressively severe, both poly- and mono-cyclic aromatics significantly decreased.

### Stability

Stability test results are given in Table II. All four samples showed excellent thermal and storage stability. As sulfur level decreased, overall results remained constant.

SMORS measured on the filtered samples after D4625 storage showed a decreasing trend with decreasing sulfur level. Only the 222 ppm sulfur and 86 ppm sulfur fuels developed significant additional SMORS relative to the amounts initially present. The 222 ppm sulfur fuel developed a quite high level of SMORS. Since all four fuels prior to D4625 testing contained no measurable phenalenones, the SMORS developed during D4625 testing must have been formed from other precursors. Also, since ASTM color did not darken much during D4625 testing, the SMORS formed must not have been very dark. This is in contrast to HS diesel fuel, where previous work indicates that SMORS contribute to aged color formation<sup>4</sup> and can correlate to aged sediment formation.<sup>10</sup> The major implication of this result is that SMORS formed in LS diesel fuel are different from SMORS formed in HS diesel fuel. In fact, the SMORS formed in HS diesel fuel may include a wide range of compounds beyond the indolyl phenalenes and indolyl phenalenones typically suggested in the literature.<sup>11</sup> This wide range of compounds may include some of the SMORS formed in LS diesel fuels. Although not published, some of these conclusions concerning the diversity of SMORS in diesel fuel have been suggested by one of the researchers who first discovered SMORS.<sup>12</sup>

Hydroperoxide susceptibility of the four progressively hydrotreated fuels was profiled by measuring the peroxide number developed after four increasingly severe storage conditions. Based on the one year ambient data, it appears that "real world" hydroperoxide susceptibility of U.S. LS diesel fuel will improve as sulfur levels are further reduced beyond the current typical levels. Although the 7 meq O/Kg value for the 222 ppm sulfur fuel is within the "problem" range cited in prior jet fuel literature, it is unlikely that much on-highway diesel fuel will be stored for one year. Previous data indicated that commercial U.S. LS fuel (with similar sulfur levels) gave negligible levels of hydroperoxides.<sup>4</sup> Those fuels represented what the end user would likely receive. Whatever level of hydroperoxide stability exists in today's LS diesel fuel, further reductions in required sulfur levels should improve that stability.

Looking at the entire peroxide number data, an interesting trend can be seen. As test storage conditions increased in severity, the maximum peroxide number observed among the four fuels shifted towards lower sulfur diesel fuel. For instance, the initial peroxide number (after one year storage in the laboratory) showed the highest level in the 222 ppm sulfur fuel. A similar pattern was observed for peroxides measured after D4625 storage (43°C, 13 weeks, 1 atm. air), although overall values after D4625 were higher than the initial values. However, after the even more severe CRC conditions (65°C, 4 weeks, 1 atm air), the maximum peroxide level shifted towards the 86 ppm sulfur fuel. After the most severe OP storage condition (100°C, 24 hours, 690 kPa O<sub>2</sub>), the maximum peroxide number was observed in the 39 ppm sulfur fuel, with much lower values for the other three fuels. These test results can be best understood by remembering that a fuel's peroxide number reflects the difference between the rates of two processes: hydroperoxide formation and hydroperoxide decomposition. Factors promoting hydroperoxide formation are apparently more important under the less severe test storage conditions. One such factor is the concentration of compounds most prone to hydroperoxide formation. As indicated previously,<sup>4</sup> compounds containing benzylic carbon are among the most prone to hydroperoxide formation. As poly-cyclic aromatics are reduced to mono-cyclic aromatics with total aromatic content remaining constant, benzylic carbon content increases. This fact has been proposed as a primary reason why hydroperoxide susceptibility under accelerated conditions is greater in commercial LS diesel fuels compared with HS diesel fuels.<sup>4</sup> However, when hydrotreating is severe enough to reduce all aromatic species, benzylic carbon content will decrease, replaced by carbons less susceptible to hydroperoxide formation. This would explain why peroxide number decreased under lower test severity as the fuel was more severely hydrotreated.

However, as test storage conditions become more severe, factors promoting hydroperoxide decomposition apparently become more important for the less hydrotreated diesel fuels. One factor that may contribute to this effect is the concentration of naturally occurring hydroperoxide decomposers in the fuels. These compounds are removed as the fuel is progressively

hydrotreated. So, at higher test severity, hydroperoxide decomposition by naturally occurring hydroperoxide decomposers will be greater in the less hydrotreated diesel fuels. Also, there is some evidence that benzylic hydroperoxides are somewhat less kinetically stable compared with non-aromatic hydroperoxides. If so, this would also tend to increase the rate of hydroperoxide decomposition in the less hydrotreated diesel fuels.

More data will be required to fully explain how these and other factors contribute to the peroxide number trends evident in the Table II data.

It is interesting to note that the most severely hydrotreated diesel fuel (11 ppm sulfur) gave only about 0.5 meq O/Kg for all test storage conditions. Without further analysis for final oxidation products, it can only be concluded that for that fuel the rates of hydroperoxide formation and decomposition were nearly equal under all test storage conditions.

## CONCLUSIONS

The work reported in this paper supports the following conclusions:

1. Current U.S. commercial LS diesel fuel has less multi-ring aromatics than HS diesel fuel, but similar total aromatic levels. With further hydrotreating, total aromatics are reduced as well, due to removal of mono-ring aromatics.
2. As diesel fuels are hydrotreated to and beyond current U.S. commercial LS diesel fuel sulfur levels, storage stability remains excellent.
3. As diesel fuels are hydrotreated to current U.S. commercial LS diesel fuel sulfur levels, hydroperoxide susceptibility remains acceptable under normal conditions of commercial transport and storage. As diesel fuels are further hydrotreated, hydroperoxide susceptibility under those same conditions should improve.
4. SMORS in non-additized LS diesel fuel do not significantly contribute to color darkening. Neither are they sediment precursors. LS diesel fuel SMORS are either chemically distinct from HS diesel fuel SMORS, or they are an innocuous subset of HS diesel fuel SMORS.

## ACKNOWLEDGMENTS

The contributions of the following people are gratefully acknowledged: Simon Kukes for providing the diesel fuel samples and the processing conditions used to generate them; Al Novak for providing some of the analytical data on the initial feed and resulting fuels; Susan Taskila for running many of the laboratory tests; Don Porter for graphically treating the data.

## REFERENCES

- (1) Palmer, L. D.; Copson, J. A. "Hydrotreatment of Light Cycle Oil for Stabilization of Automotive Diesel Fuel"; Proceedings of 2nd International Conference on Long-Term Storage Stabilities of Liquid Fuels, San Antonio, Texas, July 1986.
- (2) Martin, B.; Bocard, C.; Durand, J. P.; Bigeard, P. H.; Denis, J.; Dorbon, M.; Bernasconi, C. "Long-Term Storage Stability of Diesel Fuels: Effect of Aging on Injector Fouling; Stabilization by Additives or Hydrotreating"; presented at SAE Fuels and Lubes meeting, Tulsa, Oklahoma, 1990.
- (3) Vardi, J.; Kraus, B. J. "Peroxide Formation in Low Sulfur Automotive Diesel Fuels"; SAE Paper No. 920826, 1992.
- (4) Waynick, J. A.; Taskila, S. M. "A Comparison of Low and High Sulfur Middle Distillate Fuels in the United States"; Proceedings of the 5th International Conference on Stability and Handling of Liquid Fuels; Rotterdam, the Netherlands, October 1994.
- (5) Waynick, J. A. "Evaluation of Commercial Stability Additives in Middle Distillate Fuels"; Proceedings of the 5th International Conference on Stability and Handling of Liquid Fuels; Rotterdam, the Netherlands, October 1994.
- (6) Determination of the Hydroperoxide Potential Jet Fuels, CRC Report No. 559, April, 1988.

- (7) Black, B. H.; Hardy, D. R. "Comparison of Jet Fuel Phenolic Antioxidants Using A Serial Dilution Technique"; Proceedings of the 4th International Conference on Stability and Handling of Liquid Fuels, Orlando, Florida, November 1991.
- (8) Hardy, D. R.; Wechter, M. A. "What Are Soluble Macromolecular Oxidatively Reactive Species (SMORS)?" ACS National Meeting, Washington, D.C., August 1990.
- (9) Marshman, S. J. "Liquid Chromatographic Determination of Phenalenones in Middle Distillate Fuels"; *Fuel* 1990, 69, pp 1558-1560.
- (10) Wechter, M. A.; Hardy, D. R. "The Use of Macromolecular Oxidatively Reactive Species (SMORS) to Predict Storage Stability of Mid-Distillate Diesel Fuels"; Proceedings of the 4th International Conference on Stability and Handling of Liquid Fuels, Orlando, Florida, November 1991.
- (11) Malhotra, R. "Field Ionization Mass Spectrometric Analysis of Sediments: Chemistry of Insolubles Formation"; Proceedings of the 4th International conference on Stability and Handling of Liquid Fuels; Orlando, Florida, November 1991.
- (12) Personal communication with M. A. Wechter, Rotterdam, the Netherlands, October 6, 1994.

**TABLE I**  
**CHEMICAL COMPOSITION**

Sulfur, ppm (wt)	222	86	39	11
Total Nitrogen, ppm (wt)	75	8	4	<1
Basic Nitrogen, ppm (wt)	12	<5	<5	<5
SMORS, mg/100 ml	2.5	0.4	0.4	0.2
Phenalenones, ppm (wt)	ND <sup>1</sup>	ND <sup>1</sup>	ND <sup>1</sup>	ND <sup>1</sup>
Aromatics by Mass Spec., % (wt)				
Total	53	28	13	7.2
Mono-cyclic	43	24	11	5.3
Di-cyclic	9.7	3.3	1.1	0.8
Tri-cyclic	0.6	0.7	0.9	1.0

<sup>1</sup> Not detected

**TABLE II**  
**STABILITY**

Sulfur, ppm (wt)	222	86	39	11
Initial Color, ASTM <sup>1</sup>	<1.5	-6 <sup>2</sup>	-16 <sup>2</sup>	<1.0
Stability, D2274				
Total Insolubles, mg/100 ml	0.2	0.1	0.0	0.0
Final Color, ASTM	<2.0	<0.5	<0.5	<1.0
Nalco Pad Rating	1	1	1	1
40-Hour Stability				
Total Insolubles, mg/100 ml	0.4	0.1	0.0	0.0
Final Color, ASTM	<1.5	-6 <sup>2</sup>	-16 <sup>2</sup>	<1.0
Stability, D4625				
Total Insolubles, mg/100 ml	0.3	0.2	0.2	0.2
Final Color, ASTM	<2.0	<0.5	0.5	<1.0
SMORS, mg/100 ml				
Initial <sup>3</sup>	2.5	0.4	0.2	0.2
After D4625	11.0	1.0	0.4	0.3
Hydroperoxide Potential, ineq O/Kg				
Initial <sup>4</sup>	7.6	1.7	0.43	0.50
After D4625	193	24	1.4	0.55
CRC <sup>4</sup>	26	28	2.0	0.43
OP <sup>5</sup>	1.3	21	199	0.68

<sup>1</sup> ASTM D1500 except where noted

<sup>2</sup> Saybolt color

<sup>3</sup> Measured on fuels after 1 year ambient laboratory temperature storage

<sup>4</sup> CRC Hydroperoxide Potential Method as described in EXPERIMENTAL section

<sup>5</sup> Oxygen Overpressure Method as described in EXPERIMENTAL section

## EFFECT OF HYDROTREATING ON THE STABILITY OF SYNTHETIC CRUDE FROM WESTERN CANADA

P. Rahimi and C. Fairbridge, National Centre for Upgrading Technology,  
1 Oil Patch Drive, Suite A-202, Devon, Alberta, CANADA, T9G 1A8

M. Oballa, C. Wong and A. Somogyvari, NOVA Research and Technology  
Corporation, 2928-16th Street N.E., Calgary, Alberta, CANADA, T2E 7K7

**Keywords :** hydrocracking, distillates, hydrotreating, colour, storage stability

### ABSTRACT

The storage stability of distillates from the hydrocracking of Western Canadian bitumen atmospheric residue was studied over 60 days. naphtha-jet and gas oil fractions of the hydrocracked distillates were shown to be unstable with respect to the formation of existent gum, total insoluble materials and asphaltene. The storage stability was significantly improved when these two fractions were mildly hydrotreated. The data were used to generate correlations that predict the stability of synthetic crudes.

### INTRODUCTION

The refining industry in North America is consistently moving towards the utilization of heavier feedstocks for the production of synthetic crude. Current production of synthetic crude oil from oil sands and heavy oils is achieved by hydrogen addition as well as carbon rejection technologies. The primary products from these heavy feedstocks require different degrees of hydrotreating to obtain transportation fuels that meet current specifications. The hydroprocessing of bituminous materials and residues results in coke deposition on the catalyst as well as sludge formation in the product oil [1]. The products obtained are rather unstable, generally described as storage instability. Storage stability of hydrocarbon fuels therefore refers to their tendency to produce coloured species, soluble gums, and insoluble sediment during storage [2]. The storage and thermal stability of liquid stocks, especially diesel and jet fuel, have been topics of intense study especially by the military [3, 4]. To our knowledge, there has been very little study on the stability of hydrocracked products from the residues of Canadian heavy oils or the synthetic crude so blended after hydrotreating the hydrocracked distillate fractions.

The objective of the study was to quantify the rate of deterioration of the hydrocracked material and the hydrotreated distillates in terms of colour change and formation of soluble gums and insoluble materials, as well as to establish the presence or absence of the precursors to instability in the liquid fractions.

### EXPERIMENTAL

The feedstock for this study was 50/50 Cold Lake/Llyodminster atmospheric residue (399°C +). The hydrocracking of the residue to distillate fractions was performed on a commercial NiMo/Al<sub>2</sub>O<sub>3</sub> catalyst using a continuous bench scale stirred tank reactor. The experiments were carried out using the following conditions: Pressure < 20,685 kPa, temperature < 450°C and LHSV < 1 h<sup>-1</sup>. The catalyst was presulphided and conditioned for 120 hours. To obtain the required amount of distillate products the experiment was continued for another 16 hours. The product samples had to be analyzed as soon as they were generated and distilled to give the fractions required for further processing (hydrotreating) or analysis. Distillation of the hydrocracked materials was carried out in order to obtain fractions which were tested for storage and colour stability and further characterized to identify materials causing instability. The hydrocracked materials were distilled into naphtha, jet-fuel, diesel, gas oil and Residue. The naphtha and jet-fuel fractions were analyzed for both colour and storage stability and then combined as feedstock for hydrotreating. Similarly, diesel and gas oil fractions were analyzed for colour and storage stability and then combined as feedstock for hydrotreating. The catalysts used for naphtha-jet and diesel-gas oil hydrotreating experiments were C-411 and C-424 catalysts respectively. Detailed experimental procedures and equipment are described elsewhere [5].

### Analytical Methods and Analyses of Samples

Specific gravities were determined in triplicate at 15.5°C on a Paar DMA 48 instrument. Dynamic viscosities were determined in triplicate at 40°C using a Brookfield DV II instrument. Heptane insoluble asphaltenes were determined using the method of Pearson et.al. [6]. Existent gum was determined by the jet evaporation technique according to ASTM D 381-86. Hydrocarbon-types were determined in low boiling (IBP-249°C) distillates by the fluorescent indicator adsorption

method according to ASTM D 1319-77 and gave the volume percent of saturates, olefins and aromatics. The aniline point of the various distillate fractions was determined according to ASTM D 611-82. Bromine Numbers were determined according to procedures in ASTM D 1159-82. Carbon, hydrogen and nitrogen were determined using a CHN Analyzer. Trace nitrogen was determined on an Antek 771 pyroanalyzer coupled to an Antek chemiluminescent nitrogen detector. Basic nitrogen was determined according to procedures outlined in UOP Method 269-70T. Sulfur was determined on a Leco SC-132 sulfur analyzer. The colour of the petroleum products was determined by the Lovibond Tintometer method as described in IP 17/52. The oxidation stability of middle distillate fractions was determined according to ASTM D 2274-88 and these procedures have been found useful for estimating the storage stability of distillate fuels boiling between 175 and 370°C. The procedures in ASTM D 4625-87 were followed for the prediction of storage stability. Hydrocarbon-type analyses on the liquid samples were performed using a modified ASTM D 2007-75 and ASTM D 2579-78 procedures. The saturates and the aromatic fractions were analyzed by low resolution mass spectrometry by modifications to procedures in ASTM D 3239 and ASTM D 2786-71. The polars fraction, which contained mostly nitrogen heterocycles, was similarly analyzed via high resolution mass spectrometry.

## RESULTS AND DISCUSSION

### Effect of Hydrocracking:

The hydrocracking of the feedstock resulted in a 66.7% conversion of material boiling above 524°C (Table 1). The asphaltene content which is more or less a measure of the hydrogen deficiency of an oil was reduced to one third of its original value after hydrocracking and mainly remained in the 524°C+ fraction. The increase in the hydrogen to carbon ratio after hydrocracking was synonymous with the decrease in the asphaltene content. The viscosity and density of the hydrocracked materials decreased as expected. Of particular interest is the ratio of non-basic nitrogen to basic nitrogen in the hydrocracked sample. Some nitrogen compounds have been known to contribute to fuel instability, while others are inert. As shown in Table 1 hydrocracking reduced the total nitrogen in the feed, but the basic nitrogen increased.

### Effect of Hydrotreating :

The hydrotreating was carried out on the naphtha-jet fuel fraction as well as on the diesel-gas oil fraction. For simplicity, these hydrotreated fractions are referred to as hydrotreated naphtha-jet and hydrotreated Gas Oil respectively. The hydrotreating step not only removed the heteroatoms (S, N, O), but also refined and stabilized the products. Sulfur was released in the form of H<sub>2</sub>S, nitrogen in the form of NH<sub>3</sub>, and oxygen in the form of H<sub>2</sub>O. The following tests were performed to determine the effect of hydrotreating on the stability of different distillate fractions.

### Stability Tests:

**Total Insolubles:** The oxidation stability results performed on naphtha-jet fraction are shown in Table 1. The data indicate that the total insolubles were much higher in the unhydrotreated material than in the hydrotreated samples. This data confirmed that hydrotreating stabilized the reactive hydrocarbons thereby rendering them less reactive than they otherwise would have been. The effects of hydrotreating on the long term storage stability of different fractions are shown in Table 2 and Table 3. In the unhydrotreated naphtha jet fraction, after 60 days of storage time, the total insolubles increased from 0.03 to 19.2 mg/100ml whereas in the hydrotreated sample, the total insolubles were at 0.25 mg/100 ml after storage for 60 days. In the unhydrotreated gas oil fraction, the total insolubles were 15.9 mg/100 ml after 60 days of storage, while for the hydrotreated sample, the total insolubles were only at 3.6 mg/100 ml after 60 days of storage.

**Existent Gum:** It is generally believed that the products of initial oxidation, probably peroxides, catalyze the oxidation of normally less reactive hydrocarbons to increase the rate of gum formation. Most of the oxidation products are said to be soluble in naphtha but decompose during evaporation to give gum that is largely composed of acidic material. Some of the studies show a correlation between gum content and total nitrogen content, while in other studies the gum content is said to increase with boiling range. The results in Tables 2 show that the existent gum in the naphtha-jet fraction decreased from 8.8 mg/100 ml before hydrotreating to zero after hydrotreating. After storage of the unhydrotreated fraction for 60 days, the existent gum was 142 mg/100 ml as opposed to a hydrotreated sample stored for the same 60 days which had 0.80 mg/100 ml. Undoubtedly, hydrotreating affects the existent gum content of naphtha -jet fractions.

**Colour :** The results of the colour test are shown in Table 1. Colour is one of the most distinguishing characteristics of untreated hydrocracked distillates. On distillation after hydrocracking, the naphtha-jet fraction is from clear to pale yellow. However, when exposed to

ordinary room conditions, this hydrocracked fraction will start to darken and also to deposit gum. Colour change is therefore indicative of the aging of the sample. The naphtha-jet fraction before hydrotreating had a colour number of 0.5 to 1.0 and after hydrotreating the colour number was reduced to zero. The gas oil fraction had a colour number of 3.5 to 4.5 before hydrotreating and after hydrotreating the colour number was reduced to 1.5 to 2.

**Viscosity :** The viscosity of the fractions (Table 2 and 3) is influenced more by storage time than by hydrotreating. Both the naphtha-jet and the gas oil fractions showed an increase in viscosity with storage time.

**Aniline Point :** There is an inverse relationship between aniline point and aromatic content. Aniline Point is usually increased slightly with the molecular weight and boiling point of a sample, and rapidly with the paraffinicity of oil samples. The higher aniline point value denotes a lower aromatic content and a higher paraffin content. Tables 2 and 3 show a higher aniline content after hydrotreating for both the naphtha-jet and the gas oil fractions. In Table 4, the analyses for paraffins and aromatics confirm the above conclusions. Overall, the monocycloparaffins are being converted to dicycloparaffins, leaving a decrease in the paraffinic content after aging. Both the mono- and di-aromatic constituents of the distillates increased at the expense of the paraffinic components, which suggests that saturated paraffinic components undergo some form of condensation with aromatic constituents.

#### **SUMMARY:**

The work presented here was undertaken to address the issue of the storage stability of middle distillates obtained from Western Canadian heavy oil/bitumen. Fuel stability is the general resistance of a fuel to change. Two types of stability were investigated. The first was storage stability, which reckons the ability of the fuel to stay in storage for a long period of time with little deterioration. The second was thermal stability which is the ability of the fuel to resist with little deterioration high temperature stress for a short period. The study results show that the deterioration of the fuel through storage manifested itself in colour change, development of soluble and insoluble gum, and changes in the physical and chemical properties of the fuel, like viscosity, density, nitrogen, sulfur, aromatics and asphaltene content. The results obtained also suggest that hydrocracked or thermally cracked materials should be hydrotreated/processed as quickly as possible. The detail hydrocarbon-type analyses of different fractions before and after hydrotreating showed that hydrotreating reduced refractory materials, including polar compounds, that cause storage instability.

#### **ACKNOWLEDGEMENT :**

Our thanks go to the management of NCUT and NOVA Research & Technology Corporation for financing the project and publication of the paper.

#### **REFERENCES**

- 1- M. F. Symoniak and A. C. Frost, Oil & Gas Journal, Mar. 17, 1971, 76.
- 2- J. Ritchie, J. Inst. Petr., 1965, Vol. 51, 296.
- 3- O. K. Bahn, D.W. Brinkman, J.B. Green and B. Carley, Fuel, 1987, Vol. 66, 1200.
- 4- J. V. Cooney, E. J. Beal, M.A. Wechter, G. W. Mushrush and R. N. Hazlett, Preprints, Petroleum Chemistry Division, 1984, Vol. 29, 1003.
- 5- M.C. Oballa, C. Wong and A. Somogyvari, "Colour and Storage Stability of Synthetic Crudes & Distillates", Final Report, for Energy Mines and Resources Canada, 1992, SCC File No : 06SQ.23440-1-9014
- 6- C.D. Pearson, G.S. Huff and S.G. Garfeh, Anal-Chem., 1986, Vol. 58, 3265

**TABLE 1: COLOUR AND STORAGE STABILITY OF SAMPLES**

	FSTK <sup>(1)</sup>	HC <sup>(2)</sup>	IBP-249	249-524	After Hydrotreating	
					IBP-249	249-524
Asphaltene Content (wt%)	15.86	5.31	0.02	0.06	0.02	0.05
Viscosity @ 40 deg C (cP)	8.75E+05	22.4	0.69	24.1	0.88	11.4
Density @ 15.5 deg C (g/cc)	1.0266	0.9292	0.7934	0.9295	0.7822	0.889
API Gravity (API)	6.33	20.78	46.85	20.73	49.40	27.67
Sludge (wt%)	-	0.74	-	0	-	0
Bromine No. (mg Br/100 g)	-	17.3	-	10.7	-	1.2
<b>Hydrocarbon Types by FIA</b>						
Aromatics (Vol.%)	-	-	21.1	-	3.4	-
Saturates (Vol.%)	-	-	75.5	-	95.4	-
Olefin (Vol.%)	-	-	3.4	-	1.2	-
Aromatics by Mass Spec.	-	-	-	-	-	-
<b>Colour</b>						
IBP - 177 C	-	-	0-0.5		0	
177 - 249 C	-	-	0.5-1.0		[IBP 249]	
249 - 343 C	-	-	-	3-3.5		1.5-2.0
343 - 524 C	-	-	-	4.5-5		[249-524]
Aniline Point (deg C)	-	-	46.7	61.8	63.4	74.5
<b>Elemental Analysis</b>						
Total Nitrogen (wt%)	0.546	0.410	0.104	0.291	<1 ppm	146ppm
Basic Nitrogen (wt%)	0.117	0.129	0.088	0.125	<1 ppm	25ppm
Non-Basic Nitrogen (wt%)	0.429	0.281	0.016	0.166	<1 ppm	121ppm
C (wt%)	83.15	86.66	85.00	87.14	85.17	87.07
H (wt%)	10.36	12.33	13.03	11.08	13.84	12.50
S (wt%)	5.231	1.043	0.488	1.402	144 ppm	800ppm
H/C Ratio (Atomic)	1.49	1.70	1.83	1.52	1.94	1.71
<b>Oxidation Stability</b>						
Filterable Insolubles (mg/100ml)	-	-	3.23	-	0.11	-
Adherent Insolubles (mg/100ml)	-	-	6.00	-	0.03	-
Total Insolubles (mg/100ml)	-	-	9.23	-	0.14	-
Existent Gum (mg/100ml)	-	-	8.8	-	0	-
<b>Simulated Distillation (wt%)</b>						
IBP - 177 C	0	7.60	40.00	0	44.00	2.50
177 - 249 C	0	8.80	52.50	0.80	48.50	4.30
249 - 343 C	0.50	17.00	6.80	27.50	6.00	34.50
343 - 524 C	32.00	44.10	0.70	69.30	1.30	58.70
524 C+	67.50	22.50	0.00	2.40	0.20	0

(1) Feedstock

(2) Hydrocracked product

**TABLE 2 - NAPHTHA-JET FUEL FRACTION - EFFECT OF HYDROTREATING ON STORAGE STABILITY**

PROPERTIES	IBP - 249 °C Unhydrotreated		IBP - 249°C Hydrotreated	
	At Time 0	After 60 days storage	At Time 0	After 60 days storage
Aniline Point [°C]	46.7	47	63.4	64.2
Viscosity [CP @ 40°C]	0.69	1.22	0.88	1.03
Asphaltene Content [wt%]	0.02	0.20	0.02	0.14
Existent Gum [mg/100ml]	8.8	142	0	0.80
<b>Storage Stability [mg/100ml]</b>				
Filterable Insolubles	0.03	0.90	0	0.14
Adherent Insolubles	0	18.30	0	0.11
Total Insolubles	0.03	19.20	0	0.25

**TABLE 3 - DIESEL - GAS OIL FRACTION - EFFECT OF HYDROTREATING ON STORAGE STABILITY**

PROPERTIES	249 - 524°C Unhydrotreated		249 - 524°C Hydrotreated	
	At Time 0	After 60 days storage	At Time 0	After 60 days storage
Aniline Point [°C]	61.8	61.7	74.5	74.6
Viscosity [CP @ 40°C]	24.1	28.3	11.4	14.5
Asphaltene Content [wt%]	0.06	0.25	0.05	0.23
<b>Storage Stability [mg/100ml]</b>				
Filterable Insolubles	0.20	15.33	0.11	3.31
Adherent Insolubles	0	0.63	0	0.29
Total Insolubles	0.20	15.96	0.11	3.60

**TABLE 4 - MASS SPECTROMETRY ANALYSIS RESULTS OF THE HYDROCRACKED SAMPLES**

HYDROCARBON	NAP-JET Before Storage (wt%)	NAP-JET After Storage (wt%)	GAS-OIL Before Storage (wt%)	GAS-OIL After Storage (wt%)	HT* GAS-OIL Before Storage (wt%)	HT* GAS-OIL After Storage (wt%)
Paraffins	36.40	32.52	17.15	17.17	22.23	19.02
Cycloparaffins	39.93	39.97	29.10	29.18	46.36	47.45
Monoaromatics	22.46	24.78	29.22	27.23	25.72	25.80
Diaromatics	0.73	1.14	14.92	15.14	3.74	4.82
Triaromatics	0	0	2.29	2.52	0.36	0.55
Tetraaromatics	0	0	0	0	0	0
Pentaaromatics	0	0	0.43	0.32	0.24	0.25
Unidentified	0	0	0.03	0.01	0	0
Aromatic Sulfur	0.03	0.43	2.97	3.35	0.97	1.56
Polar Compounds	0.45	1.16	3.89	5.08	0.38	0.55

\* Hydrotreated

# A COMPARISON OF LOW AND HIGH SULFUR MIDDLE DISTILLATE FUELS IN THE UNITED STATES

J. Andrew Waynick  
Amoco Petroleum Products  
150 West Warrenville Road  
Naperville, Illinois 60563-8460

## ABSTRACT

Sixty-nine low sulfur (LS) and twenty-six high sulfur (HS) No. 2 diesel fuel samples were collected from twenty-four marketers throughout the United States in early 1994. Fuel samples were tested for chemical composition and stability. Statistical analysis of the data indicated that other than sulfur and nitrogen levels, the main compositional difference between LS and HS diesel fuels was a partial saturation of poly-aromatics to mono-aromatics in LS fuel. Storage stability via ASTM D4625 was improved in LS fuels compared to HS fuels. Hydroperoxide susceptibility of LS and HS fuels was equivalent and acceptable under conditions of ambient fuel transport and storage. However, under progressively severe thermal and oxidative stress, LS fuels appeared increasingly less stable than HS fuels.

## INTRODUCTION

Before October 1993, No. 2 distillate fuel sold in the United States contained 0.2-0.4 % (wt) sulfur. As of October 1993, No. 2 distillate fuel used for on-highway vehicles was required to have a sulfur level no greater than 0.05 % (wt), i.e. 500 ppm (wt). This sulfur level reduction has been achieved by increasing the severity by which diesel fuel feedstocks are hydrotreated.

Limited data indicates that such low sulfur diesel fuels will have improved storage stability<sup>1-3</sup>, i.e. form less sediment and dark-colored fuel-soluble materials. However, there have been concerns that resulting low sulfur diesel fuels may be more prone to form hydroperoxides upon storage.

The objective of the work reported in this paper was to compare the storage stability and hydroperoxide susceptibility of a large number of low and high sulfur No. 2 diesel fuels throughout the United States.

## EXPERIMENTAL

### Fuel Samples

Ninety-five No. 2 diesel fuel samples were collected during the period of February-March 1994. Sixty-nine samples were low sulfur (LS) diesel fuels; twenty-six were high sulfur (HS) fuels. Samples were collected in five geographic areas of the United States: Northern Midwest, Southern Midwest, Texas Gulf Coast, Rocky Mountains, and East Coast. Fuel samples spanned twenty-four marketers of diesel fuel, and were taken from both company-operated terminals and service stations. A few samples were taken directly from product pipelines. No attempt was made to determine if samples had been co-mingled during fungible pipeline shipment, or delivered segregated from the refinery. However, all samples represent diesel fuel being sold by the various marketers in the United States during early 1994.

All samples were shipped to the Amoco Research Center, Naperville, Illinois, by overnight express mail from the sampling points, and were stored at 40°F except when being tested.

### Tests

Fuel samples were tested for chemical composition and stability using the following procedures:

Chemical Composition	Stability
Total Sulfur by Dispersive X-Ray Fluorescence (ASTM D4294)	Storage Stability (ASTM D4625) Initial Peroxide Number (ASTM D3703)
Total Nitrogen (ASTM D4629, modified) SMORS	Peroxide Number after ASTM D4625 (ASTM D3703)
Paraffins/Aromatics by Mass Spectrometry	Hydroperoxide Potential, CRC Procedure Hydroperoxide Potential, Oxygen Overpressure (OP) Procedure

Initial color (ASTM D1500) and ASTM D4625 final color were usually not determined for HS diesel fuel samples, since nearly all of those samples were dyed. The CRC Hydroperoxide Potential Procedure was originally developed for jet fuels<sup>6</sup> and involves heating a 100 ml fuel sample at 65°C and 1 atmosphere air for four weeks. Peroxide number is then determined as an indication of the fuel's hydroperoxide susceptibility. The OP procedure for hydroperoxide potential was adapted from previously documented work involving jet fuels<sup>5</sup>. The procedure involves heating a 50 ml fuel sample at 100°C and 690 kPa (100 psia) O<sub>2</sub> for 24 hours. The peroxide number is then determined. The modification to the total nitrogen procedure was that the fuel sample was delivered to the combustion tube by a platinum boat rather than by standard syringe injection. SMORS (Soluble Macromolecular Oxidatively Reactive Species) are believed to be sediment precursors, and the procedure for measuring them has been previously documented<sup>6</sup>.

### Statistical Treatment of Data

Data was statistically analyzed using SAS 6.08 for Windows. Statistical analysis was executed in three steps:

1. Distribution analysis
2. Analysis of geographic variance
3. Two sample t-testing of LS and HS fuels

Distribution analysis of the LS and HS results was done to ensure that normal distributions existed before running t-tests. When certain fuel test results gave non-normal distributions, a conversion to their logarithms usually gave the normal distributions required for valid t-testing. For a few tests, large numbers of zeros required the use of a non-parametric procedure known as the Median Scores test instead of the more commonly used t-test. Before t-tests were performed, the variance of data in each geographic area was analyzed to allow a stronger statistical treatment of the entire data pool. Two sample t-testing was then done to determine the statistical probability that a given mean test value was different for LS fuels compared to HS fuels. The confidence level (in percent) that the mean LS test value and mean HS test value is different was calculated. For the purposes of this paper, a difference in LS and HS mean test results was not considered statistically significant unless the confidence level was at least 90%. However, confidence levels that were somewhat lower were not entirely dismissed.

## RESULTS AND DISCUSSION

### Chemical Composition

Results of the statistical analysis of chemical composition tests are given in Table I. None of the LS fuels significantly exceeded the 500 ppm(wt) maximum allowed value for sulfur. Sulfur and nitrogen values reflected the already demonstrated fact<sup>2</sup> that hydrotreating removes sulfur-containing compounds more easily than nitrogen-containing compounds. Surprisingly, SMORS did not significantly decrease in LS fuels compared to HS fuels. The mass spectrometric data indicated that while LS fuels had more mono-aromatics and less poly-aromatics than HS fuels, they did not have significantly less total aromatics.

### Stability

Results of the statistical analysis of stability tests are given in Table II. ASTM D4625 storage stability of all fuels was generally acceptable. LS fuel total insolubles averaged half that of HS fuel total insolubles, a statistically significant difference. This agrees with earlier work indicating that when diesel fuels are hydrotreated to reduce sulfur levels to less than 500 ppm(wt), conventional storage stability improves<sup>3</sup>. Dyeing practices prevented the determination of final color for the HS diesel fuels. However, the mean LS value (1.2, ASTM) appeared to be significantly improved from the typical HS values seen over the years in our laboratory. This also confirms previous observations that increased hydrotreating improves storage stability color, a significant result in view of the general inability of currently available additives to accomplish the same thing<sup>2</sup>.

All fuels except one LS fuel gave zero initial hydroperoxides via the ASTM D3703 titrametric procedure. Previous researchers found the same result when examining field samples of HS diesel fuels. They concluded that HS diesel fuels were stable with respect to hydroperoxide formation<sup>3</sup>. Since the sixty-nine LS fuels in this study were also taken from the field, the same line of reasoning would indicate that LS diesel fuels are also stable with respect to hydroperoxide formation under commercial transport and storage conditions.

Differences in peroxide susceptibility between LS and HS diesel fuels varied directly with the severity of the sample storage conditions. Under ASTM D4625 conditions (13 weeks, 43°C, 1 atm. air), LS fuels developed hydroperoxide levels that were higher than HS fuels by a modestly significant amount (C. L. = 83.9%). Under the CRC conditions (4 weeks, 65°C, 1 atm. air), the same trend was observed, but the difference was very significant (C. L. = 99.2%). Under the OP conditions (24 hours, 100°C, 690 kPa O<sub>2</sub>), the difference was even more significant (C. L. = 99.9%). It should also be noted that in all three hydroperoxide susceptibility tests, the mean final hydroperoxide level for LS fuels was far above the 1.0 meq O/Kg maximum level imposed on freshly refined JP-5 fuel. Hydroperoxide susceptibility for HS fuels exceeded this limit only for the most severe oxygen overpressure method.

The trend in hydroperoxide susceptibility is exactly what is expected, based on prior reported work and known chemical principles. Hydroperoxides in fuels are known to form via the well known peroxidation chain mechanism<sup>7</sup>. Very often, a slow initial stage of fuel oxidation, the induction period, occurs after which a more rapid rate of hydroperoxide formation is observed<sup>8</sup>. The length of the induction period will be determined by many factors including the level and efficacy of any naturally occurring or intentionally added antioxidants. Removal of those antioxidants by hydrotreating will reduce the induction period at any given set of incubation conditions (temperature, oxygen partial pressure, time). At very mild incubation conditions, the induction period may not be exceeded for most or all fuels. In that case, little or no difference in peroxidation susceptibility would be observed. As the incubation conditions become more severe, eventually the less stable fuels would exceed their induction period and rapid peroxidation would onset. These fuels would then be observed as more unstable. As the incubation conditions continue to become more severe, the separation of less stable and more stable fuels would become increasingly apparent up to a point.

Based on these observations, it appears that LS diesel fuels produced in the United States may be as hydroperoxide stable as HS diesel fuels under conditions they experience while getting to the end user. Also, results suggest that all three hydroperoxide susceptibility procedures used in this study may overpredict actual hydroperoxide levels generated by LS fuels under ambient conditions of fuel transport and storage. However, there is a real decrease in the peroxidation stability of LS diesel fuels compared to HS diesel fuels that could become apparent if the fuel is sufficiently stressed.

## CONCLUSIONS

Major conclusions regarding the U.S. diesel fuels evaluated in this paper include the following:

1. Other than reduced sulfur and nitrogen content, the main statistically significant compositional difference between LS and HS diesel fuels was a partial saturation of poly-aromatics to mono-aromatics in LS fuels. There did not appear to be a strong statistical difference in total aromatics between LS and HS fuels.
2. Conventional storage stability as measured by ASTM D4625 was improved by a statistically significant amount in LS diesel fuels compared to HS diesel fuels. Both total insolubles and final color appeared to be improved.
3. Hydroperoxide susceptibility appeared to be equivalent and satisfactory for both LS and HS diesel fuels under the ambient conditions encountered during fuel transport and storage. However, under progressively severe thermal and oxidative stress, LS fuels appeared increasingly less stable than HS fuels.

## ACKNOWLEDGMENTS

The contributions of the following people are gratefully acknowledged: Mike Dattalo, Teresa Myczek, and Jack Treadman for running much of the laboratory tests; Don Porter for performing the statistical analysis of data.

## REFERENCES

1. Palmer, L. D.; Copson, J. A. "Hydrotreatment of Light Cycle Oil for Stabilization of Automotive Diesel Fuel," Proceedings of 2nd International Conference on Long-Term Storage Stabilities of Liquid Fuels, San Antonio, Texas, July 1986.

2. Martin, B.; Bocard, C.; Durand, J. P.; Bigeard, P. H.; Denis, J.; Dorbon, M.; Bernasconi, C. "Long-Term Storage Stability of Diesel Fuels: Effect of Ageing on Injector Fouling; Stabilization by Additives or Hydrotreating," presented at SAE Fuels and Lubes meeting, Tulsa, Oklahoma, 1990.
3. Vardi, J.; Kraus, B. J. "Peroxide Formation in Low Sulfur Automotive Diesel Fuels," SAE Paper No. 920826, 1992.
4. Determination of the Hydroperoxide Potential of jet Fuels, CRC Report No. 559, April 1988.
5. Black, B. H.; Hardy, D. R. "Comparison of Jet Fuel Phenolic Antioxidants Using A Serial Dilution Technique," Proceedings of the 4th International Conference on Stability and Handling of Liquid Fuels, Orlando, Florida, November 1991.
6. Hardy, D. R.; Wechter, M. A. "What Are Soluble Macromolecular Oxidatively Reactive Species (SMORS)?" ACS National Meeting, Washington, D.C., August 1990.
7. Lundberg, W. O. (Ed.) *Autooxidation and Antioxidants*. Interscience (John Wiley and Sons), 1961.
8. Fodor, G. E.; Naegali, D. W.; Kohl, K. B. "Peroxide Formation in Jet Fuels," *Energy and Fuels* 1988, 2, pp 729-734.

**Table I**  
**Results of the Statistical Analysis**  
**Chemical Composition**

Test	Low Sulfur Mean	Low Sulfur St Dv	High Sulfur Mean	High Sulfur St Dv	Conf. Level for Diff.	Test Metric <sup>1</sup>
Total Sulfur, ppm(wt)	296	92	2082	902	99.9	Log
Total Nitrogen, ppm(wt)	74.3	47.4	156.1	79.5	99.9	Original
SMORS, mg/100ml	.59	.50	.53	.35	35.4	Original
Mass Spectrometry Analysis, %(vol)						
Total Saturates	69.9	5.2	68.7	4.7	68.0	Original
Total Aromatics	30.1	5.2	31.3	4.7	68.0	Original
Mono-Aromatics	23.9	4.4	19.6	3.4	99.9	Original
Poly-Aromatics	6.3	2.2	11.7	3.3	99.9	Original

1. Test Metric indicates whether original data or natural logarithms were used to generate statistical information. See EXPERIMENTAL section for more information.

**Table II**  
**Results of the Statistical Analysis**  
**Stability**

Test	Low Sulfur Mean	Low Sulfur St Dv	High Sulfur Mean	High Sulfur St Dv	Conf. Level for Diff.	Test Metric <sup>1</sup>
Storage Stability, ASTM D4625						
Total Insolubles, mg/100ml	.30	.31	.67	.67	99.9	Log
Final Color, ASTM	1.20	.514	.750 <sup>2</sup>	--	--	Log
Hydroperoxide Analysis, meq O/Kg						
Initial Peroxide Number, ASTM D3703	.071 <sup>4</sup>	.590	0.00	0.00	--	Original
Peroxide Number after ASTM D4625 <sup>3</sup>	21.3	156.0	.78	1.42	83.9	Original
Hydroperoxide Potential, CRC <sup>3</sup>	23.6	131.3	.10	.53	99.2	Original
Hydroperoxide Potential, OP	339	545	19.8	11.2	99.9	Log

1. Test Metric indicates whether original data or natural logarithms were used to generate statistical information. See EXPERIMENTAL section for more information.

2. High sulfur results based on 1 observation

3. Because of the large number of zeros, the Median Scores test results are reported

4. Only one of the sixty-nine LS fuel samples had a non-zero result.

# EFFECT OF C<sub>60</sub> ON OXIDATIVE STABILITY OF FUELS

R. Malhotra

SRI International, Menlo Park, CA 94025

D. R. Hardy, E. J. Beal, R. E. Morris, B. H. Black

Naval Research Laboratory, Code 6180, Washington DC 20036

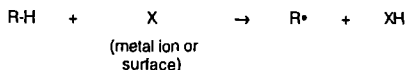
## ABSTRACT

Prompted by the ability of fullerenes to intercept radical chain processes, we investigated their possible application as additives to enhance thermal and storage stabilities of fuels. The thermal stability was evaluated using a gravimetric JFTOT apparatus, and the storage stability was assessed using the oxygen overpressure test. At a doping of 24 ppm, we found a significant beneficial effect of C<sub>60</sub> in enhancing the thermal stability of jet fuels, but only a marginal effect for the storage stability of diesel fuels. In addition, we found that the presence of fullerenes had no effect on hydroperoxide formation as long as the fuel was kept in the dark. However, exposure to ambient light led to the build up of substantial quantities of hydroperoxides.

## INTRODUCTION

Formation of insolubles in the fuel is a general problem. It can happen under various conditions, such as thermal stressing of jet fuels at 250 - 400°C during a flight, or during long term (years) storage of diesels under ambient conditions (10 - 45°C). The formation of insoluble materials can lead to many problems such as plugging of filters or fouling of engine parts.<sup>1,2</sup> In the extreme case when fuel flow is completely blocked, the consequence is extremely serious. Autoxidation has been implicated as a key step in the chemical scheme resulting in insolubles formation. This process involves generation of radical species, which initiate a chain reaction with oxygen to give oxidized hydrocarbons. The scheme, as originally proposed by Hazlett, is shown below:

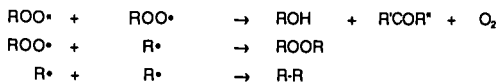
### INITIATION:



### PROPAGATION:



### TERMINATION:



In view of the ability of  $C_{60}$  to scavenge radicals<sup>3</sup> we decided to test the effect it would have on (i) thermal stability of jet fuels, (ii) storage stability of diesels, and (iii) hydroperoxide formation.

## RESULTS AND DISCUSSION

Numerous studies have been conducted on the chemistry leading to insolubles formation in jet fuels at elevated temperatures.<sup>1</sup> Key reactions are the thermal decomposition of alkyl chains by the Rice Herzfeld mechanism and autoxidation. The thermal stability tests were conducted using a gravimetric JFTOT apparatus with two JP-5 fuels (J1 and J2) and commercial Jet A fuel (JA). The JFTOT strip was heated to 260°C and 450 mL of fuels were pumped over it at 3.0 mL/min. The weight of the deposits on the strip as well as those collected on the filter were determined. The strip deposit is often very small (about 5-10%) of the total deposit. However, addition of 24 ppm  $C_{60}$  reduced deposit formation on the strip as well as the filtered deposit by about 50%. The data for the total deposits are displayed in Figure 1. The reduction in the fuel J1, which had a commercial additive package in it, is particularly noteworthy, because  $C_{60}$  was able to further reduce the very small amount of the deposit. An additive-free jet fuel (J2), which gave 15 mg/L of deposits, gave only 5.5 mg/L when doped with 24 ppm  $C_{60}$ . Finally, a commercial jet fuel, Jet A, which also had the additive package in it, showed no beneficial effect upon doping with  $C_{60}$ .

The chemistry of insolubles formation during long term storage is fairly complex and involves many different reactions. A possible scenario includes oxidation of sulfur species to sulfonic acids which catalyze the nucleophilic reaction of alkyliindoles with phenalenones, which are also formed by autoxidation.<sup>4</sup> Tests on the storage stability of diesels were conducted with two diesel fuels (D1 and D2) by the oxygen over pressure (oop) test developed at the Naval Research Laboratory.<sup>5</sup> Both of the fuels are a 20% light cycle oil blend with the straight run diesel. The fuels were stressed for 16 h at 90°C with 100 psig  $O_2$ . The results are shown in Table 1.

Table 1. Effect of  $C_{60}$  on the Insolubles formation in diesel fuels during the oxygen overpressure test (90°C, 16 h, 100 psig  $O_2$ )

Fuel ID	Neat	+24 ppm $C_{60}$	% Redn.
D1	56	47	16
D2	44	34	23

At the doping level of 24 ppm both fuels responded to the addition of  $C_{60}$ , although the more unstable fuel, Fuel D1, exhibited a modest 16% reduction deposit formation. At a similar level of doping with an alkyl amine additive, these fuels showed a reduction in deposit formation of about 70%. Thus,  $C_{60}$  is not a particularly effective agent for enhancing the storage stability of diesel fuels.

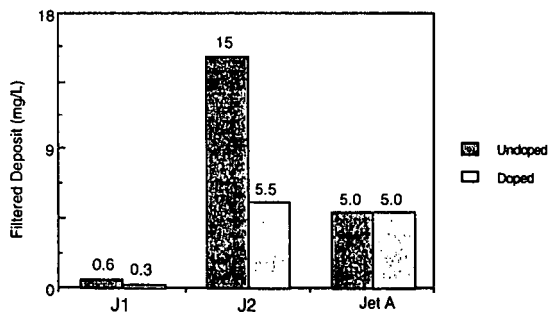
Finally development of hydroperoxides in an unstable JP-5 fuel, held in the dark at 102°C under 50 psia air, was monitored over a 150-h duration. The results are illustrated in Figure 2. Initially,  $C_{60}$  (@24 ppm) accelerated the hydroperoxide formation, but at the end (~140 hr), both samples—additive free and doped—show the same low values. Experiments were also

conducted with a stable JP-5 at ambient temperatures under a fluorescent light in the presence of 0, 5, 10, and 20 ppm C<sub>60</sub>. In control experiments, there was no formation of hydroperoxides in the dark, but C<sub>60</sub> had a profound influence on the formation of hydroperoxides in the light. These results further illustrate the ability of C<sub>60</sub> to photosensitize the oxidation of other substrates.

These preliminary data show that although C<sub>60</sub> reduces the deposit formation in jet fuels, it can also have deleterious effects, particularly if the fuel were to be exposed to light. Further work with functionalized fullerenes is currently under way.

## REFERENCES

1. R. N. Hazlett, "Thermal Oxidation Stability of Aviation Turbine Fuels," ASTM Publications, Philadelphia, PA, 1991.
2. A. Z. Fathoni and B. D. Batts, *Energy Fuels* 1992, 6, 681.
3. C. N. McEwen, R. G. McKay, and B. S. Larsen, *J. Am. Chem. Soc.* 1992, 114, 4412-4414.
4. R. N. Hazlett, D. R. Hardy, and R. Malhotra, *Energy Fuels* 1994, 8, 774.
5. D.R. Hardy, R.N. Hazlett, E.J. Beal and J.C. Burnett, *Energy Fuels* 1989, 3, 20.



## FUELS

J1: JP5 (contains additives)

J2: Fresh blend (unstable)

Jet A: Commercial aviation fuel (contains additives)

Doping at 24 mg/L

Figure 1. Effect of C<sub>60</sub> on the thermal stability of jet fuels as determined in a gravimetric JFTOT test conducted at 260°C.

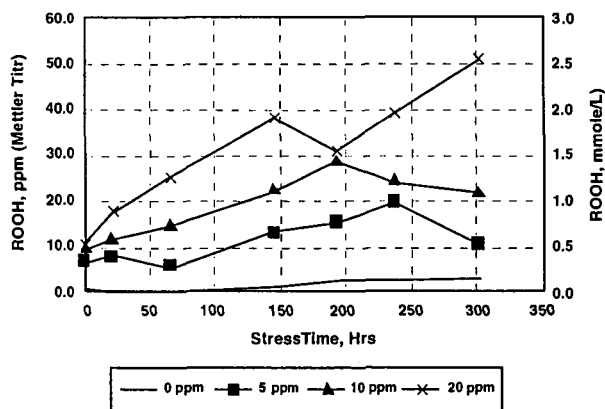
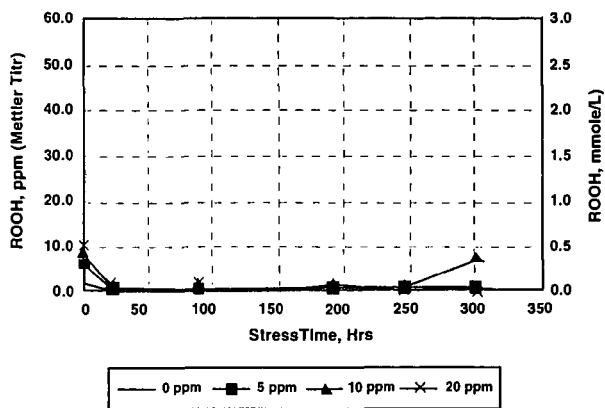


Figure 2. Effect of C<sub>60</sub> on the peroxide formation at 25°C in aviation fuel 91-7 in (a) dark and (b) in light.

# EFFECTS OF CARBON SURFACES ON THERMAL DECOMPOSITION OF HYDROCARBONS

Philip H. Chang and Semih Eser  
Fuel Science Program  
Department of Materials Science & Engineering  
209 Academic Projects Building  
The Pennsylvania State University, University Park, PA 16802, USA

## INTRODUCTION

Deposition of carbonaceous solids on metal surfaces in the fuel system has been a major concern for the development of advanced aircraft with high thermal loads (Heneghan et al., 1996; Eser, 1996). In our previous studies we showed that the presence of high surface area activated carbon PX-21 prevented solid deposition on reactor walls and reduced the extent of decomposition of *n*-alkanes (Eser et al., 1992; Gergova et al., 1994; Gergova et al., 1996). We have suggested that the active sites of PX-21 carbon act to stabilize the pyrolysis products and enhance the H-transfer reactions. There are other reports on the activity of solid carbons in catalyzing the reactions of hydrocarbons (Szymanski and Rychlicki, 1993; Grunewald and Drago, 1990).

In this study, we compare the effects of activated carbon and other carbon additions on thermal decomposition of *n*-dodecane, cyclohexane, and ethylbenzene, as three different types of hydrocarbons present in jet fuels, and investigate the influence of oxygen complexes present on the carbon surface on thermal decomposition of cyclohexane and ethylbenzene.

## EXPERIMENTAL

Thermal stressing experiments were carried out on 10 ml *n*-dodecane, cyclohexane and ethylbenzene in 316 stainless steel batch reactors at 450°C for 1 to 23 hours in a nitrogen atmosphere (Gergova et al., 1996). The high surface area activated carbon (PX-21), the carbon black (FW200), and another activated carbon (Asbury 5562) were obtained from Amoco Oil company, Degussa company in Germany, and Asbury company, respectively. Approximately 200mg of each carbon was added to model compounds prior to thermal stressing. The  $N_2$ -BET surface areas of the three carbons are given below.

	PX-21	FW200	Asbury5562
Surface area(m <sup>2</sup> /g)	3000	500	1200

Gas chromatography (GC) of liquid samples was conducted using a Perkin-Elmer 8500 GC with fused silica capillary column. Gas products were also analyzed by Perkin-Elmer Auto System GC. Compounds in the liquid products were identified by capillary Gas Chromatography-Mass Spectrometry (GC-MS) using a Hewlett-Packard 5090 II GC coupled with 5971A mass selective detector.

Boehm titrations (Boehm, ) were performed with the three carbons to determine the concentrations of surface functional groups. For titrations, two- or three-gram samples of carbons were added in 200ml of various acidic and basic solutions prepared previously; all the solutions were 0.1M except Na<sub>2</sub>CO<sub>3</sub> which was 0.05M. The solutions with added carbons were agitated for 48 hours, and filtered prior to titration. A 10 ml sample of filtered solutions was titrated with either 0.1M HCl or 0.1M NaOH solution depending on whether the acidic or basic functional groups are determined. Phenolphthalein or methylorange was used as an indicator in titrations.

The Asbury 5562 AC was bathed in strong nitric solution to oxidize its surface. A 20 g of activated carbon was bathed with 4M nitric acidic solution at 75°C for 2 hours. After bathing with acidic solution, the activated carbon was rinsed with distilled water until the washing water is neutral. The washed sample was dried in a vacuum oven. Boehm titrations were carried out on the oxidized carbon also to determine the acidic and basic functional groups on the surface.

## RESULTS AND DISCUSSION

**Thermal Decomposition of *n*-Dodecane.** Despite the large differences in their BET surface areas the activated carbon PX-21 and the carbon black FW200 showed the same effect on thermal decomposition of hydrocarbons. Therefore, no results will be presented on the behavior of FW200 in thermal stressing experiments. Figure 1 shows the total concentrations of cycloalkanes and aromatics in the products obtained from stressing of *n*-dodecane at 450°C for 1 and 3 h with and without added PX-21. When PX-21 is added, higher concentrations of aromatic compounds are obtained in the products, indicating that the carbon surface promotes dehydrogenation reactions, possibly through hydrogen shuttling activity, as proposed before (Gergova et al., 1996) and discussed below.

In gaseous products, hydrogen and ethane concentrations were higher, whereas ethylene concentration was lower with PX-21 compared to those obtained without PX-21. Higher ethane and lower ethylene concentrations with PX-21 can be attributed to the stabilization of ethyl radicals (formed by  $\beta$ -scission reactions) on the carbon surface. Combined with the data on the concentrations of cycloalkanes and aromatics in the liquid products, the gas analysis suggests

that the carbon surface shuttles hydrogen from cycloalkanes to stabilize the free radicals produced by thermolysis of n-dodecane. In other words, the carbon surface appears to be active in both dehydrogenation (e.g., of cycloalkanes) and hydrogenation (e.g., of ethyl radicals) reactions. One possible mechanism for the proposed hydrogen shuttling activity is the sequential hydrogenation and dehydrogenation of aromatic ring systems on the carbon surface. The stabilization of free radicals on carbon surface can explain why thermal decomposition of n-dodecane is suppressed with inhibition of solid deposition on metal surfaces (Gergova et al., 1996).

**Thermal Decomposition of Cyclohexane.** Thermal stressing of cyclohexane with/without PX-21 gave similar results to those obtained from stressing n-dodecane. The addition of PX-21 inhibited the thermal cracking of cyclohexane and gave much higher concentrations of benzene in the liquid products. The data shown in Figure 2 clearly demonstrates the dehydrogenation activity of PX-21 which produced in long duration experiments almost 30 times higher benzene concentrations compared to that obtained without PX-21. Similar to the results obtained with n-dodecane, the analysis of gaseous products showed that the presence of PX-21 gave higher concentrations of hydrogen and ethane, and lower concentrations of ethylene compared to those obtained without PX-21.

**Thermal Decomposition of Ethylbenzene.** In contrast to the results obtained from stressing n-dodecane and cyclohexane, the additions of PX-21 promoted cracking reactions and increased the amount of carbonaceous deposit on the reactor wall. The liquid products obtained with PX-21 was much darker. Figure 3 shows that much higher concentrations of benzene, methylbenzene, dimethylbenzene, styrene and methylethylbenzene were obtained when PX-21 was added to ethylbenzene. The major product was dimethylbenzene.

The gas analyses showed the same trends as those observed with n-dodecane and cyclohexane, that is, higher concentrations of hydrogen, ethane (and methane), and lower concentrations of ethylene were obtained when PX-21 was present. There was almost no ethylene present in the gases obtained with PX-21. These results suggest that the carbon surface still acts as a hydrogen shuttler to methyl and ethyl radicals, but compared to n-dodecane and cyclohexane reactions, there is much less amount of hydrogen to shuttle. It appears that demethylation of the ethyl group (producing a resonance stabilized benzyl radical) and methylation of subsequently formed methylbenzene (to produce dimethylbenzene) are the major reactions. The higher extents of cracking observed with PX-21 can be attributed to the abstraction of hydrogen by the carbon surface which, in this case, appears to destabilize the pyrolysis system.

**Surface Characterization of Carbons using Boehm Titration.** Based on the Boehm titration results, the equivalent numbers of each basic and acidic solution neutralization were calculated. As shown in Table 1, small concentrations of basic groups are present on the surface of PX21 and 5562AC, but no basic groups are detected on the FW200. There are large concentrations of acidic groups present on both PX21 and FW200 surfaces, but relatively small concentrations of acidic groups are detected on 5562AC surface. If the acidic groups are divided into four individual groups, large concentrations of carboxyl and lactone groups are found on the surface of both PX-21 and FW200, but none is present on 5562AC. Compared to carboxyl and lactone groups, phenolic and carbonyl groups are less abundant on PX21 and FW200 surfaces than those on 5562AC.

It appears that PX21 and FW200 with high concentrations of surface acid groups, especially carboxyl and lactone groups, are very active during thermal decomposition of hydrocarbons. In contrast, 5562AC with low concentrations of acidic groups, but relatively high concentrations of phenolic and carbonyl groups did not show much activity during thermal stressing of hydrocarbons. These results suggest that oxygen functional groups are important for the activity of carbon surfaces during thermal decomposition of hydrocarbons.

**Effects of Oxidation of 5562 Asbury Activated Carbon on Thermal Degradation of Ethylbenzene and Cyclohexane.** Upon oxidation of 5562 Asbury activated carbon with nitric acid solution, all basic groups are decreased from 0.48 meq/g to 0.3 meq/g, and all acidic groups are increased from 0.65 meq/g to 2.1 meq/g (see Table 1). The oxidation treatment increased the concentrations of all major acidic groups except the phenolic group.

Untreated and oxidized Asbury 5562 activated carbon were used in thermal stressing experiments with ethylbenzene and cyclohexane. The thermal stressing of ethylbenzene and cyclohexane (10ml) was done with 300mg of as-received and oxidized 5562AC. Liquid product analysis shows that oxidized 5562AC shows the same effect during ethylbenzene pyrolysis as that observed with PX-21 and FW200, that is, more extensive cracking of alkyl side-chain was obtained with oxidized 5562AC than that observed with as-received 5562AC present. The addition of oxidized 5562AC promotes cracking reactions and increases the amount of carbonaceous deposit on the reactor wall. The liquid products obtained with the oxidized 5562AC was much darker in color. Figure 4 shows that the addition of the oxidized carbon gave much higher concentrations of benzene, methylbenzene, dimethylbenzene, styrene and methylethylbenzene compared to those obtained with the untreated 5562AC. The major product was dimethylbenzene. The amount of ethylbenzene remaining was drastically reduced when the oxidized 5562AC was added during pyrolysis experiments (see Fig. 5). These results are the same as those obtained from the pyrolysis of ethylbenzene with PX21 or FW200.

In contrast to ethylbenzene pyrolysis, the addition of oxidized 5562AC inhibited the thermal cracking of cyclohexane and gave much higher concentrations of benzene in the liquid products

(see Fig. 6,7). The data shown in Figure 3 clearly demonstrates the dehydrogenation activity of oxidized 5562AC indicated by the increase in benzene concentration, however the isomerization activity (i.e., cyclohexane to methylcyclopentane) was reduced with the oxidized 5562AC. These results suggest that oxidized 5562AC behaves like PX-21 and FW200 in promoting hydrogen transfer reactions.

It is important to note that even a very inactive carbon like Asbury 5562AC became active upon simple oxidation with nitric acid. These results confirm that oxygen functional groups, in particular acidic groups, on carbon surfaces play an important role during pyrolysis of hydrocarbons in the presence of added carbons. Some important reactions which appear to be catalyzed by active carbon surfaces include dehydrogenation of hydrocarbons, stabilization of free radicals at early stage of pyrolysis, and cracking of side chains on alkylaromatics.

## CONCLUSIONS

Thermal decomposition behavior of hydrocarbons is strongly influenced by the presence of an activated carbon PX-21 and a carbon black FW200. The addition of PX-21 and FW200 inhibits thermal decomposition of n-dodecane and cyclohexane and solid formation on reactor walls, but promotes the decomposition of, and solid formation, from ethylbenzene. The increased stability of n-dodecane and cyclohexane systems is explained by effective hydrogen shuttling on the carbon surface. Increased extents of cracking and solid formation from ethylbenzene can be attributed to the hydrogen deficiency of the aromatic compound compared to the two alkanes.

Boehm titrations showed the most active carbons such as PX-21 and FW200 contain large concentrations of acidic, but low concentrations of basic surface groups. Especially carboxyl and lactone type groups are present in high concentrations on the surfaces of PX-21 and FW200, whereas no carboxyl and lactone groups are found on the surface of Asbury 5562AC. The nitric acid oxidation process effectively produced oxygen functional groups on Asbury 5562AC and increased its activity during thermal stressing of hydrocarbons. Oxygen functional groups appear to play a key role in determining the activity of carbon surfaces during thermal stressing of hydrocarbons.

## ACKNOWLEDGMENT

Funding was provided by the US DOE under contract DE-FG22-92PC92104. We thank Mr. W. E. Harrison III of Wright Laboratory/Aero Propulsion and Power Directorate, Wright-Patterson AFB and Dr. S. Rogers of U.S. DOE for many helpful discussions.

## REFERENCES

- Heneghan, S. P., Zabarnick, S., Ballal, D. R., Harrison III, W. E., in *Proceedings 34<sup>th</sup> Aerospace Sciences Meeting & Exhibit*, Nevada, USA, 1996, AIAA Paper No 96-0403.
- Boehm, H. P., *Carbon*, 1994, 32, 759.
- Eser, S., *Carbon*, 1996, 34, 539.
- Eser, S., Gergova, K., Arumugam, R., and Schobert, H. H., in *Proceedings Carbon '92*, Essen, Germany, Paper E11, 1992, p. 519.
- Gergova, K., Eser, S., Arumugam, R. and Schobert, H. H., in *Proceedings of the 5<sup>th</sup> International Conference on Stability and Handling of Liquid Fuels*, Rotterdam, the Netherlands, 1994, p.227.
- Gergova, K., Arumugam, R., Chang, P. and Eser, S., *Preprints ACS Div. Pet Chem.*, New Orleans, USA, 1996, 41(2), p.513.
- Szymanski, G. S. and Rychlicki, G., *Carbon*, 1993, 31, 247.
- Grunewald, G. C. and Drago, R. S., *J. Mol. Catal.*, 1990, 58, 227.

Table 1. Surface functional groups of different carbons.

	PX21, meq/g	FW200, meq/g	5562AC, meq/g	Acid treated 5562AC, meq/g
All Basic Groups	0.40	0	0.48	0.3
All Acidic Groups	3.3	3.3	0.65	2.1
Carboxyl	1.1	1.3	0	0.52
Lactone	1.9	1.6	0	0.86
Phenolic	0.1	0.1	0.2	0.12
Carbonyl	0.2	0.3	0.45	0.60

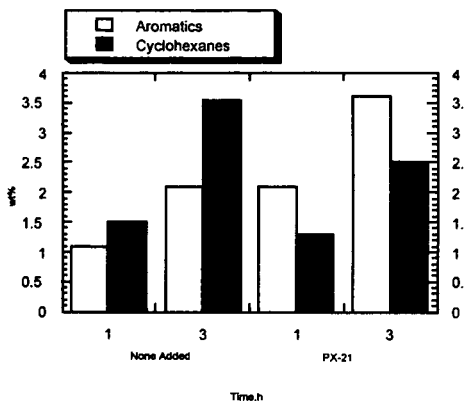


Figure 1. The concentrations of aromatics and cycloalkanes in the liquid products from the thermal decomposition of n-dodecane with/without PX-21.

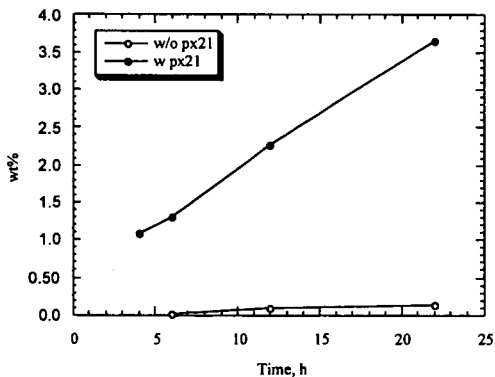


Figure 2. Benzene concentration in the liquid products from the thermal decomposition on cyclohexane with/without PX-21.

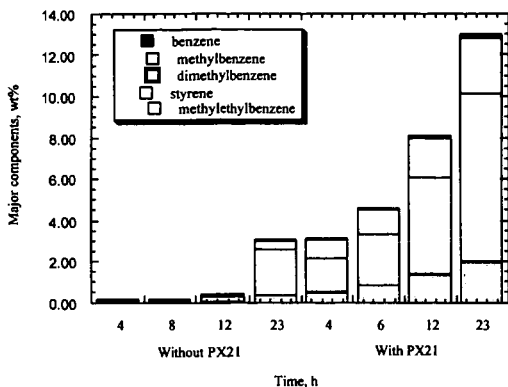


Figure 3. Concentrations of major components in the liquid products from the thermal decomposition of ethylbenzene with/without PX-21.

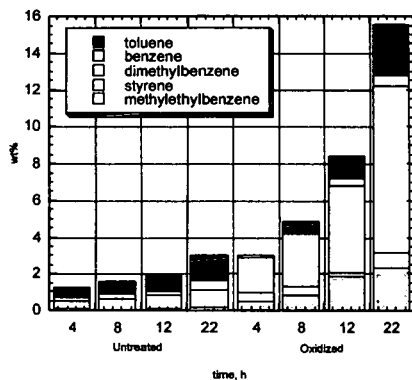


Figure 4. Major components from ethylbenzene pyrolysis with untreated/oxidized 5562AC.

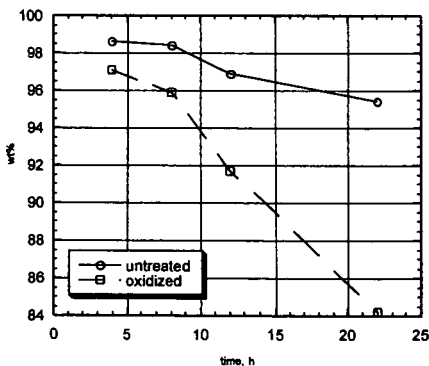


Figure 5. Ethylbenzene concentration from ethylbenzene pyrolysis with untreated/oxidized 5562AC.

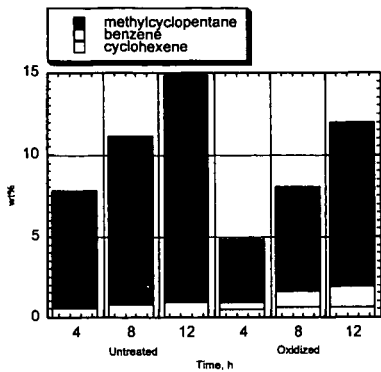


Figure 6. Major components from cyclohexane pyrolysis with untreated/oxidized 5562AC

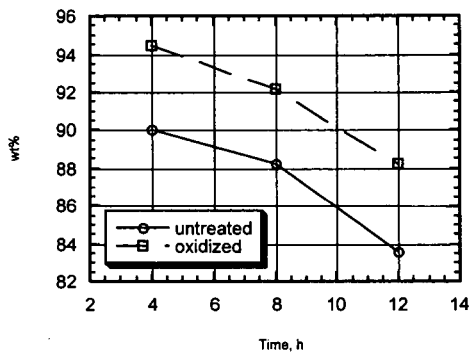


Figure 7. Ethylbenzene concentration from ethylbenzene pyrolysis with untreated/oxidized 5562AC.

## USE OF MATHEMATICAL EXPRESSIONS FOR THE ESTIMATION OF SELECTED DIESEL FUEL PROPERTIES

D. Karonis, E. Lois, S. Stourmas, F. Zannikos  
National Technical University of Athens  
Laboratory of Fuels and Lubricants Technology  
Iron Polytechniou 9, Athens 157 80, Greece

### ABSTRACT

Mathematical expressions are presented, which predict some of the most important properties of diesel fuels. The experiments were performed using a fuel matrix of 128 gas oils, which covered the cetane index range 23-62. Although other parameters were also considered, the majority of the predictions were based on the distillation curve and the density of the fuels. Very good predictions were obtained for the aniline point, the kinematic viscosity at 40 °C, and for the fuels' aromatic content. The adjusted correlation coefficients in all cases is over 0.96.

### LIST OF SYMBOLS

a,b,c,d,e,f,g,h,i	constants
ANIL	aniline point (°C)
AROM	aromatic content of the fuel (vol %)
DENS	fuel density (g/mL at 15 °C)
D <sub>10</sub>	distillation temperature for the 10% vol. of the fuel (°C)
D <sub>50</sub>	distillation temperature for the 50% vol. of the fuel (°C)
D <sub>90</sub>	distillation temperature for the 90% vol. of the fuel (°C)
FBP	final boiling point of the fuel (°C)
p	probability, the t-test to give a number equal or higher than t-ratio
R <sup>2</sup>	correlation coefficient
R <sup>2</sup> <sub>adj</sub>	adjusted correlation coefficient
S	sulphur content of the fuel (wt %)
s	standard deviation

### Greek Letters

$\nu_{40}$	kinematic viscosity (cSt at 40 °C)
------------	------------------------------------

### INTRODUCTION

The properties of the gas oil streams in a modern refinery, vary widely, depending on the nature of the feedstock and the operating conditions. Straight atmospheric or cracking processes produce gasoils with properties that usually do not meet commercial specifications. Critical properties, such as the ignition quality, expressed with the cetane number increasingly become more severe, mainly for environmental reasons. Following production, the quality of the final gas oil products (diesel fuel) is adjusted by blending various gas oil streams in adequate quantities.

Modern blending processes need mathematical expressions that can predict accurately the amounts of each component to be blended, in order to meet the specifications of the market. The traditional use of tables and nomograms from the refineries for the estimation of the fuel blend properties, cannot satisfy the needs of the automated processes used in modern blending facilities [1-3]. Therefore, it would be desirable to find mathematical expressions for the most important specifications, using such parameters as the fuel distillation curve and density.

In the past, several investigators tried to identify the impact of the various fuel properties, either on the engine operating conditions or on emissions. The cetane number, as measured in a standard CFR engine, is the most significant property of diesel fuels, and for calculation purposes it can be approximated by the calculated cetane index [4-6]. The diesel fuel aromatic content, a property usually determined using chromatographic methods was found to correlate well with emissions from diesel engines [7-12]. The aniline point is related to the ignition quality of diesel

fuels through the diesel index [13, 14]. The kinematic viscosity is related to particulate emissions and performance of diesel engines, because of its impact on the droplet size distribution of the fuel at the injection system [15,16].

This work is an effort to present reliable mathematical expressions for the fuel's aromatic content, aniline point, and kinematic viscosity mainly using data from the distillation curve and the density.

### EXPERIMENTAL SECTION

Sixteen gasoils with different properties were used as base fuels in this course of experiments, with their cetane index in the range of 23-62. They included straight run fuels from atmospheric distillation and cracking processes, i.e. light cycle oil from a fluid catalytic cracking unit and gasoils from visbreaker and hydrocracker. From these base fuels, 120 blends were prepared, covering a large spectrum of specifications that reflect both current and future trends. The properties of the total 126 fuels (base fuels and their mixtures), are listed in Table 1. All measurements were done according to the appropriate ASTM procedures.

### STATISTICAL ANALYSIS

The data of the various fuel properties were analysed using standard statistical techniques. For each property, the parameters considered were the standard deviation  $s$ , the correlation coefficient  $R^2$ , and the adjusted correlation coefficient  $R^2_{adj}$ , which gives a more accurate behaviour of the model used. Each expression was tested through the t-test and probability number  $p$ , to ensure that only significant terms are used in the mathematical expressions [17]. All statistical parameters of the fuel properties considered in this paper, are listed in Table 2.

### ESTIMATION OF THE KINEMATIC VISCOSITY

The kinematic viscosity of the fuel  $\nu$ , was determined at 40 °C. The best results were obtained from the following equation:

$$\nu_{40} = a \cdot \text{DENS} + b \cdot \text{DENS}^2 + c \cdot D_{10}^2 + \frac{d}{D_{10}} + e \cdot D_{50}^2 + \frac{f}{D_{50}^2} + g \cdot D_{90}^2 + \frac{h}{D_{90}} + i \quad (1)$$

Statistical parameters are given in Table 2. The results are depicted in Figure 1, where it can be seen that most of the points are close to the diagonal.

### ESTIMATION OF THE ANILINE POINT

Aniline point is a simple procedure that gives an indication of the aromatic content of the fuel. The proposed equation for the aniline point is given below:

$$\text{ANIL} = a \cdot \text{DENS} + b \cdot (e^{-3.5 \cdot (\text{DENS} - 0.85)} - 1) + c \cdot (D_{10} - 215) + d \cdot (D_{10} - 215)^2 + e \cdot (D_{30} - 260) + f \cdot (D_{90} - 310) + g \cdot (D_{90} - 310)^2 + h \cdot S^2 + i \quad (2)$$

In this case all variables have very high t-ratios and p-values equal to zero. The statistical parameters are given in Table 2. This means that all the predictor variables are significant. The results are given graphically in Figure 2.

### ESTIMATION OF THE AROMATIC CONTENT

The aromatic content for diesel fuels is an important property since it affects both the density and the resulting emissions. The experimental determination of this specification requires special columns and it takes several hours to complete, ASTM D1319. Chromatographic techniques such as HPLC and SFC are also employed, but their instrumentation is very expensive. Modern techniques as FTIR give fast and good results. A mathematical expression for the calculation of aromatic content would be attractive. The following equation was found to give very good results:

$$\text{AROM} = a \cdot \text{DENS}^2 + b \cdot D_{10}^2 + \frac{c}{D_{10}} + \frac{d}{D_{50}} + e \cdot D_{90}^2 + \frac{f}{D_{90}} + g \cdot \text{ANIL}^2 + h \cdot S^2 + i \quad (3)$$

In Table 2 are given the statistical parameters of the above equation. Graphical representation of the results shows that practically all the points are very well behaved, Figure 3.

### CONCLUSIONS

Mathematical expressions which predict some important properties of diesel fuels have been experimentally determined, using a fuel matrix of 128 base fuels and blends. Very good predictions were obtained for the kinematic viscosity at 40 °C, the aniline point and the aromatic content. In all cases the adjusted correlation coefficients were just less than unity. These expressions can be used for a very accurate prediction of the actual values of these properties, when they cannot be measured directly.

### ACKNOWLEDGEMENTS

The authors would like to thank Hellenic Aspropyrgos Refineries, Athens, Greece and Motor Oil Hellas Refineries, Athens, Greece, for supplying the gasoils that were used in this study.

### REFERENCES

- [1] Lois, E.; Stournas, S.; Karonis, D. Mathematical Expressions of Some Nonadditive Properties of Gas Oil-Residual Fuel Blends. *Energy and Fuels*. 1991, 5, 855.
- [2] Obert, E. F. *Internal Combustion Engines and Air Pollution*; 3rd Edition, Intext Educational Publishers: New York, 1973.
- [3] Diesel Fuels - SAE J313, SAE Handbook, 1992, Jun 89, 3.
- [4] Standard Method for Ignition Quality of Diesel Fuels by the Cetane Method; ASTM D-613, 1996.
- [5] Standard Method for Calculated Cetane Index of Distillate Fuels; ASTM D-976, 1993.
- [6] Standard Test Method for Calculated Cetane Index by Four Variables Equation; ASTM D-4737, 1996.
- [7] Aromatic Hydrocarbon Types in Diesel Fuels and Petroleum Distillates by High Performance Liquid Chromatography with Refraction Index Detection; IP 391/90, 1996.
- [8] Standard Method for Hydrocarbon Type Analysis in Liquid Petroleum Products by Fluorescent Indicator Adsorption; ASTM D-1319, 1996.
- [9] Standard Test Method for Determination of Aromatic Content of Diesel Fuels by Supercritical Fluid Chromatography; ASTM D-5186, 1996.
- [10] Li, X.; Chippior, W. L.; Gülder, Ö, L. Effects of Cetane Enhancing Additives and Ignition Quality on Diesel Engine Emissions. SAE Paper 972968, 1997.
- [11] Lange, W. W.; Cooke, J. A.; Gadd, P.; Zürner, H. J.; Schlögl, H.; Richter, K. Influence of Fuel Properties on Exhaust Emissions from Advanced Heavy-Duty Engines Considering the Effect of Natural and Additive Enhanced Cetane Number. SAE Paper 972894, 1997.
- [12] Ryan III; T. W., Erwin, J. Effects of Fuel Properties and Composition on the Temperature Dependent Autoignition of Diesel Fuel Fractions. SAE Paper 922229, 1992.
- [13] Standard Test Method for Aniline Point and Mixed Aniline Point of Petroleum Products and Hydrocarbon Solvents; ASTM D-611, 1996.
- [14] Diesel Index; IP 21, 1991.
- [15] Standard Test Method of Kinematic Viscosity of Transparent and Opaque Liquids; ASTM D-445, 1996.
- [16] Owen, K.; Colley T. *Automotive Fuels Handbook*; SAE, Warrendale, PA, 1991.
- [17] Ryan, B.; Joiner, B.; Ryan, T. *Minitab Handbook*; 2nd Edition, PWS-KENT Publishing Company: Boston, 1992.

Table 1. Fuel Properties

Cetane Index	IBP (°C)	D <sub>10</sub> (°C)	D <sub>50</sub> (°C)	D <sub>90</sub> (°C)	FBP (°C)	Density 15°C (g/ml)	V <sub>40</sub> (cst)	Autiline Point (°C)	Aromatic Content (% vol)	Total Sulfur (% wt)
23.5	188	250	288	346	372	0.9550	3.85	20.9	73.0	1.82
24.3	154	242	276	341	369	0.9510	3.21	1.4	77.4	0.33
26.0	166	238	275	344	368	0.9420	3.16	7.0	74.3	0.30
27.0	185	235	274	340	366	0.9330	3.11	12.4	71.1	0.27
27.2	191	239	285	347	369	0.9330	3.62	19.8	69.4	0.28
27.3	190	249	290	355	372	0.9403	3.79	27.9	67.5	1.64
28.4	188	233	272	337	364	0.9240	3.06	17.5	67.9	0.24
28.6	188	252	288	347	373	0.9326	3.75	32.0	61.3	1.53
29.0	180	242	293	370	380	0.9346	3.85	20.4	65.8	0.34
30.2	193	233	270	334	360	0.9150	3.01	22.6	64.8	0.21
31.1	196	232	269	333	357	0.9060	2.96	27.6	61.6	0.18
32.4	194	247	296	354	369	0.9154	4.20	36.5	61.1	0.24
32.7	195	251	287	334	363	0.9100	3.64	43.0	51.9	1.22
34.0	205	252	290	356	382	0.9136	3.99	44.2	52.2	1.29
34.2	198	232	268	331	355	0.8970	2.92	32.1	58.5	0.15
35.8	185	228	254	332	361	0.8889	2.99	43.2	43.8	1.05
36.0	198	231	267	326	351	0.8880	2.87	36.8	55.4	0.12
36.8	189	247	287	338	361	0.8930	3.57	50.4	45.0	0.97
36.9	201	250	304	358	373	0.9012	4.78	46.8	54.2	0.19
37.5	185	225	257	337	369	0.8827	2.84	48.4	41.1	1.11
37.6	206	254	292	357	385	0.9012	4.07	50.6	46.3	1.12
38.3	200	230	267	323	348	0.8790	2.83	41.3	52.2	0.09
39.2	190	249	307	359	379	0.8941	4.91	55.1	52.2	0.18
40.2	185	223	262	353	369	0.8757	3.08	52.8	38.2	1.18
40.6	200	239	265	319	348	0.8700	2.78	45.9	49.0	0.05
40.8	206	255	294	357	383	0.8905	4.25	56.6	41.1	0.95
41.6	186	220	265	337	379	0.8706	3.17	55.0	45.9	1.25
42.9	198	227	265	313	344	0.8610	2.77	50.2	45.9	0.02
43.7	183	214	272	368	373	0.8642	3.42	58.5	32.2	1.32
43.8	185	218	272	363	376	0.8642	3.42	58.5	32.1	1.32
44.0	188	243	284	321	347	0.8691	3.48	60.3	33.8	0.64
44.1	206	256	295	359	386	0.8810	4.35	61.2	36.3	1.23
44.2	183	209	275	368	379	0.8618	3.50	60.8	30.7	1.35
44.5	185	215	275	368	379	0.8618	3.50	60.8	30.9	1.35
44.5	165	251	296	351	369	0.8771	4.01	59.1	38.1	0.12
44.7	196	229	268	323	353	0.8595	2.97	53.4	43.1	0.02
44.8	198	229	268	314	341	0.8578	2.85	53.8	42.3	0.05

Table 1. Fuel Properties (Continued)

Cetane Index	IBP (°C)	D <sub>10</sub> (°C)	D <sub>50</sub> (°C)	D <sub>90</sub> (°C)	FBP (°C)	Density 15°C (g/ml)	V <sub>40</sub> (cst)	Autiline Point (°C)	Aromatic Content (% vol)	Total Sulfur (% wt)
45.7	202	230	266	320	345	0.8561	2.80	55.1	41.2	0.03
45.8	182	210	284	365	375	0.8511	3.14	62.7	26.5	1.15
46.2	194	231	272	329	360	0.8580	3.11	56.4	40.0	0.02
46.5	185	215	284	372	385	0.8592	3.72	62.4	29.3	1.39
46.5	197	231	272	314	340	0.8550	2.93	56.9	39.1	0.07
46.7	219	257	316	362	381	0.8772	5.65	60.5	44.2	0.13
47.1	199	247	297	352	373	0.8691	4.11	63.8	32.8	0.18
47.5	208	257	297	340	386	0.8720	4.43	65.4	31.9	0.69
47.5	188	219	251	346	369	0.8459	2.8	65.2	23.5	0.91
47.5	206	231	265	321	347	0.8511	2.83	59.7	36.6	0.03
47.7	158	254	299	352	371	0.8701	4.13	65.4	33.9	0.10
47.8	225	268	327	371	384	0.8752	6.35	66.0	38.3	0.20
48.1	210	259	314	362	381	0.8742	5.29	61.9	42.1	0.12
48.1	194	235	278	338	363	0.8565	3.32	60.0	37.2	0.02
48.5	196	234	276	314	338	0.8518	3.02	60.6	35.5	0.10
48.5	188	225	261	355	388	0.8472	2.98	63.7	24.8	0.56
48.9	194	220	244	324	367	0.8355	2.45	64.5	20.5	0.66
48.9	182	210	284	365	375	0.8511	3.14	62.7	26.4	1.15
49.0	189	225	257	351	394	0.8435	2.88	64.1	23.4	0.92
49.0	214	261	302	360	386	0.8704	4.48	67.2	30.6	0.63
49.2	191	220	238	256	322	0.8247	2.06	65.6	16.2	0.28
49.4	195	220	240	270	354	0.8274	2.23	65.2	17.7	0.41
49.4	192	237	282	340	366	0.8550	3.56	63.0	34.2	0.02
49.4	203	232	264	323	347	0.8462	2.87	64.3	32.3	0.04
49.6	202	252	305	360	375	0.8638	4.67	68.7	29.2	0.27
49.6	191	225	252	346	391	0.8396	2.62	64.4	22.0	0.79
49.7	195	235	278	314	336	0.8500	3.08	62.7	33.1	0.11
49.8	195	226	246	333	395	0.8357	2.46	64.7	20.5	0.69
49.8	197	222	238	256	322	0.8239	2.06	65.6	16.2	0.28
50.2	191	224	246	359	381	0.8336	2.92	69.6	16.8	0.16
50.5	205	231	269	369	385	0.8462	2.58	73.8	18.9	0.17
50.5	170	257	300	354	373	0.8641	4.25	65.5	31.6	0.08
50.7	206	259	301	360	386	0.8650	4.55	69.8	28.1	0.36
50.9	190	239	287	342	368	0.8535	3.76	66.2	31.4	0.03
50.9	197	224	237	248	265	0.8200	1.94	66.4	14.7	0.15
50.9	209	258	299	361	388	0.8638	4.51	68.6	27.8	0.38
51.1	180	221	272	342	368	0.8430	3.16	68.6	28.0	0.28

Table 1. Fuel Properties (Continued)

Cetane Index	IBP (°C)	D <sub>16</sub> (°C)	D <sub>50</sub> (°C)	D <sub>80</sub> (°C)	FBP (°C)	Density @ 15°C (g/ml)	viscosity (cSt)	ANiline Point (°C)	Aromatic Content (% vol)	Total Sulfur (% wt)
51.4	195	236	281	314	334	0.8475	3.15	65.3	30.5	0.13
51.6	205	227	241	257	301	0.8225	2.03	67.4	14.9	0.19
51.6	208	235	263	270	301	0.8412	2.90	68.9	27.6	0.05
51.6	198	228	240	270	354	0.8226	2.23	65.2	17.6	0.41
51.9	205	229	242	278	377	0.8282	2.18	67.8	15.2	0.18
52.0	165	214	279	349	372	0.8420	3.28	70.2	22.5	-
52.1	204	238	263	327	391	0.8404	3.33	72.4	16.7	0.26
52.1	228	274	333	375	388	0.8732	7.20	71.3	32.0	0.26
52.2	201	236	275	375	392	0.8452	3.77	73.8	17.2	0.30
52.4	214	237	254	368	390	0.8349	2.83	71.8	16.2	0.23
52.4	196	234	246	352	385	0.8302	2.49	68.2	15.7	0.22
52.4	187	219	268	333	359	0.8374	2.88	68.0	27.8	0.12
52.9	207	235	282	343	364	0.8460	3.57	70.1	24.1	0.28
53.0	203	239	273	337	358	0.8432	3.22	70.2	26.4	0.04
53.1	193	239	283	314	332	0.8451	3.23	67.9	27.7	0.16
53.2	188	247	292	348	370	0.8520	3.98	69.0	28.5	0.03
53.3	207	241	285	377	395	0.8475	4.07	75.2	17.4	0.32
53.8	195	230	267	290	302	0.8335	2.62	66.8	24.6	0.78
54.0	202	234	256	301	327	0.8303	2.57	69.0	18.5	0.18
54.1	210	259	299	365	390	0.8561	4.61	77.6	18.2	0.24
54.1	198	248	301	354	373	0.8530	4.52	72.2	23.2	0.15
54.2	195	243	282	345	361	0.8451	3.59	71.8	25.1	0.04
54.5	161	259	301	355	374	0.8554	4.41	71.0	26.0	0.05
54.7	191	244	284	314	331	0.8431	3.29	70.2	25.4	0.25
54.8	186	251	296	349	370	0.8505	4.26	71.6	25.6	0.03
54.8	210	244	334	370	385	0.8589	4.02	76.8	21.0	0.17
55.0	204	241	302	378	392	0.8492	4.43	75.4	17.7	0.32
55.1	186	238	270	311	330	0.8355	2.27	70.6	20.6	0.19
55.4	202	235	270	297	309	0.8350	2.71	70.3	19.2	0.62
55.6	186	248	293	351	367	0.8471	4.23	73.1	23.9	0.03
55.6	198	225	253	273	282	0.8213	2.24	66.5	20.3	0.68
55.9	195	238	279	309	328	0.8370	3.06	70.6	22.5	0.09
56.0	232	290	340	380	390	0.8712	8.16	76.7	25.7	0.33
56.0	212	254	303	353	380	0.8510	4.60	72.8	25.3	1.07
56.1	218	252	297	353	379	0.8483	4.16	74.3	20.5	0.89
56.3	225	270	320	364	385	0.8597	5.81	77.2	21.2	1.01
56.5	210	254	305	367	390	0.8505	4.57	73.8	23.1	0.15

Table 1. Fuel Properties (Continued)

Cetane Index	IBP (°C)	D <sub>16</sub> (°C)	D <sub>50</sub> (°C)	D <sub>80</sub> (°C)	FBP (°C)	Density @ 15°C (g/ml)	viscosity (cSt)	ANiline Point (°C)	Aromatic Content (% vol)	Total Sulfur (% wt)
56.9	185	252	290	324	350	0.8431	3.60	72.8	23.0	0.15
57.1	184	255	293	335	356	0.8451	3.87	73.3	22.9	0.11
57.1	211	250	291	341	366	0.8432	3.69	71.2	22.1	1.00
57.2	180	260	300	353	369	0.8490	4.55	-	22.6	0.07
57.2	183	258	289	346	364	0.8470	4.19	73.9	22.7	0.03
57.6	188	249	285	313	329	0.8411	3.36	72.2	23.1	0.19
57.6	214	263	304	346	368	0.8500	4.51	72.8	22.6	1.23
57.8	194	260	305	360	388	0.8493	4.44	74.8	22.0	0.25
58.5	231	286	338	383	405	0.8662	7.85	77.2	23.4	0.20
58.8	221	281	324	363	385	0.8586	5.96	75.2	26.4	1.18
59.2	195	235	270	295	306	0.8252	2.81	74.6	17.5	0.03
59.9	216	285	335	380	397	0.8603	6.35	78.6	20.8	0.34
60.6	207	254	304	362	392	0.8410	4.53	81.0	18.6	0.08
61.5	239	312	351	382	390	0.8692	9.33	81.9	19.6	0.40
62.8	222	276	325	375	398	0.8489	6.12	83.4	19.2	0.09

Table 2. Statistical Parameters of Estimating Equations

Parameter	Equation (1)	Equation (2)	Equation (3)
a	124.080E+0	-12.248E+2	83.020E+0
b	-69.740E+0	-20.747E+1	24.970E-4
c	18.222E-5	38.215E-2	70.080E+2
d	38.601E+2	-24.400E-4	-11.009E+3
e	6.760E-5	12.106E-2	-32.528E-5
f	152.261E+3	55.730E-3	-19.659E+3
g	2.580E-5	87.490E-5	-71.388E-4
h	10.611E+2	34.537E-1	42.522E-1
i	-91.250E+0	10.945E+2	93.290E+0
s	2.472E-1	2.481E+0	1.654E+0
R <sup>2</sup>	9.620E-1	9.780E-1	9.890E-1
R <sup>2adj</sup>	9.590E-1	9.770E-1	9.880E-1

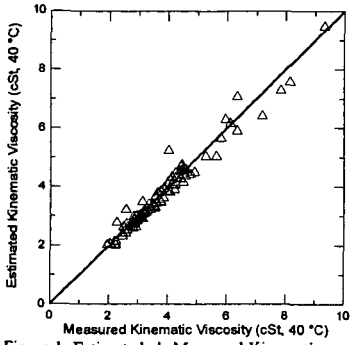


Figure 1. Estimated v's Measured Kinematic Viscosity

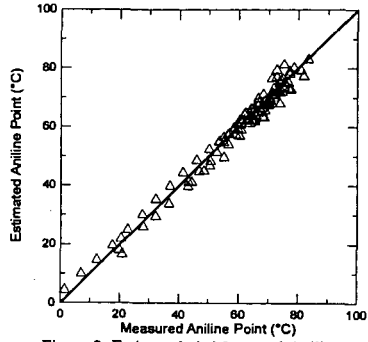


Figure 2. Estimated v's Measured Aniline Point

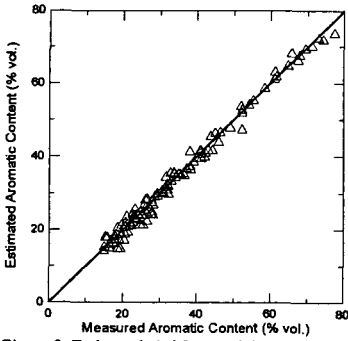


Figure 3. Estimated v's Measured Aromatic Content

# CHARACTERIZATION OF AUTO-OXIDATION PRODUCTS OF AVIATION JET FUELS BY GAS CHROMATOGRAPHY COUPLED WITH MASS SPECTROMETRY

Jouni Enqvist (1), Esko Ranta (2) and Maarit Enqvist (3)

(1) VTT Chemical Technology, P.O.Box 1402, SF-33101 Tampere, Finland, (2) Laboratory of Organic Chemistry, P.O.Box 55, FIN-00014 University of Helsinki, (3) J&M Group Ky, P.O.Box 61, FIN 33961 Pirkkala, Finland

## ABSTRACT

Hydroperoxides are important products in the liquid phase oxidation reactions of jet fuel hydrocarbons. For better understanding of the reasons for the differences in oxidative stability between different jet fuels, it would be useful to monitor the formation of oxidation products, especially hydroperoxides, from individual hydrocarbons. In this work, hydroperoxides were analyzed from fresh, long-time stored and high temperature oxidized jet fuel samples. The analytical procedure includes extraction of the hydroperoxides into deionized water, re-extraction into diethyl ether, subsequent trimethyl silylation and GCMS analysis. Tentative identification of two isomeric cymene hydroperoxides, the tetralin 1-hydroperoxide, isomeric methylindan hydroperoxides, and higher molecular weight substituted tetralin and indan hydroperoxide trimethylsilyl derivatives was obtained. Assignment of individual hydroperoxide isomers was not possible by mass spectra.

## INTRODUCTION

Development of the aircraft and particularly of the jet engines seems to place more and more demands on the heat-sink efficiency of the jet fuel. The hydrocarbon mixture should resist higher fuel system component temperatures without thermal oxidative degradation or pyrolysis. Strategic long-term storing, also, places high demands for auto-oxidative and microbial degradation resistance of fuels.

Hydroperoxides are the principal primary auto-oxidation products of most hydrocarbons.<sup>1</sup> Oxidative degradation of jet fuel, which may appear as development of gums and insoluble deposits, unpredictable changes in lubricity, increased corrosiveness, poor water separation properties etc., correlates strongly with the formation of hydroperoxides, at least as intermediates. Soluble oxygen containing products may have useful effects on formation of boundary lubrication films chemically bonded on fuel system surfaces like the friction surfaces of fuel pumps but small amount of insoluble small molecular weight or polymeric secondary products may be harmful by causing fouling of critical engine components like fuel nozzles, augmentors etc. If the role of each oxidation-susceptible molecule in the degradation of the jet fuel could be understood, modifications of the refinery processes or design of more specific antioxidants could be possible, which in turn would result in better thermal and long term stability for the fuel.

Standard jet fuel oxidation tests do not give information about which individual chemical compounds are oxidized most rapidly. A jet fuel is comprised of at least hundreds of saturated paraffin, alicyclic (naphthenic) and aromatic hydrocarbons and may also contain some unsaturated olefinic hydrocarbons and trace amounts of sulfur, oxygen and nitrogen compounds. It is known that olefinic and several aromatic hydrocarbons oxidize much more rapidly than the saturated hydrocarbons. However, there is deficiency of even qualitative information about the individual products formed in oxidative degradation of jet fuels.

Direct detection of individual hydroperoxides and other oxidation products in a jet fuel is very difficult due to the complexity of the product mixtures and low concentration of each product. On the other hand, hydroperoxides are labile compounds and often decompose rapidly at optimal temperatures for GCMS analysis<sup>2</sup> or when treated with acids or bases.<sup>3</sup> Analysis of hydroperoxides by GCMS generally requires derivatization or other conversion into more thermally stable compounds.<sup>4</sup>

The objectives of this investigation were 1) to develop a practical method for the enrichment of hydroperoxides from oxidized jet fuels, and 2) to characterize the molecular structures of the enriched hydroperoxides by conversion into thermally stable derivatives followed by GCMS analysis. The aim of this article is to describe an analytical procedure for hydroperoxides based on water extraction of oxidized fuel samples followed by trimethyl silylation

of the hydroperoxide -OOH groups to the more stable -OOSi(CH<sub>3</sub>)<sub>3</sub> groups<sup>4</sup> and application of GCMS technique for characterization of molecular structures of the most abundant hydroperoxides found in differently oxidized Jet A-1 samples.

## EXPERIMENTAL

*Materials.* A fresh and differently oxidized Jet A-1 fuel samples were treated by procedures described below to obtain samples for GCMS analysis of hydroperoxides as their corresponding peroxytrimethylsilanes. One Jet A-1 sample (obtained from Sabena Airlines Depot, Brussels Airport, Belgium) was allowed to stand 2.5 years at room temperature in a sealed glass flask which was occasionally opened to air (to take samples for NMR). A 10 ml sample of this was extracted once with 50 ml of deionized water. The extract was then allowed to evaporate into dryness at room temperature. The evaporation residue was trimethylsilylated as described below to obtain Sample 1.

Other samples were a 100 ml fresh Jet A-1 (obtained from Finnish Air Force, Satakunnan lennosto, Tampere, Finland), a 50ml Jet A-1 sample oxidized 24 hours at reflux under oxygen atmosphere and a similarly oxidized 50 ml sample of a Jet A-1 sample that had been extracted three times with identical volume of deionized water. The corresponding GCMS samples (Sample 2, Sample 3 and Sample 4) were obtained as described below.

Jet A-1 samples (except the aged one) was extracted three times with identical volume of deionized water, the water phases were combined, saturated with sodium chloride (p.a., Riedel-De Haen, Seelze, Germany) and extracted three times with one third volume of diethyl ether (glass distilled grade, Rathburn, Walkerburn, UK). Ether phases were combined and ether was evaporated with rotatory evaporator. 50 ml acetone (nanograde, Mallinckrodt, Paris, Kentucky, USA) was then added and evaporated with rotatory evaporator to dry the residue.

*Derivatization and GCMS analysis.* Trimethylsilylation: a 100  $\mu$ l sample (for Sample 3 and Sample 4) or the whole evaporation residue (for Sample 1 and Sample 2) was mixed with 100  $\mu$ l of BSTFA (Merck, Darmstadt, Germany) and 1 ml of toluene (nanograde, Mallinckrodt, USA) or diethyl ether (for Sample 1) was then added. At least two hours of reaction was allowed prior to analysis by GCMS. Analyses were conducted with a GC (HP 5890) equipped with a quadrupole mass selective detector (HP 5970A series). For all analyses the EI electron energy was 70 eV and the ion source temperature 280 °C. All samples were introduced as 1.0  $\mu$ l aliquots by autosampler. Sample 1 was analyzed with a 25 m x 0.2 mm capillary column (HP-1, polydimethylsiloxane, 0.11  $\mu$ m film thickness), 90 °C injector temperature, split injection at 1:8.4 split ratio, and scan range from 30 to 300 amu. The temperature program for Sample 1 was 4 min at 60 °C, then to 200 °C at 5 °C/min, then to 280 °C at 20 °C/min, and 3 min hold at 280 °C. Sample 2, Sample 3 and Sample 4 were analyzed with a 30 m x 0.2 mm capillary column (RTx-200, trifluoropropylmethyl polysiloxane, 0.10  $\mu$ m film thickness), 200 °C injector temperature in splitless injection mode. For these samples the temperature program was 1.0 min at 70 °C, then to 120 °C at 2 °C/min, then to 200 °C at 4 °C/min and then to 280 °C at 8 °C/min, and the mass analyzer was scanned from 33 to 300 amu the first 10 min and from 33 to 500 amu the rest of the analysis time.

## RESULTS AND DISCUSSION

Extraction into water was found to be a useful method for the isolation of hydroperoxides from hydrocarbons of the jet fuel. Many other oxidation products were also water extractable, and the extracts from the oxidized samples were actually quite complicated mixtures, especially those that were oxidized at high temperature (Sample 3 and Sample 4). On the other hand, the yield of the extraction from the fresh Jet A-1 sample (Sample 2) was so low that individual components could not be identified due to low signal to noise ratio (data not shown). Analysis of Sample 2 thus confirmed that the water extractables of the oxidized Jet fuel samples were essentially oxidation products. The water extraction for Sample 4 differed from the other samples in that considerable amount of insoluble gum was formed when water was added into oxidized mixture.

There may have been decomposition of hydroperoxides in the water extracts due to presence of carboxylic acids that were detected among the oxidation products. Partially because of this possibility, Sample 2, Sample 3 and Sample 4 were immediately re-extracted into diethyl ether. The other reason for the re-extraction was that azeotropic evaporation with water of some extracted components was detected in early experiments. Evaporation of diethyl ether can also be

done rapidly at a low temperature. Removal of the residual moisture by azeotropic distillation with acetone has the same benefits.

The effectiveness of the silylation reagent BSTFA was tested with cumene hydroperoxide (data not shown). MSTFA has been successfully used for trimethylsilylation of cumene hydroperoxide<sup>4</sup> and the product obtained by using BSTFA was confirmed to be the same by comparing the mass spectra. No side products were detected and the reaction appeared to be complete within an hour.

The trimethylsilyl derivatives of hydroperoxides, or more shortly, peroxytrimethylsilanes seem to usually yield, at best, weak molecular ions by 70 eV EI ionization. Loss of the trimethylsilyloxy radical from molecular ion usually produces abundant  $[M - 105]^+$  ion.<sup>4</sup> Important lower mass fragments often appear at  $m/z$  values 89  $[C_3H_9SiO]^+$ , 75  $[C_2H_7SiO]^+$ , 73  $[C_3H_9Si]^+$ , 59  $[C_2H_7Si]^+$  and/or  $[CH_3SiO]^+$ , and 45  $[CH_3Si]^+$  and/or  $[HSiO]^+$ . Peak  $m/z$  91 which appears in EI mass spectra of cumylperoxytrimethylsilane and 1-tetralylperoxytrimethylsilane may have contribution from ion  $[C_2H_7SiO_2]^+$ .

TIC chromatogram of Sample 1 is represented in Figure 1. The most abundant analyte peaks in the chromatogram of Sample 1 correspond silylated products that have the fragmentation characteristics of peroxytrimethylsilanes. Examples of the mass spectra are represented in Figures 2 and 3. In Figure 3 there is also a reference spectrum of 1-tetralylperoxytrimethylsilane obtained by trimethylsilylation of tetralin hydroperoxide in an auto-oxidized tetralin sample. Mass spectrum in Figure 2 (RT 10.93 min) is interpreted to correspond a TMS derivative of an unknown isomer of cymene hydroperoxide. Peak assignments:  $M^+$  at  $m/z$  238,  $m/z$  133 (-105 amu, loss of trimethylsilyloxy radical),  $m/z$  119 ( $[CH_3C_6H_4CO]^+$  and/or  $[C_3H_9SiOOCH_2]^+$  and/or  $[CH_3C_6H_4CHCH_3]^+$ ), low mass ions as described in the previous paragraph. A TMS derivative of another isomer of cymene hydroperoxide at RT 11.78 min yielded almost identical mass spectrum (not shown). There are other significant analyte peaks in the TIC chromatogram of Sample 1 that are due to products that produce mass spectra consistent with peroxytrimethylsilanes with indan and tetralin ring structures up to molecular weight 264 which corresponds compounds with trimethylindan/dimethyltetralin moieties (data not shown).

Figure 1. TIC chromatogram of Sample 1

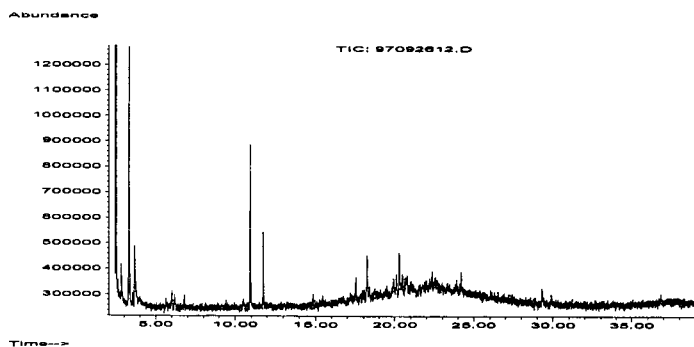


Figure 2. Mass spectrum of a compound (RT 10.93min) tentatively identified as a TMS derivative of an unknown isomer of cymene hydroperoxide.

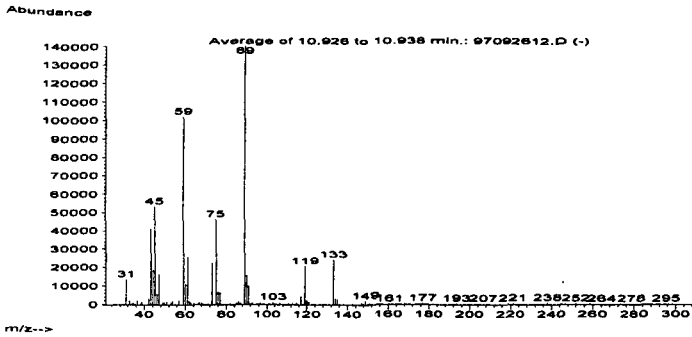
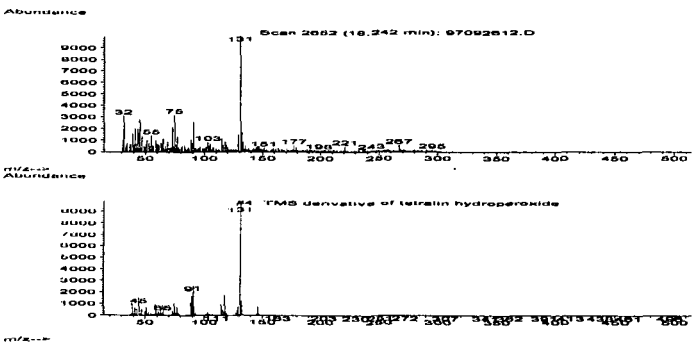


Figure 3. Mass spectra of a compound tentatively identified as tetralin hydroperoxide from Sample 1 and from an auto-oxidized tetralin sample.



TIC chromatogram of Sample 3 is represented in Figure 4. In this sample only one distinct peroxytrimethylsilane peak was detected (Figure 5), and it appeared to be a cymene hydroperoxide derivative. Many types of silylated and nonsilylated oxidation products were found in Sample 3. Among the most abundant peaks were those of TMS ethers of phenols (Figure 6) indicating that phenols are important oxidation products. The phenols are probably formed by decomposition of benzylic alkylbenzene hydroperoxides via hydrolytic mechanism catalyzed by carboxylic acids which were also detected among the oxidation products in Sample 3.

Figure 4. TIC chromatogram of Sample 3.

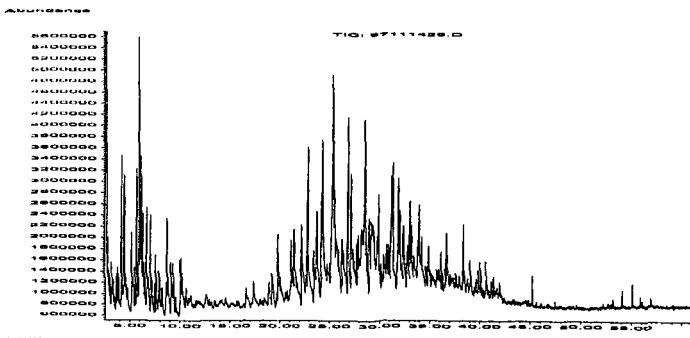


Figure 5. A partial TIC chromatogram of Sample 3. The peak at 5.5min is tentatively identified as a TMS derivative of an isomer of cymene hydroperoxide.

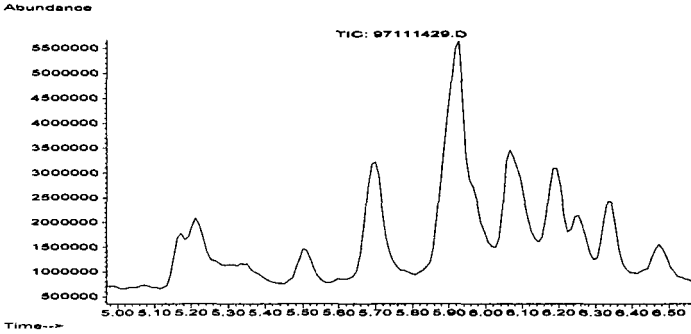
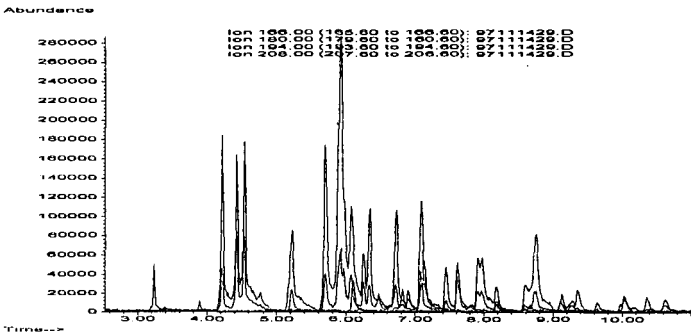


Figure 6. Reconstructed ion chromatograms showing the TMS derivatives of phenol (at 3.2 min), cresols (4.2-4.6 min), dimethyl- (or ethyl-) phenols (5.6-7.2 min), and trimethyl- (or isomeric) phenols in Sample 3.



TIC chromatogram of Sample 4 is represented in Figure 7. This sample consisted of larger variety of oxidation products than Sample 3. The water extracted fuel was clearly more severely degraded during the oxidation than the normal fuel and yielded more of water extract and insoluble products. The darkening of the water extracted jet fuel was also much stronger. The TMS derivative of the suggested cymene hydroperoxide peak present in Sample 3, was also present in Sample 4.

Figure 7. TIC mass chromatogram of Sample 4.

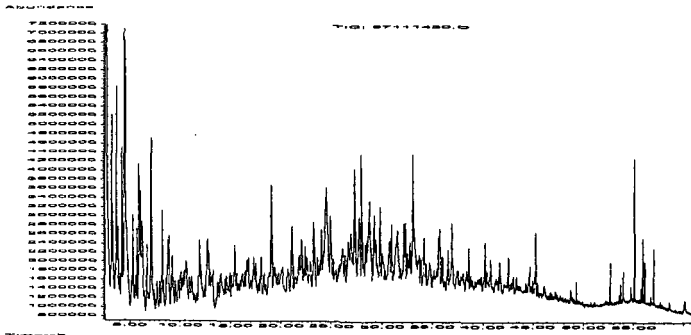


Table 1. Summary of the Experiments.

Samples	Oxidation Conditions	Results
<u>Sample 1:</u> Brussels Jet A-1 Oxidized as such	Two and a half years under air at ambient temperature	Several cymene, tetralin and indan hydroperoxides
<u>Sample 2:</u> Tampere Jet A-1 fresh	Not oxidized	No oxidation products could be identified due to low yield of extraction
<u>Sample 3:</u> Tampere Jet A-1 Oxidized as such	Refluxed 24 h under oxygen atmosphere.	Low on hydroperoxides, various other oxidation products, small amount of insolubles formed
<u>Sample 4:</u> Tampere Jet A-1 water extracted	Oxidized like sample 3	Dark brown product with deposits, oxidation products in the extract similar to as in Sample 3

The water extract of the fresh jet fuel served as the zero sample. The oxidation of the water extracted fuel produced a sample with the characteristics of heavily oxidized fuel, and indicated that separation of water may reduce the antioxidative resistency of Jet A-1 fuel and that presence of water may increase the amount of insolubles formed. The hydroperoxides formed during long-time storing are accumulated since they decompose slowly at low temperatures. In the water extract of the aged sample hydroperoxides were thus the main products. At fuel reflux temperatures the hydroperoxides were no more stable but mostly decomposed producing large variety of secondary products.

Jet fuel samples and oxidation procedures of this investigation are just examples of sample materials where analysis of individual hydroperoxides and other oxidation products could produce useful information about the chemical and tribological condition of the fuel in the molecular level. The four samples described in Table 1 represent examples of different crude oils, different refinery processes and different auto-oxidation conditions (oxidation time and temperature, presence and absence of antioxidant) that may be found in practical applications where determination of individual hydroperoxides would give useful information.

The present work by us is aimed for refinement of the GCMS method for quantitative determination of individual hydroperoxides with the emphasis of elucidation of molecular structures of the isomeric compounds by different spectroscopic techniques as well as characterization of secondary products.

Although all oxidation products cannot be analyzed by the method described, we believe that application of this method can result in better understanding of oxidative degradation and chemical change in long-term storing of middle distillate fuels in general. The method can be routinely applied to monitor of certain key hydroperoxides and other important oxidation products like phenols in the fuels. Effects of fuel additives into oxidation stability of the fuel can be now monitored in molecular level.

## REFERENCES

1. Nonhebel, D. C., and Walton, J. C. in *Free-radical chemistry*, University Printing House, Cambridge, 1974, p 393
2. Foglia, T. A., Silbert, L. S., and Vail, P.D., *Journal of Chromatography*, 637 (1993), p 157
3. Mageli, L. O., and Sheppard, C. S., in Swern D., (Editor), *Organic Peroxides*, Vol. 1, Wiley-Interscience, New York, 1970, Ch. 1, pp 19-20
4. Turnipseed, S. B., Allentoff, A. J., and Thompson, J. A., *Analytical Biochemistry*, 213 (1993) 218

## ACKNOWLEDGEMENTS

Jet fuel specialists at Finnish Air Force and Sabena Airlines Depot are acknowledged for the samples and useful discussions, and Neste Oy Foundation for the financial support.

## AUTOXIDATION OF DILUTED AVIATION FUELS

E. Grant Jones and Lori M. Balster  
Innovative Scientific Solutions, Inc.  
2786 Indian Ripple Road  
Dayton, OH 45440-3638

Keywords: Autoxidation, Fuel Blend

### INTRODUCTION

In addition to its role in combustion, aviation fuel serves as the primary heat sink for cooling component systems in military aircraft.<sup>1</sup> The efficiency of heat exchangers and the operation of many other critical fuel-line components can be compromised by fouling of surfaces caused by the accumulation of intractable gums. Products from autoxidation are the major source of surface fouling at temperatures below 400°C.<sup>2</sup> Although pure paraffins and hydrotreated fuels have high thermal stability, i.e., a low propensity for fouling surfaces, they can oxidize very rapidly in the absence of antioxidant protection. Species containing heteroatoms (present in low concentrations in most fuels) tend to inhibit or retard oxidation by acting as antioxidants. However, on the basis of the high relative abundance of O, S, and N in insoluble products, these same types of species have been implicated in surface fouling.

The thermal stability of lesser quality aviation fuels can be improved through hydro-treatment processes at the refinery which reduce the concentration of many heteroatomic species as well as dissolved metals and alkenes.<sup>3</sup> More severe hydro-treatment can also lower the concentration of aromatics. Thermal stability can be improved at a lower cost by the introduction of additives or additive packages.<sup>4</sup>

Our laboratory has been investigating the effect of fuel blending upon autoxidation.<sup>5,6</sup> Adding a small amount of a straight-run fuel that contains naturally occurring antioxidants to a hydrotreated fuel whose natural antioxidants have been removed during refining is equivalent to adding a small amount of antioxidant.<sup>5-7</sup> Conversely, the addition of a severely hydrotreated fuel to a straight-run fuel can be viewed as a means of diluting the concentration of many deleterious fuel components including antioxidants as well as aromatics. Such dilution causes compositional changes analogous to those achieved during hydrotreatment. In the present study this concept was explored by investigating the autoxidation of neat and diluted fuels and the changes in autoxidation arising from the introduction of some simple additives.

### EXPERIMENTAL

Blends (1:10) are prepared by stirring together 10% aviation fuel and 90% Exxsol D-110, the latter being a mixture of paraffins and cycloparaffins containing no antioxidants and less than 1% aromatics. The methodology has been described in detail previously.<sup>5</sup> Liquid-phase oxidation occurs as air-saturated fuel passes through a single-pass heat exchanger operated isothermally at 185°C. A system pressure of 2.3 MPa ensures a single reaction phase with no headspace. It is assumed that the amount of dissolved O<sub>2</sub> is approximately the same for each fuel and blend.<sup>8</sup> Fuel reaction time (residence time) in the 0.81-m tube (i.d. 0.216 cm) is varied by changing the flowrate. Dissolved O<sub>2</sub> in the stressed fuel is measured by the GC method developed by Rubey and co-workers.<sup>9</sup> For the oxidation experiments, tubing treated with the Silcosteel process<sup>10</sup> was used to minimize catalysis that occurs on the surfaces of stainless-steel tubing. Additives employed in this study include the DuPont metal deactivator N,N'-disalicylidene-1,2-propanediamine [designated MDA (2 mg/L)], the hindered phenol antioxidant BHT (25 mg/L), and the Betz proprietary dispersant 8Q405 (100 mg/L).

### RESULTS AND DISCUSSION

**Oxidation of neat and diluted fuel: effect of additives on POSF-3084.** POSF-3084 is a Jet-A fuel of low thermal stability containing 35 ppb of Cu. The oxidation behavior of neat and diluted fuel at 185°C is shown in Figure 1. In each case oxidation is autocatalytic as a result of formation and subsequent thermal and Cu-catalyzed<sup>11</sup> dissociation of hydroperoxides, which increases the source of free radicals. The impact of autocatalysis is reduced somewhat in the neat fuel because of the abundance of naturally occurring antioxidants which act either as primary antioxidants in a radical chain-breaking mechanism or as secondary antioxidants by destroying hydroperoxides. Diluted fuel contains fewer secondary antioxidants, resulting in higher hydroperoxide concentrations and more rapid oxidation at high conversion.

Dilution also reduces the concentration of dissolved Cu to ~ 4 ppb. Thus, Cu-catalyzed initiation is expected to be less important in diluted fuel than in neat fuel. By chelating the dissolved Cu with MDA, most of the effects of metal-catalyzed initiation can be eliminated. The results of introducing 2 mg/L of MDA into neat and diluted fuel are

shown in Figures 2a and 2b, respectively. With regard to slowing oxidation, MDA has a significant effect on the neat fuel and a minimal effect on the diluted fuel. This observation illustrates that ten-fold dilution of POSF-3084 almost totally removes any contribution from dissolved metals.

Hydrotreated fuels usually require the addition of a hindered-phenol antioxidant, such as BHT, for improved storage stability to offset the removal of natural antioxidants. Such fuels are sensitive to the introduction of additional BHT. For example, concentrations of BHT up to 70 mg/L have been shown to have an approximately linear effect in extending the delay in autoxidation of the severely hydrotreated JPTS fuel POSF-2976.<sup>12</sup> Figures 3a and 3b show the effect of introducing BHT into neat and diluted fuel, respectively. Both fuels exhibit delays in autoxidation, but the response to BHT is greater in the diluted fuel.

Dispersants are not expected to alter autoxidation. However, in some metal-containing fuels (POSF-3084, -3119) autoxidation has been reported to be slowed by the introduction of 8Q405.<sup>4</sup> It has been suggested that this behavior is due to metal deactivation rather than a radical chain-breaking mechanism.<sup>4,13</sup> Response to the addition of dispersant 8Q405 is shown in Figures 4a and 4b. The reduced sensitivity following dilution is not consistent with 8Q405 acting as a primary antioxidant; rather it supports another role, possibly related to metal deactivation.

Finally, is the oxidation behavior of diluted POSF-3084 similar to that of hydrotreated fuels? Figure 5 shows the similarity between diluted POSF-3084 and three severely hydrotreated fuels.

**Oxidation of a series of diluted fuels.** The oxidation behavior of twelve diluted aviation fuels is shown in Figure 6. This series includes fuels covering a broad range of thermal stability. Three points can be made. First, the fuel discussed in detail above is a representative example of this series. Second, with one significant exception (namely, POSF-2985), the curves are very similar in shape but rapid reaction is delayed in the same manner as we observed previously at this temperature with the addition of a primary antioxidant such as BHT to JPTS.<sup>12</sup> Since dilution has removed most of the impact of species such as metals and secondary antioxidants which require interaction with hydroperoxides, the observed delays may provide an indirect measure of the efficiency of naturally occurring primary antioxidants in slowing oxidation of the diluent.

## CONCLUSIONS

Results presented here show that fuels diluted ten-fold with paraffins exhibit behavior more characteristic of hydrotreated fuels than of the original undiluted fuel with regard to autoxidation and response to additives. This is attributed to a reduction in the impact of dissolved metals and heteroatomic species that is analogous to compositional changes achieved during hydrotreatment.

## ACKNOWLEDGMENTS

This work was supported by the Air Force Research Laboratory, Propulsion Directorate, Wright-Patterson Air Force Base, Ohio, under USAF Contract No. F33615-95-C-2507. The authors would like to thank Mr. Walter Balster for valuable discussions and Mrs. Marian Whitaker for editorial assistance.

## REFERENCES

1. Edwards, T.; Anderson, S. D.; Pearce, J. A.; Harrison, W. E., III, High-Temperature JP Fuels--An Overview, AIAA Paper No. 92-0683, Presented at the 30th Aerospace Sciences Meeting and Exhibit, Reno, NV, 6-9 January 1992.
2. Hazlett, R. N. *Thermal Oxidation Stability of Aviation Turbine Fuels*, ASTM Monograph 1; American Society for Testing and Materials: Philadelphia, 1991, p 111.
3. Gary, J. H.; Handwerk, G. E. *Petroleum Refining*; Marcel Dekker: New York, 1994, p 187.
4. Jones, E. G.; Balster, W. J.; Balster, L. M. *ASME J. Eng. Gas Turb. Power* 1997, 119, 830-835.
5. Jones, E. G.; Balster, L. M.; Balster, W. J. *Energy Fuels* 1996, 10, 509-515.
6. Balster, L. M.; Balster, W. J.; Jones, E. G. *Energy Fuels* 1996, 10, 1176-1180.
7. Zabarnick, S.; Zelesnik, P.; Grinstead, R. R. *ASME J. Eng. Gas Turb. Power* 1996, 118, 271-277.
8. Striebich, R. C.; Rubey, W. A. *Prepr.-Am. Chem. Soc., Div. Pet. Chem.* 1994, 39(1), 47-50.
9. Rubey, W. A.; Striebich, R. C.; Tissandier, M. D.; Tirey, D. A.; Anderson, S. D. *J. Chromat. Sci.* 1995, 33, 433-437.
10. Restek Corporation, Bellfonte, PA.
11. Pedersen, C. J. *Ind. Eng. Chem.* 1956, 48, 1881-1884.
12. Jones, E. G.; Balster, L. M., *Energy Fuels* 1997, 11, 610-614.

13. Balster, W. J.; Balster, L. M.; Jones, E. G. *Prepr.-Am. Chem. Soc., Div. Pet. Chem.* 1996, 41(2), 446-451.

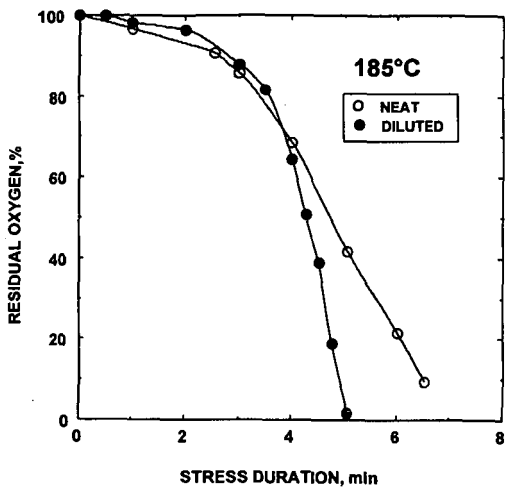


Figure 1. Autoxidation of neat and diluted POSF-3084.

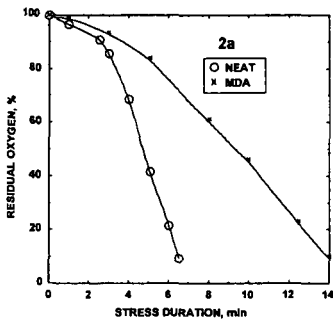


Figure 2a. Effect of MDA (2 mg/L) on neat fuel.

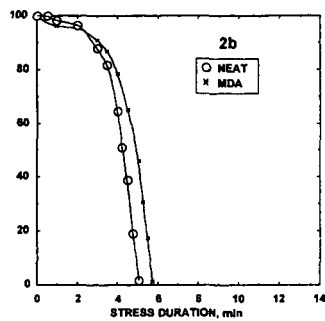


Figure 2b. Effect of MDA (2 mg/L) on diluted fuel.

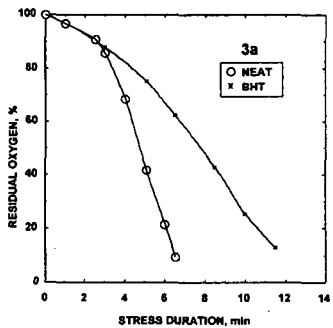


Figure 3a. Effect of BHT (26 mg/L) on neat fuel.

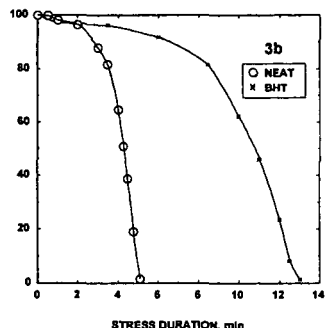


Figure 3b. Effect of BHT (26 mg/L) on diluted fuel.

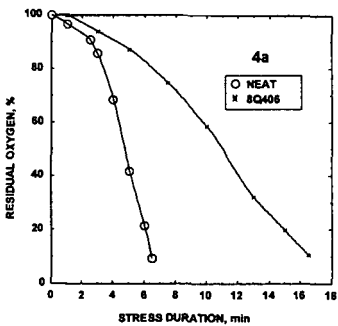


Figure 4a. Effect of BQ408 (100 mg/L) on neat fuel.

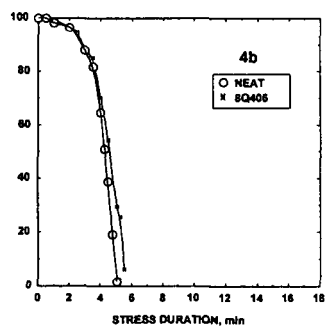


Figure 4b. Effect of BQ408 (100 mg/L) on diluted fuel.

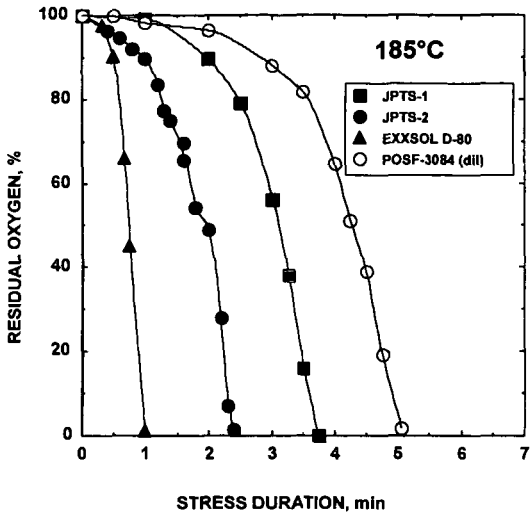


Figure 5. Comparison of diluted POSF-3084 with severely hydrotreated fuels.

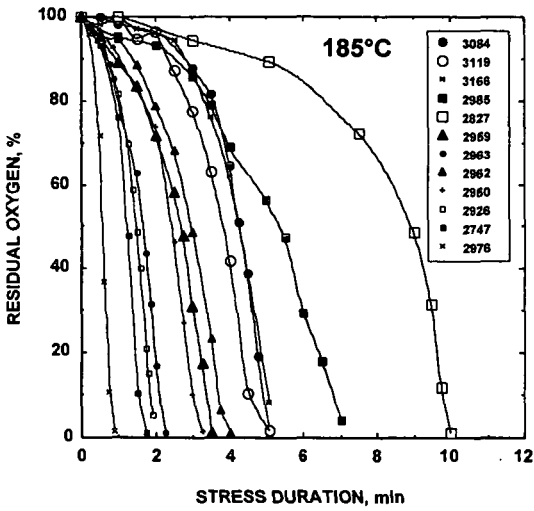


Figure 6. Oxidation of a series of diluted fuels.

## AUTOXIDATION OF AVIATION FUEL BLENDS

Lori M. Balster and E. Grant Jones  
Innovative Scientific Solutions, Inc.  
2786 Indian Ripple Road  
Dayton, OH 45440-3638

Keywords: Autoxidation, Fuel Blend, Surface Fouling

### INTRODUCTION

The use of aviation fuel to cool component systems in military aircraft creates conditions under which fuel containing dissolved  $O_2$  is exposed to hot surfaces. Liquid-phase oxidation from fuel heating during this application can lead to fouling of critical fuel-line surfaces; problems associated with surface fouling are predicted to become more severe in future aircraft where additional heat dissipation will be required.<sup>1</sup> Low-cost additives including antioxidants have been successful in reducing such fouling in both automotive<sup>2</sup> and aviation<sup>3</sup> fuels. A variation on the introduction of additives is the blending of two fuels. For example, adding a small amount of straight-run fuel which contains many natural antioxidants to a second fuel whose antioxidants have been reduced by refining techniques is equivalent to adding a small amount of antioxidant.<sup>4-6</sup> In an effort to better understand autoxidation and changes resulting from antioxidants and blending, the depletion of dissolved  $O_2$  has been monitored in aviation fuels and fuel blends under high-pressure and elevated-temperature conditions that simulate, to some extent, the thermal oxidative stress experienced in aviation fuel lines.

In the present study we tracked depletion of dissolved  $O_2$  at 185°C in a series of eight aviation fuels and many of their 1:1 blends. The selected fuels, summarized in Table 1, include JPTS, JP-7, JP-8, and Jet-A examples covering a broad range of thermal stability. The fuels are numbered approximately in order of decreasing thermal stability, and a blend of Fuels 1 and 8 is designated (1/8). The total quantity of surface insolubles measured for these fuels under the current test conditions ranges from 0.1 to 5  $\mu\text{g/mL}$ . In general, after 22 min of stressing under these reaction conditions, fuels with high thermal stability deposit < 1  $\mu\text{g/mL}$  of insolubles and fuels with low thermal stability deposit > 3  $\mu\text{g/mL}$ .<sup>7</sup> The complex oxidation behavior of each fuel and fuel blend was tracked; the time,  $t$ , required to deplete dissolved  $O_2$  by 50% was interpolated from the data and used as a simple measure of oxidation time.

The overall goal of these efforts is the reduction of surface fouling. The specific goal of this study was twofold: first, to investigate whether knowledge of the oxidation behavior of two neat component fuels would be sufficient to predict the oxidation behavior of their 1:1 blend and, second, to identify cases in which blending causes significant delays in autoxidation and search for corresponding delays or reduction in surface fouling. Any method of slowing autoxidation has potential for reducing the extent of surface fouling.

### EXPERIMENTAL

Blends are prepared by stirring together equal volumes of the component fuels. The amount of dissolved  $O_2$  is assumed to be approximately the same for each fuel.<sup>8</sup> The methodology used in this study has been described in detail previously.<sup>5</sup> Oxidation and deposition reactions occur as fuel that is saturated with respect to air at room temperature passes through single-pass heat exchangers (NIFTR's) operated isothermally at 185°C. A system pressure of 2.3 MPa ensures a single reaction phase with no headspace. Fuel reaction time (residence time) in the 0.81-m tube (i.d. 0.216 cm) is varied by changing the flowrate. Dissolved  $O_2$  in the stressed fuel is measured by the GC method developed by Rubey and co-workers.<sup>9</sup>

Deposition experiments are performed separately using 1.6-m tubes at a fixed flow of 0.25 mL/min. Surface deposits are quantified using conventional surface-carbon burnoff of 5.1-cm sections cut from the tube at the completion of a 72-hr test.

### RESULTS AND DISCUSSION

Oxidation behavior at 185°C for three representative fuels is shown in Figure 1. For the JP-7 Fuel 1—a paraffin/cycloparaffin mix—oxidation is very rapid (< 1 min) and cannot be followed accurately with current methods, whereas for Fuel 6 oxidation is quite slow (> 14 min). All of the remaining fuels oxidize at rates between these two limits. The dependence of Fuel 2 is representative of the behavior of a hydrotreated fuel with added hindered phenol as a synthetic antioxidant. The values of  $t$  for Fuels 1, 2, and 6 are ~ 0.6, 3.4, and 6.3 min, respectively. The main constituents of fuels are paraffins, cycloparaffins, aromatics, and alkenes. Many constituents of lesser abundance that contain hetero-atoms such as O, S, and N are very important as natural primary anti-

oxidants that serve to terminate free-radical chains or as natural secondary antioxidants that act to reduce self-initiation by destroying hydroperoxides. Hydroperoxides and dissolved metals in trace amounts can act as pro-oxidants by increasing the free-radical pool. The overall distribution of the major constituents, including antioxidants and pro-oxidants, determines the oxidation behavior. Fuels behave differently under conditions of thermal oxidative stress because each has a unique distribution of components.

Assuming that linear combinations of fuel constituents are achieved in the blends, exactly one-half of the antioxidants and pro-oxidants from each neat fuel is present in a 1:1 blend. In a simplistic view with the blend containing an average of the antioxidants and pro-oxidants from each fuel, the oxidation time may be the average of the times for the component fuels. This model can be checked by comparing the measured times and average calculated times, as shown in Figure 2. Only one-half of the blends approach the simple prediction indicated by the dashed line. The other blends oxidize more slowly than predicted and, in fact, usually oxidize more slowly than either component fuel. The origin of this effect that was originally reported<sup>6</sup> for fuel system (1/6) is not well understood. However, constituents of the slower oxidizing component seem to be more important in determining the oxidation of the blend. This effect occurs in blending two fuels with large differences in oxidation times, one being a severely hydrotreated fuel with reduced aromatic concentration and the other a slower oxidizing fuel of lower thermal stability containing naturally occurring pro-oxidants (dissolved metals) and antioxidants.

The results for many of the blends can be rationalized. For example, the pro-oxidant effect of dissolved metals in Fuel 8 is expected to be reduced by dilution with Fuel 1, and oxidation in that blend will be additionally slowed. An alternative explanation is based on the fact that phenolic antioxidants operate best at an optimum concentration. It can be argued that because lesser quality fuels contain a large excess of phenolic antioxidants, dilution may optimize their antioxidant effect. Both explanations can qualitatively account for the observations, but reliable prediction of the oxidation time for blends cannot be made at this time simply from knowledge of the oxidation behavior of the individual component fuels. The very complicated composition of aviation fuels plays an important role in determining the oxidation time not only for each fuel but also for blends. The presence of naturally occurring antioxidants and dissolved metals as well as the frequent addition to fuels of synthetic antioxidants and metal deactivators preclude simple predictions for blends.

The time dependence of surface fouling was studied in three blends (1/6, 1/7, 1/8) exhibiting unusually slow oxidation. Figure 3 shows the relative difference in surface fouling that resulted from mixing the paraffin Fuel 1 with Fuels 6, 7, and 8. Negative and positive values indicate decrease and increase, respectively, in the extent of surface fouling. Under conditions of 8 - 12 min of stressing, reductions are observed on the order of 0.8 - 1.6  $\mu\text{g}/\text{mL}$ , reflecting the observed delays in oxidation. Dilution of Fuels 6, 7, and 8 of lower thermal stability with the severely hydrotreated Fuel 1 creates blends with improved thermal stability.

## CONCLUSIONS

The oxidation behavior of 18 blends made from 1:1 mixing of eight component fuels has been studied. Knowledge of the oxidation behavior of the component fuels is not sufficient to permit prediction of the oxidation behavior of blends on the basis of averaging antioxidant and pro-oxidant effects. This is attributed to the complex interaction of fuel constituents including aromatics, naturally occurring antioxidants, and dissolved metals as well as synthetic antioxidants and metal deactivators. Many instances of unusually slow oxidation of blends involving straight-run and severely hydrotreated fuels have been observed. In several of these cases, surface fouling was found to be reduced at shorter stress times in agreement with observed slowing of autoxidation.

## ACKNOWLEDGMENTS

This work was supported by the Air Force Research Laboratory, Propulsion Directorate, Wright-Patterson Air Force Base, Ohio, under USAF Contract No. F33615-95-C-2507. The authors would like to thank Mrs. Marian Whitaker for editorial assistance.

## REFERENCES

1. Edwards, T.; Anderson, S. D.; Pearce, J. A.; Harrison, W. E., III, High-Temperature JP Fuels—An Overview, AIAA Paper No. 92-0683, Presented at the 30th Aerospace Sciences Meeting and Exhibit, Reno, NV, 6-9 January 1992.
2. Kalghatgi, G. T. Combustion Chamber Deposits in Spark-Ignition Engines: A Literature Review, SAE Paper No. 952443, 1995.
3. Hazlett, R. N. *Thermal Oxidation Stability of Aviation Turbine Fuels*, ASTM Monograph 1; American Society for Testing and Materials: Philadelphia, 1991, p 111.

4. Zabarnick, S.; Zelesnik, P.; Grinstead, R. R. *ASME J. Eng. Gas Turb. Power* 1996, 118, 271-277.
5. Jones, E. G.; Balster, L. M.; Balster, W. J. *Energy Fuels* 1996, 10, 509-515.
6. Balster, L. M.; Balster, W. J.; Jones, E. G. *Energy Fuels* 1996, 10, 1176-1180.
7. Balster, W. J.; Jones, E. G.; Balster, L. M. Manuscript in preparation.
8. Striebich, R. C.; Rubey, W. A. *Prepr.-Am. Chem. Soc., Div. Pet. Chem.* 1994, 39(1), 47-50.
9. Rubey, W. A.; Striebich, R. C.; Tissandier, M. D.; Tirey, D. A.; Anderson, S. D. *J. Chromat. Sci.* 1995, 33, 433-437.

Table 1. Fuels studied.

NO	FUEL	TYPE	TREATMENT	AROMATICS (% vol)	TOTAL SURFACE INSOLUBLES FORMED AT 185°C (µg/mL)	TOTAL SULFUR (ppm)	METALS (ppb)
1	Exxsol D-80	JP-7	hydrotreated	<1	0.5	3	
2	POSF-2976	JPTS	hydrotreated	8	0.1	0	
3	POSF-2747	Jet-A-1	hydrotreated	19	0.1	37	Cu, <5
4	POSF-2980	Jet-A	Mercox-treated	17	1.6	614	Cu, <5; Fe, <5
5	POSF-2934	JP-8	straight-run	18	1.9	755	Cu, 44*
6	POSF-2827	Jet-A	straight-run	19	2.6	790	Cu, <5; Fe, 8
7	POSF-3119	Jet-A	straight-run	~20	4.5	1000	Cu, 7; Fe, 26
8	POSF-3084	Jet-A	straight-run	18	4.8	527	Cu, 35; Fe, <5

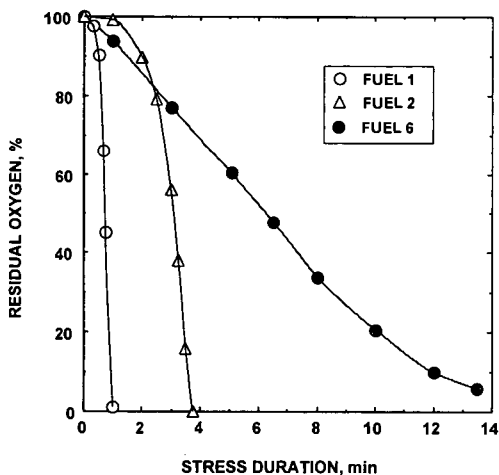


Figure 1. Autoxidation of representative fuels at 185°C.

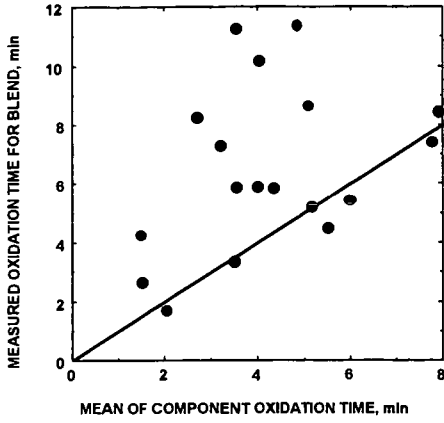


Figure 2. Comparison of measured and calculated oxidation times

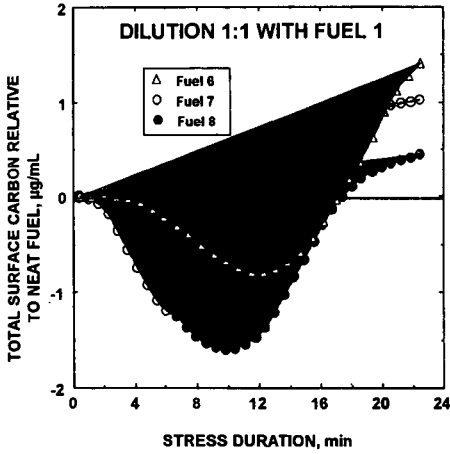


Figure 3. The effect of blending on total surface carbon.

## LIQUID-PHASE OXIDATION KINETICS OF AVIATION FUELS

E. Grant Jones  
Innovative Scientific Solutions, Inc.  
2786 Indian Ripple Road  
Dayton, OH 45440-3638

James M. Pickard  
Kinetica, Inc.  
Mound Advanced Technology center  
720 Mound Avenue  
Miamisburg, OH 45343

Keywords: Autoxidation, Fuels, Oxidation Kinetics

### INTRODUCTION

Liquid-phase oxidation occurs when fuel that contains dissolved  $O_2$  is used as the primary heat sink for cooling aircraft subsystems.<sup>1</sup> Insoluble products of oxidation reactions can foul heated surfaces, resulting in expensive downtime for cleaning and replacement of heat exchangers, fuel-control valves, and injectors. Computational fluid dynamics (CFD) models<sup>2</sup> have been successful in calculating the extent of surface fouling in selected fuel systems. The general application of such models depends on calibration using experimental fouling data and is limited by simple representations of very complicated oxidation chemistry. Furthermore, the fact that each fuel is unique in its distribution and abundance of components adds to the complexity of the oxidation processes. More detailed knowledge of oxidation kinetics of several representative aviation fuels is needed to assist in improving CFD calculations and the understanding of the fundamentals of fuel autoxidation.

Over the past several years, our laboratory has been measuring the depletion of dissolved  $O_2$  under elevated-temperature (150-225 °C), elevated-pressure, and isothermal conditions to simulate the thermal oxidative stress conditions existing in aircraft fuel lines. An important factor in these studies has been the reduction of surface catalysis. Stainless-steel surfaces were found to catalyze autoxidation; however, the use of passivated tubing (Silcosteel process)<sup>3</sup> enabled the study of autoxidation with minimal effects from surface catalysis.<sup>4</sup>

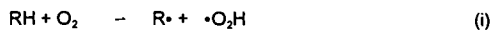
This paper summarizes recent kinetic studies of the oxidation of several representative aviation fuels. Results are reviewed for a Jet-A fuel, POSF-2827, that has been studied both as a neat fuel<sup>5</sup> and as a mixture catalyzed by  $Fe_2O_3$ .<sup>5</sup> New data are presented which extend the range of studied fuels to include both a rapidly oxidizing paraffin blend, Exxsol D-80, which is analogous to a JP-7 fuel, and a hydrotreated Jet-A fuel, POSF-3428.

## EXPERIMENTAL

The methodology used in NIFTR (Near-Isothermal-Flowing-Test-Rig) studies of oxidation and deposition has been described in detail previously<sup>7</sup>. Liquid-phase oxidation occurs as air-saturated fuel passes through a single-pass heat exchanger operated isothermally at 185 °C. A system pressure of 2.3 Mpa ensures a single reaction phase with no head space. Fuel reaction time (residence time) in the 0.81-m tube (i.d. 0.216 cm) was changed by varying the flowrate. Dissolved O<sub>2</sub> in the stressed fuel was measured by the GC method developed by Rubey and co-workers.<sup>8</sup> In experiments where the initial O<sub>2</sub> concentration was varied, fuel was sparged with different gas blends of O<sub>2</sub> and N<sub>2</sub> using a Porter CM 4 interface module and F200 thermal mass flow controllers.

## RESULTS AND DISCUSSION

**POSF-2827.** POSF-2827 is a Jet-A fuel with a thermal stability ranging from average to below average. Reduced thermal stability coupled with very slow oxidation, as shown at 458 K in Figure 1, has been attributed to a large excess of natural antioxidants.<sup>5</sup> The overall effect of these antioxidants is a low steady-state concentration of hydroperoxide, ROOH, and the absence of autocatalysis at higher O<sub>2</sub> conversion. Such a system with an approximately constant rate of initiation provided an excellent test for application of the NIFTR technique in collecting data for evaluating Arrhenius kinetic parameters. Since the reaction is 0.5 order in O<sub>2</sub>, it is explained according to the following simplified autoxidation mechanism:



where  $R\cdot$  is a radical,  $RO_2\cdot$  is a peroxy radical, and  $RO_2H$  is the hydroperoxide. Reactions (i) and (i') represent initiation, (ii) and (iii) are propagation, and (iv) termination. Reaction (i') is the major initiation reaction in hydrotreated fuels; it is of minor importance in fuels containing large concentrations of heteraromatic species and natural antioxidants. Data analysis over the temperature range 438–478 K yielded  $\log(k_{ap}/M^{-1/2}s^{-1}) = (12.9 \pm 0.4) - (36.9 \pm 0.8)/\theta$ , where  $k_{ap}$  is the apparent rate coefficient and  $\theta$  is  $2.303 RT \text{ kcal mol}^{-1}$  ( $R$  is the ideal gas law constant and  $T$  is absolute temperature). At lower temperature, the self-initiation of the autoxidation is negligible.

The addition of an external initiator (2,2'-azobis[2-methylpropionitrile], AIBN) over the temperature range 393–414 K resulted in  $\log(k_d/(2k_t)^{1/2}/M^{-1/2}s^{-1/2}) = (7.08 \pm 0.3) - (18.6 \pm 0.5)/\theta$ .<sup>5</sup>

**POSF-2827 (4 ppm  $Fe_2O_3$ ).** Figure 1 shows changes arising from the introduction of 4 ppm of  $Fe_2O_3$  into POSF-2827.  $Fe_2O_3$  acts as a heterogeneous catalyst in accelerating autoxidation. The kinetic data for oxidation in the presence of  $Fe_2O_3$  are consistent with reaction acceleration from dissociation of an  $Fe_2O_3$ -ROOH adduct formed by the adsorption of ROOH on the  $Fe_2O_3$  surface; and subsequent H-atom abstraction by surface adsorbed radicals. Data analysis yielded  $\log(k_{ap}/M^{-1/2}s^{-1}) = (11.7 \pm 0.5) - (27.7 \pm 0.9)/\theta$  for the catalytic oxidation. The average value of  $E_{ii} - E_{iv}/2 = 18.6 \text{ kcal mol}^{-1}$  determined from AIBN initiation coupled with  $E_{ap} = 27.7 \text{ kcal mol}^{-1}$  implies  $E_i = 18 \text{ kcal mol}^{-1}$  for initiation by  $Fe_2O_3$ .<sup>6</sup>

**Paraffin/cycloparaffin blend (Exxsol D-80).** This blend is representative of the highly thermally stable JP-7 fuel (in the absence of a lubricity additive) as used in high performance military aircraft such as the SR-71. With very low concentrations of aromatics (< 1%) and no natural or synthetic antioxidants, Exxsol D-80 oxidizes rapidly. Depletion of  $O_2$  over the low-temperature range 408–438 K is given in Figure 2. Unlike POSF-2827 oxidation, this system is dominated by thermal dissociation of ROOH, as evidenced by acceleration at higher conversion. The kinetic data are described by  $\log(k_{ap}/M^{-1/2}s^{-1}) = (9.5 \pm 0.2) - (26.3 \pm 0.4)/\theta$ ; the solid lines illustrate fits from these parameters. Oxidation has been studied at 413 K for different initial concentrations varying from 10 to 100%  $O_2$ -saturation at room temperature. The results, shown in Figure 3, are also fitted with the same kinetic parameters. Initial rates are independent of  $O_2$  concentration, consistent with initiation by trace quantities of ROOH. Analysis of the ROOH data led to  $\log(k_d/(2k_t)^{1/2}/M^{-1/2}s^{-1/2}) = (3.3 \pm 1.3) - (12.5 \pm 2.6)/\theta$ .

**POSF-3428.** The fuels discussed above represent two extremes both in thermal stability and oxidation behavior. POSF-3428 is more representative of a broad spectrum of aviation fuels having intermediate stability and reaction rates controlled by hydroperoxides. The oxidation behavior shown in Figure 4 is autocatalytic and the solid lines were calculated using the same mechanism as that for Exxsol D-80, with thermal decomposition of ROOH as the dominant source of initiation. The kinetic data are summarized by  $\log(k_{app}/M^{-1/2}s^{-1/2}) = (12.3 \pm 0.9) - (34.7 \pm 1.8)/\theta$

## CONCLUSIONS

The apparent rate coefficients describing liquid-phase oxidation have been measured in four fuel systems using the NIFTR apparatus. The fuel reactivities may be ranked inversely according to the magnitudes of the apparent activation energies for autoxidation. Apparent activation energies follow the trend: POSF-2827 > POSF-3428 > POSF-2827 (4 ppm Fe<sub>2</sub>O<sub>3</sub>) > Exxsol D-80. The most unreactive fuel with respect to autoxidation is POSF-2827; the reason being that the fuel the fuel contains heteroaromatic species (sulfur compounds) that scavenge ROOH. The most reactive fuel is Exxsol-D80 which contains less than 1% aromatics and is devoid of natural ROOH scavengers. The extremes in reactivity are also reflected by the rates of initiation. Since appreciable ROOH does not accumulate in neat POSF-2827, initiation is controlled by reaction (i). This results in  $E_i = 37 \text{ kcal mol}^{-1}$  for the spontaneous initiation of POSF-2827. For Exxsol D-80, initiation is dominated by ROOH dissociation with  $\log(k_i/s^{-1}) = 16 - 33/\theta$ .

## ACKNOWLEDGMENTS

This work was sponsored by the Air Force Research Laboratory, Propulsion Directorate, Wright-Patterson Air Force Base, Ohio, under Contract No. F33615-95-C-2507. The authors would like to thank Ms. Lori Balster for conducting the dissolved O<sub>2</sub> measurements and Mrs. Marian Whitaker for editorial assistance.

## REFERENCES

1. Edward, T.; Anderson, S. D.; Pearce, J. A., Harrison; W. E., III, High-Temperature JPFuels—An Overview, AIAA Paper No. 92-0683, Presented at the 30<sup>th</sup> Aerospace Sciences Meeting and Exhibit, Reno, NV, 6-9 January 1992.

2. Katta, V. R.; Jones, E. G.; Roquemore, W. M. "Development of Global-Chemistry Models for Jet-Fuel Thermal Stability Based on Observations from Static and Flowing Experiments," AGARD-CP-536, Paper No. 19., 1993.
3. Restek Corporation, Bellefonte, PA.
4. Jones, E. G.; Balster, L. M.; Balster, W. J. *Energy Fuels*, **1996**, *10*, 831-836.
5. Pickard, J. M.; Jones, E. G. *Energy Fuels*, **1996**, *10*, 1074-1077.
6. Pickard, J. M.; Jones, E. G. *Energy Fuels*, **1997**, *11*, 1232-1236.
7. Jones, E. G.; Balster, L. M.; Balster, W. J. *Energy Fuels*, **1996**, *10*, 509-515.
8. Rubey, W. A.; Striebich, R. C.; Tissandier, M. D.; Tirey, D. A.; Anderson, S. D. J. *Chromat. Sci.* **1995**, *33*, 433-437.

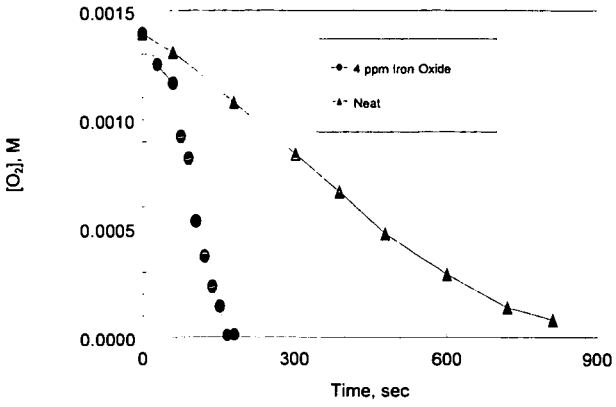


Figure 1. Oxygen depletion vs time for neat and iron-oxide (4 ppm)-treated fuel.

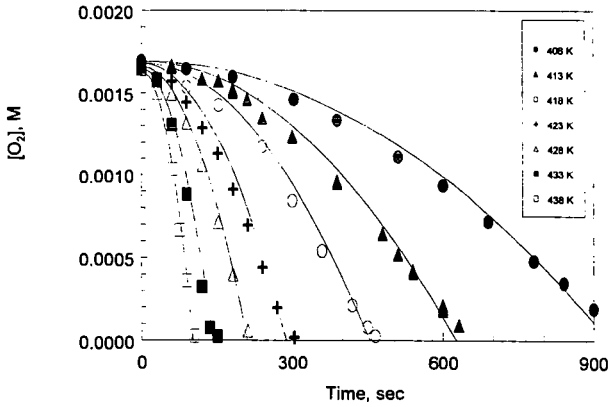


Figure 2. Influence of temperature on oxygen depletion : air-saturated Exxsol D-80 from 408 to 438 K.

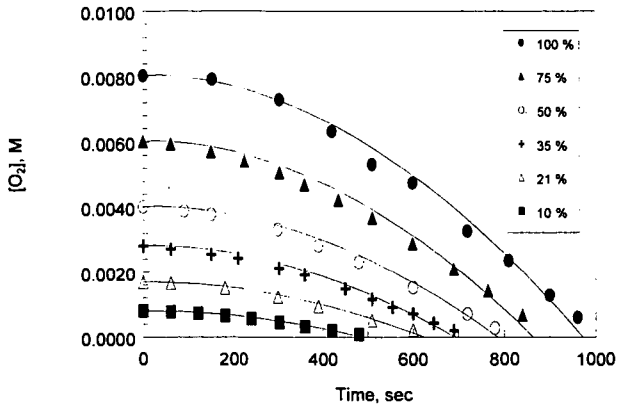


Figure 3. Influence of oxygen concentration on oxygen depletion: air-saturated Exxsol D-80 at 413 K.

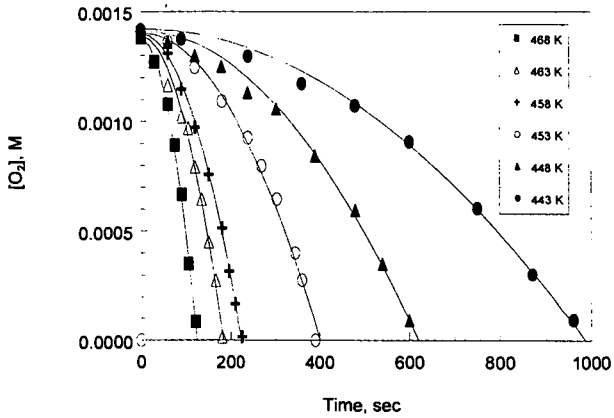


Figure 4. Influence of temperature on oxygen depletion: air-saturated POSF-3428 from 408 to 438 K.

## JET FUEL SYSTEM ICING INHIBITORS: SYNTHESIS AND STABILITY

<sup>a,b</sup>George W. Mushrush, <sup>b</sup>Erna J. Beal, <sup>b</sup>Dennis R. Hardy, <sup>a</sup>Wayne M. Stalick, <sup>a</sup>Subhash Basu, <sup>c</sup>Dennis Grosjean, and <sup>d</sup>John Cummings

<sup>a</sup>George Mason University, Fairfax, VA 22030, <sup>b</sup>Navy Technology Center for Safety and Survivability, Washington, DC 20375, <sup>c</sup>Innovative Scientific Solutions Inc., 2786 Indian Ripple Road, Dayton, OH 45440, and <sup>d</sup>Naval Air-Warfare Center, Trenton, NJ 08628

### ABSTRACT

The current fuel system icing inhibitor additives, used both by the military and commercial aviation, are ethylene glycol monomethyl ether (EGME) and diethylene glycol monomethyl ether (DiEGME). These deicing compounds are toxic at the concentrations that are required for effective deicing. This observation points to an immediate need for non-toxic, inexpensive, and biodegradable deicing compounds. The synthesis of polar sugar derivatives represents viable alternatives to glycol based additives. The synthesis and characterization of acetals, ketals, ethers, and esters of oxoacids will be discussed. These alternative deicing compounds are cheap, fuel stable, and exhibit similar icing inhibitor characteristics to EGME and DiEGME.

### INTRODUCTION

The literature of deicing additives for jet fuels is rather sparse. Those articles that have appeared are related to concentration determination, stability in fuels, and health implications of these additives (1, 2). Currently the fuel icing inhibitor additives, ethylene glycol monomethyl ether (EGME) and diethylene glycol monomethyl ether (DiEGME), are mandatory in all military aircraft fuels and are optional in world-wide commercial aviation fuels depending on route, flight length, and season. Unfortunately, ethylene glycol based deicing compounds are toxic at the concentrations that are required for effective deicing (2). These additives are leached out of the fuel and into water bottoms and when this water is drained from fuel system sumps, filters and storage tanks it contains EGME and/or DiEGME thus creating a personnel health hazard. Also, glycols exert high oxygen demand for decomposition and when they get into the environment they cause the death of aquatic organisms as dissolved oxygen is depleted. These observations all point to an immediate need for non-toxic, inexpensive, and biodegradable deicing compounds. The approach of our laboratory is to utilize the large U.S. surplus of sugars as the basis for the synthesis of biodegradable deicing compounds. These potential deicing candidates must satisfy many constraints. They must be soluble in jet fuel, soluble in water, fuel stable during storage, and exhibit similar or enhanced ice inhibiting characteristics to currently used deicing compounds.

The latter of these constraints, concerning the behavior of deicing compounds in fuels, is being investigated in our laboratory since there are no readily available software programs to estimate either the physical or colligative properties of middle distillate fuels. A large number of physicochemical and toxicological properties are prerequisite to a reasonable hazard assessment of a chemical (1). However, environmental fate, and toxicity of chemicals can be estimated using computer models. These predicted values provide the guidance towards synthesizing safer icing inhibitors for this project.

### EXPERIMENTAL

The general synthesis procedure followed for the synthesis of the glycerol acetals and ketals was that reported for the synthesis of the 2,2-dimethyl-1,3-dioxolane-4-methanol, compound I (3). The procedure was modified for the synthesis of the formaldehyde (compound II), and acetaldehyde (compound III), adducts. Acetone (232g, 4.5 moles), or acetaldehyde (197g, 4.5 moles), or formaldehyde (135g, 4.5 moles), was added to glycerol (100 g, 1.1 moles) in a toluene solvent (300 mL), containing 3.0 g *p*-toluene sulfonic acid and 255 g of 5A molecular sieves all in a 2,000 mL two-necked, round-bottomed flask fitted with a mechanical stirrer and a condenser. A freezing mixture of ethylene glycol and water at -25.0 °C was circulated through the condenser. The stirred reaction mixture was heated under gentle reflux for 33 hrs using a heating mantle. After reflux, the condenser was disconnected and excess acetaldehyde was allowed to evaporate. The acidic reaction mixture was neutralized with 3.0 g sodium acetate. The molecular sieves were separated by vacuum filtration using a Büchner funnel. The resulting liquid was distilled under vacuum. The colorless organic product distilling at 80-82°C/10 mm was collected for the acetone derivative to give a yield of 88%; for the acetaldehyde derivative the

product distilling at 85-90 °C/10mm was collected to give a yield of 80 %; and for the formaldehyde derivative the product distilling at 95-96°C/10 mm was collected (4).

Computational Methods. In order to estimate environmental fate and certain physical properties, a suite of programs developed by Syracuse Research Corporation was used (5). Well established computational methods are used in these programs.

## DISCUSSION

The reaction products of aldehydes and ketones with glycerol have been known for more than 100 years. These compounds were usually regarded as intermediates in synthetic procedures and little interest was expressed in them. The compounds in this study are simpler than the carbohydrates and carbohydrate derivatives so they were the subject of this initial investigation. Acetal and ketal formation is catalyzed by either mineral acids or Lewis acids. The intermediate hemi-acetal or hemi-ketal is not usually isolated. The compounds were subjected to testing for deicing characteristics and compared to EGME, DiEGME, and dipropylene glycol. Dipropylene glycol was included because industries and the Federal Aviation Administration have recommended it as a replacement for the ethylene based deicers. The freezing point tests were conducted in a one gallon simulator rig. The data showed that both compounds **II** and **III** were effective deicers and closely paralleled the behavior of EGME and DiEGME(6). Compounds **II** and **III** show similar time vs temperature dependence. The compounds were also tested for fuel instability and incompatibility reactions. They were tested for storage stability by ASTM method D5304-92 in JP-8 (7).

### Additives in this Study

These compounds, along with their estimated physical properties and environmental toxicity profile, are presented in Table I. Compound **I** appears to have excellent potential properties as a deicing agent. This compound has been well characterized in the literature and is considered to be relatively non-toxic (8). It is used commercially as a solvent, plasticizer, and solubilizing and suspending agent in pharmaceuticals. Additionally, it is miscible in hydrocarbons, gasolines, turpentine, oils, and water, making it an ideal candidate as an icing inhibitor. Although Compound **I** has a higher dermal dose per event than current deicers this is countered by its lower toxicity and dermal permeability, due, perhaps in part, to its higher lipophilicity. Compound **I** is decomposed in the atmosphere at a rate comparable to current deicers. Like current deicers, it is not rapidly volatilized from aquatic systems. Upon ingestion, possibly at mouth pH but certainly at stomach pH, this compound is readily broken down into acetone and glycerol. Both of these compounds have relatively low toxicity and environmental concerns. The second of the compounds synthesized, compound **III**, exhibits a lower dermal permeability and dermal dose per event than any of the other compounds in this study. The decomposition products upon ingestion, which are glycerol and acetaldehyde, are also relatively non-toxic; acetaldehyde is even less toxic than acetone. Acetaldehyde is one of the metabolized products of ethanol.

Compound **II** was dismissed due to the formation of formaldehyde upon decomposition under mildly acidic conditions. Formaldehyde is a known toxic and carcinogenic agent and the use of formaldehyde adducts in this study was ceased for this reason. This concern aside, compound **II** exhibits similar properties to the other compounds in this study, with a lower dermal dose per event.

All three compounds were found to be soluble in jet fuel at the levels necessary for inhibiting the formation of ice; and closely paralleled the behavior of EGME and DiEGME(4). Accelerated fuel instability and incompatibility studies using ASTM method D5304-92 in JP-8 (7) showed negligible formation of solids (<0.01 mg) and no increased peroxidation.

## CONCLUSION

Testing and evaluation of these new deicing compounds derived from sugars showed that they exhibited properties that make them ideal candidates for the next generation of deicing compounds. Both Compounds **I** and **III** are predicted to be environmentally benign and relatively nontoxic at the concentrations necessary for inhibiting ice formation. Compound **I** has been well characterized due to its current commercial applications, and the need for further investigation into the toxicity of Compound **II** is indicated. Other analogs from reduced sugars have been synthesized and evaluated and will be reported on in subsequent papers. The substituted forms of reduced sugars have the potential for the ideal combination of lipophilic and hydrophilic character necessary for deicing applications.

## ACKNOWLEDGMENT

The authors would like to express appreciation to Syracuse Research Corporation, the Air Force Office of Scientific Research (AFOSR) under grant number 5-25016, and the Office of Naval Research for research support.

## REFERENCES

- (1) Basak, S. C., Niemi, G. J., Veith, G. D. J. of *Mathematical Chemistry*. 4, 185 (1990).
- (2) U. S. Department of Health & Human Services, Agency for Toxic Substances and Disease Registry, Tech. Rpt for Ethylene Glycol/Propylene Glycol Rprt 205-88-0608, May 1993.
- (3) Organic Synthesis Collective Volume 3, ed. E.C. Horning, pp 502-504, Wiley:New York, 1965.
- (4) Mushrush, G.W., Stalick, W.M., Beal, E.J., Basu, S.C., Slone, J.E., Cummings, *Petroleum Science & Technology*. 15(3,4), 237 (1997).
- (5) Meylan, W., Syracuse Research Corporation. *DERMAL for Windows*, Version 1.23, (1996). (a). *MPBP for Windows*, Version 2.51, (1996); (b). *WSKOW for Windows*, Version 1.20, (1996); (c). *HENRY for Windows*, Version 2.51, (1995); (d) *AOP for Windows*, Version 1.80, (1996); (e). *KOC for Windows*, Version 1.57, (1995); (f) *Estimation Program Interface for Windows*, Version 2.00, (1995).
- (6) Stirling, K. Q., Ripley, D. L. Partition Coefficients of Icing Inhibitors in JP-4 and JP-5 Jet Fuel, U. S. Department of Energy and Naval Air Propulsion Center, Final Report DE-FC22-83FE60149, October 1990.
- (7) ASTM ?Standard Test Method for Assessing Distillate Fuel Storage Stability by Oxygen Over pressure,? Annual Book of ASTM Standards; ASTM:Philadelphia, Part 0.05.01, ASTM D5304-92, (1992).
- (8) Sanderson, M. D. J. *Pharm. Pharmacol.* 11, 150 (1959) and 11, 446 (1959).

	<u>Compound I</u>	<u>Compound II</u>	<u>Compound III</u>
Dermal permeability K <sub>p</sub> , cm/hr	5.00 x 10 <sup>-3</sup>	6.94 x 10 <sup>-4</sup>	1.17 x 10 <sup>-3</sup>
Dermal dose per event (at concentration of 100 mg/cm <sup>3</sup> for 0.25 hr) in mg/cm <sup>2</sup>	0.0430	0.0048	0.0079
log K <sub>ow</sub> (lipophilicity)	1.07	-0.50	-0.09
Vapor pressure in mmHg	0.0647	0.2700	0.1140
Water solubility in mg/L	3.459 x 10 <sup>4</sup>	9.918 x 10 <sup>5</sup>	3.914 x 10 <sup>5</sup>
Henry's Law Constant in atm x m <sup>3</sup> /mol	1.91 x 10 <sup>-9</sup>	1.08 x 10 <sup>-9</sup>	1.44 x 10 <sup>-9</sup>
OH rate constant in cm <sup>3</sup> /molecules x sec	2.50420 x 10 <sup>-11</sup>	2.68248 x 10 <sup>-11</sup>	2.99376 x 10 <sup>-11</sup>
Atmospheric half-life in hrs.	5.125	4.785	4.287
Soil adsorption coefficient K <sub>oc</sub>	1.00	1.00	1.00
Volatilization from model river in years (half-life)	60.30	94.712	75.62
Volatilization from model lake in years (half-life)	38.60	688.76	550.00
Biological Oxygen Demand in days (half-life)	2-15	2-15	2-15
LC <sub>50</sub> in ug/L for <i>Pimephales Promelas</i>	1.67 x 10 <sup>7</sup>	2.36 x 10 <sup>7</sup>	-----
Bioconcentration factor for <i>Pimephales promelas</i>	1	1	1

Table 1. Compounds based upon the reduced sugar mannose

	Ethylene glycol mono- methyl ether (EGME)	Di(ethylene glycol) mono-methyl ether (DiEGME)
Dermal permeability $K_p$ in cm/hr	$4.98 \times 10^{-4}$	$2.97 \times 10^{-4}$
Dermal dose per event (concentration of $100 \text{ mg/cm}^3$ for 0.25 hr) in $\text{mg/cm}^2$	$4.66 \times 10^{-3}$	$1.3 \times 10^{-3}$
$\log K_{ow}$ (lipophilicity)	-0.77	-1.18
Vapor pressure in mmHg	9.2200	0.2160
Water solubility in mg/L	$1.000 \times 10^6$	$1.000 \times 10^6$
Henry's Law Constant in atm	$4.19 \times 10^{-8}$	$6.50 \times 10^{-10}$
$\times \text{m}^3/\text{mol OH}$ rate constant in $\text{cm}^3/\text{molecule} \times \text{sec}$	$1.19983 \times 10^{-11}$	$2.60139 \times 10^{-11}$
Atmospheric half-life in hours	10.698	4.934
Soil adsorption coefficient $K_{oc}$	1.00	1.00
Volatilization from model river in years (half-life)	11.32	6660.27
Volatilization from model lake in years (half-life)	82.30	$4.4844 \times 10^5$
Biological Oxygen Demand (BOD) in days (half-life)	2-16	2-16
$LC_{50}$ in $\mu\text{g/L}$ for <i>Pimephales promelas</i>	$2.15 \times 10^7$	$2.96 \times 10^7$
Bioconcentration factor (BCF) for <i>Pimephales promelas</i>	1	1

Table 2. Estimated values for current FSII additives

## STUDIES OF SILYLATION AGENTS AS THERMAL-OXIDATIVE JET FUEL ADDITIVES

S. Zabarnick, M.S. Mick, R.C. Striebich, R.R. Grinstead, and S.P. Heneghan  
University of Dayton Research Institute Aerospace Mechanics Division,  
300 College Park, Dayton OH 45469-0140

### INTRODUCTION

Derivatization techniques are well known methods to alter species structures to make them more amenable to chemical analysis. Silylation is one type of derivatization process, in which species which contain reactive hydrogen atoms are reacted with an appropriate agent resulting in the conversion of these reactive hydrogen sites to relatively unreactive trimethyl silyl sites (1). Silylation is widely practiced in chromatographic analysis to improve analytical quantitation and transport, increase detectability, increase volatility, and decrease surface interactions. In general, silylating agents are able to react with the active hydrogens in the following species: acids, alcohols, thiols, amines, amides, and enolizable ketones and aldehydes. A variety of agents are known, which vary in their reactivity, selectivity, side reactions, and character of reaction by-products.

Jet fuel is used as a coolant in advanced military aircraft; the hot fuel reacts with dissolved oxygen forming oxidized products. These oxidized products include gums and solid deposits which can coat fuel system surfaces resulting in filter plugging, fouling of close tolerance valves, valve hysteresis, and other problems. Various chemical additives and additive combinations have been utilized to inhibit oxidation and/or reduce deposition. For example the U.S. Air Force JP-8+100 additive package contains a dispersant, an antioxidant, and a metal deactivator. It is generally agreed that the advanced military aircraft being presently conceived will have significantly higher heat loads which will be dumped into the fuel. This higher fuel temperature will result in substantially increased oxygen consumption and subsequent increased deposition.

The substantially higher fuel system temperatures of advanced aircraft will result in complete or near complete oxygen consumption. Additives which delay oxidation, such as antioxidants, metal deactivators, and hydroperoxide decomposers, will be unable to provide significant benefits in reducing deposition under time/temperature conditions where dissolved oxygen consumption is assured. Thus alternative additive techniques need to be explored. Dispersant additives can still be useful under these conditions.

In this study we explore the use of silylation agents as jet fuel additives for reducing oxidative deposition. Silylation agents have the ability to react with the heteroatomic species, such as phenols, which have been implicated in deposit producing mechanisms. Thus they have the potential to chemically transform these species into relatively innocuous silylated products. In this work we study the effect that silylation agents have on jet fuel oxidation and deposition. We show that these additives result in an increased oxidation rate and substantially reduced deposition. These results show that silylation agents may be useful as jet fuel additives for preventing oxidative deposition in advanced aircraft fuel systems including endothermic fuel systems. Silylation agents may also prove to be useful in easing identification of fuel components, particularly those detrimental to fuel thermal stability.

### EXPERIMENTAL

Fuel oxidation and deposition characteristics were evaluated in the quartz crystal microbalance/Parr bomb system (QCM) which has been described in detail previously (2,3). All fuel oxidation tests were run at 140C and one atmosphere of air initial pressure. It is heated with a clamp-on band heater and its temperature is controlled by a PID controller through a thermocouple immersed in the fuel. The reactor contains an rf feedthrough, through which the connection for the quartz crystal resonator is attached. The crystals are 2.54 cm in diameter, 0.33 mm thick and have a nominal resonant frequency of 5 MHz. The crystals were acquired from Maxtek Inc. and are available in crystal electrode surfaces of gold, silver, platinum, and aluminum. For the studies reported here gold crystal electrodes were used. The QCM measures deposition (i.e., an increase in mass) which occurs on overlapping sections of the two sided electrodes. Thus, the device responds to deposition which occurs on the metal surface and does not respond to deposition on the exposed quartz.

The device is also equipped with a pressure transducer (Sensotec) to measure the absolute headspace pressure and a polarographic oxygen sensor (Ingold) to measure the headspace oxygen concentration. Previous studies have demonstrated the value of determining the oxidation characteristics of fuels and fuels with additives. A personal computer is used to acquire data at one minute intervals during the experimental run. The following data are recorded during a run: temperature, crystal frequency, headspace pressure, headspace oxygen concentration, and crystal damping voltage.

The reactor is charged with 60 mL of fuel, which is sparged with the appropriate gas for one hour before each test. The reactor is then sealed and the heater is started. All runs in this study were performed at 140C; heat-up time to this temperature is 40±5 minutes. Most runs are conducted for 15 hours, after which the heater is turned off and the reactor allowed to cool. Surface mass measurements can only be determined during the constant temperature (±0.2C) portion of an experimental run. The crystal frequency is converted to a surface mass measurement using the process described below.

The theory that relates the measured frequency changes to surface mass has been presented in detail elsewhere (4). The frequency change of a crystal immersed in a liquid fuel can be due to two effects: the first results from changes in the surface mass density, the second is due to changes in the liquid density and viscosity. At constant temperature and relatively small extents of chemical conversion the liquid properties remain constant and the frequency change can be related to surface deposition via the equation

$$\rho_s = -\left(2.21 \times 10^5 \text{ g / (cm}^2\text{s)}\right) \frac{\Delta f}{f_0^2} \quad (1)$$

where  $f_0$  is the unperturbed resonant frequency,  $\Delta f$  is the change in resonant frequency, and  $\rho_s$  is the surface mass density (mass/area). The reproducibility of the mass deposition measurements on fuels is limited to ±20% for the QCM technique. The fuels studied and some of their properties are listed in Table I. The fuels were acquired from the Fuels and Lubricants Division of Wright Laboratory, Wright-Patterson AFB, OH, and are referred to by the Wright Lab assigned accession number. Silylation agents were acquired from Pierce Chemical.

The fuels were tested at 140C for 15 hours in a static reactor which utilizes a quartz crystal microbalance (QCM) for measuring deposition, and a polarographic oxygen sensor which monitors the oxygen concentration in the reactor headspace, for monitoring the oxidation process. The experimental apparatus has been described in detail previously (2).

## RESULTS AND DISCUSSION

Jet fuel is a complex mixture which is primarily composed of branched and straight chain alkanes, cycloalkanes, and alkyl-substituted aromatics. In addition, various heteroatomic species may be present at relatively small concentrations, including but not limited to: phenols, peroxides, alcohols, organic acids, sulfides, thiols, thiophenes, and amines. In the absence of these heteroatomic species, this hydrocarbon mixture oxidizes readily at elevated temperature via the classic hydrocarbon autooxidation mechanism. For example, a pure alkane, such as dodecane, or a highly treated petroleum fraction, such as Exxsol D-110, will completely consume all available oxygen in the QCM system on the order of minutes at 140C. But, real jet fuels oxidize much more slowly. Even severely hydrotreated fuels require two to five hours to consume the available oxygen at this temperature. Less severely processed fuels can require 5 to 60 hours to consume the available oxygen. These real fuels oxidize more slowly than pure hydrocarbons, due to the presence of these heteroatomic species. These species slow oxidation by intercepting alkyl peroxy radicals and/or by decomposing alkyl hydroperoxides to non-radical products (3,4). Thus the removal of such species should result in a significant increase in the oxidation of the fuel. This effect is illustrated in the hydrotreatment process, which removes heteroatomic species and results in highly oxidizable fuel. These same species which slow oxidation of fuel, also play important roles in forming surface and bulk deposits upon fuel oxidation. Thus, a fuel which is treated to remove such heteroatomic species will oxidize rapidly and display reduced deposition formation.

Treating jet fuel with silylating agents results in the reaction of species with active hydrogens to form trimethylsilyl derivatives. For the case of an alkyl phenol, the following reaction occurs:



We are converting a phenol with a reactive hydrogen to its trimethylsilyl derivative, which is much less reactive and does not contain an active hydrogen. The resulting compound is not reactive towards alkylperoxy radicals (relative to the original phenol) and thus does not interfere with the fuel autoxidation chain. Analogous reactions to the above are also possible for other compounds with active hydrogens.

To explore the effect that silylation has on jet fuel we added one mL of hexamethyldisilazane (HMDS) to 60 mL of fuel F-3119 and stressed this additized fuel in the QCM at 140C for 15 hours. The resulting oxygen sensor and QCM deposition plots for the neat and additized fuel are shown in Figure 1 and 2. The headspace oxygen plot shows that HMDS causes a substantial increase in the oxidation rate of the fuel. The resulting oxygen decay is nearly as fast as a pure hydrocarbon solvent (oxidation complete in 2 to 2.5 hours). The deposition plot shows that HMDS causes a >90% decrease in deposition during the run. It is apparent that treatment of this fuel with HMDS results in significant removal of species which delay oxidation. In addition, removal of these species results in reduced deposition.

It is interesting to compare these results with another technique which removes heteroatomic species, solid-phase extraction (SPE). Of the heteroatomic species present, silica gel SPE removes only those that have significant polarity. Previously, we have demonstrated that SPE treatment reduces deposition significantly, but does not increase oxidation as substantially (2).

To investigate the chemical changes that occur in the fuel upon silylation treatment we used gas chromatography-mass spectrometry (GC-MS) after preconcentration of the polar fuel species via SPE with subsequent methanol back extraction. This technique is particularly useful for identification of phenol species in the fuel. The results of these analyses (not shown) demonstrate substantial conversion of fuel phenols to their silylated derivatives.

There exist a variety of silylation reagents which display varying silylation selectivity, reactivity, side reactions, and character of reaction by-products. For example, while HMDS requires elevated temperatures for reaction, silylation with N,O-bis[trimethyl]acetamide (BSA) can be performed at room temperature. We therefore have the ability to control the time and/or temperature at which the silylation reaction occurs. The ability to remove phenols within aircraft fuel lines during the heating of the fuel in its transport through the fuel system is highly desirable. The presence of phenols can be desirable during fuel storage as they inhibit oxidation, but their presence is undesirable in fuel systems due to their contribution to fouling. By proper choice of a silylation additive, we may be able to design a fuel where the silylation reaction occurs at a location of choice in the fuel system with subsequent rapid consumption of oxygen.

The promise of silylation additives does not come without potential disadvantages. These include cost, water sensitivity, and problems due to product formation in combustors. Presently, silylation additives are relatively expensive, when compared to common jet fuel additives, as they are produced in relatively small quantities for derivatization in chemical analysis. Silylation reagents react rapidly with water and humid air forming undesirable silanols. It is expected that silylating reagents and silylated products will be rapidly oxidized to silicon dioxide within the combustion chamber. This may have a negative effect on combustor and turbine materials depending on the physical form of the silicon dioxide product.

## CONCLUSIONS

In this study we explore the use of silylation agents as jet fuel additives for reducing oxidative deposition. Silylation agents have the ability to react with the heteroatomic species, such as phenols, which have been implicated in deposit producing mechanisms. Thus they have the potential to chemically transform these species into relatively innocuous silylated products. In this work we study the effect that silylation agents have on jet fuel oxidation and deposition. We show

that these additives result in an increased oxidation rate and substantially reduced deposition. These results show that silylation agents may be useful as jet fuel additives for preventing oxidative deposition in advanced aircraft fuel systems including endothermic fuel systems. Silylation agents may also prove to be useful in easing identification of fuel components, particularly those detrimental to fuel thermal stability.

#### ACKNOWLEDGMENTS

This work was supported by the US Air Force, Fuels and Lubrication Division, Air Force Research Laboratory, Wright-Patterson AFB, OH under contract Nos. F33615-92-C-2207 and F33613-97-C-2719 with Mr. Charles Frayne as technical monitor.

#### REFERENCES

1. Pierce, A.E. *Silylation of Organic Compounds*; Pierce Chemical Co., Rockford, IL 1968
2. Zabarnick, S. *Ind. Eng. Chem. Res.* **1994**, 33, 1348-1354
3. Heneghan, S.P., Zabarnick, S. *Fuel* **1994**, 73, 35-43
4. Zabarnick, S. *Energ. Fuels*. **1997**, submitted.

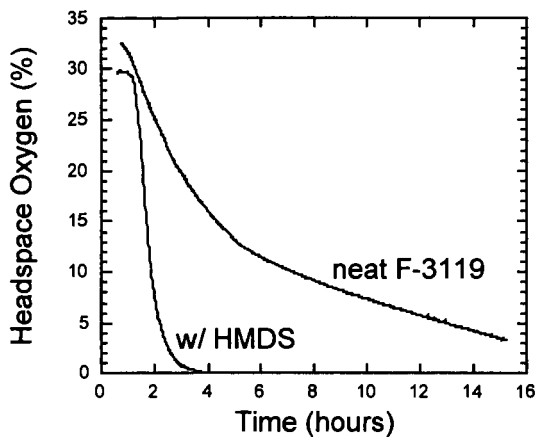


Figure 1. Plots of Headspace Oxygen for Fuel F-3119 with and without HMDS.

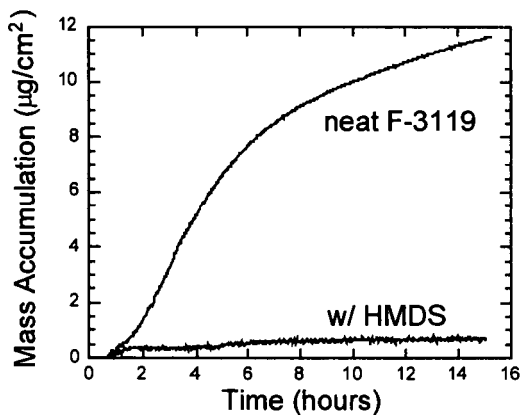


Figure 2. Plots of Mass Accumulation for Fuel F-3119 with and without HMDS.

## REACTION KINETICS IN SUPERCRITICAL FLUIDS

Robert E. Morris<sup>a</sup> and Robert F. Brady, Jr.<sup>b</sup>

<sup>a</sup>Navy Technology Center for Safety & Survivability, Code 6181  
and <sup>b</sup>Materials Synthesis and Processing Branch, Code 6123,  
Naval Research Laboratory, Washington, DC 20375

**KEYWORDS:** supercritical fluids, kinetics, AIBN, jet fuel oxidation

### INTRODUCTION

Supercritical fluids constitute a unique medium for synthesis and processing, particularly near the critical point of the solvent where large changes in solvent properties can be obtained with relatively small changes in pressure. There is relatively little information available concerning the impact of pressure on reaction rates in the vicinity of the solvent critical point, particularly in free-radical processes. In studies of spin-exchange reactions between nitroxide free radicals near the critical point of ethane, Randolph and Carlier (1) found that rate constants were independent of radical concentrations. However, extreme effects of local radical density augmentation were observed due to solvent clustering near the critical point. Cluster lifetimes compared to solute-solute collision probabilities were a determining factor in the ten-fold increase in reaction rates at the critical point. The nature of the transition state will determine how solvent clustering and reactant mobilities will impact reaction rates as the solvent moves from sub- to supercritical conditions. First-order rate constants for the thermal decomposition of  $\alpha$ -chlorobenzyl methyl ether in supercritical 1,1-difluoroethane demonstrated (2) that the greatest impact of small changes in pressure on the rate constants were in those regions where the solvent compressibility was high, i.e., near the critical point. This was explained in terms of changes in dielectric strength of the supercritical solvent, which can influence the solvatochromic transition energy. Partial molar volumes of solutes can reach negative thousands of  $\text{cm}^3/\text{mol}$  in highly compressible near-critical fluids in contrast to very small values in liquid solvents. Such large negative activation volumes and entropies suggest that solvent clusters are more ordered around the transition state than the reactants. Such solvent clustering will exert a significant impact on the reactivity of free radicals in a supercritical fluid.

As fuel temperatures approach approximately 350° - 375°C, many researchers have observed a decline in the amounts of thermal deposits. This has been explained in terms of chemical and physical effects. Since hydroperoxides thermally decompose at approximately 280 - 300°C, this was taken as evidence that deposition is linked to the presence of hydroperoxides. Another explanation proposed for this behavior is that, at these temperatures, components of the fuel can reach a supercritical state. Thus, the increased solvency of the supercritical fuel components was thought to be responsible for redissolving the insoluble products. The critical point of JP-5 fuel has been calculated(3) to occur in the range of 382° - 415°C at 300 - 380 psi (21 - 26 bar). In a series of single tube heat exchanger experiments, Edwards and Zabarnick (4) demonstrated that fuel oxidation chemistry was the determining factor in the amounts of insoluble products formed under those conditions and not simple supercritical solvency effects. However, this work did not address the impact of supercritical conditions on the free radical chemistry. Fuels subjected to conditions where components can reach their critical point may undergo chemical changes that would not necessarily form insoluble products at that time. Electron transfer reactions between metals and fuel constituents would also be mediated by solvent cluster lifetimes, which may play a role in the influence of catalytic metals on fuel properties.

In an effort to bridge the gap between gas phase and liquid phase chemistry, this work has been directed towards elucidating the impact of temperature and pressure on the free radical autoxidation mechanism of hydrocarbons near the critical point. This paper describes the apparatus and methods developed to obtain *in-situ* measurements of reaction kinetics in sub- and supercritical solvents. Some preliminary results of kinetic

measurements of the thermal decomposition of a free-radical initiator, 2,2'-azobis(isobutyronitrile) (AIBN) in supercritical CO<sub>2</sub> are presented.

## EXPERIMENTAL

**Materials.** Carbon dioxide (SCF grade 99.99%, Matheson) was passed through a Chromtech high pressure oxygen and moisture trap and a Chromtech high pressure activated carbon trap to remove hydrocarbons. 2,2'-azobis(isobutyronitrile) (AIBN, Aldrich, 98%) was recrystallized from methanol.

**Apparatus.** The apparatus used to perform *in-situ* optical kinetic measurements is shown in Figure 1. Two ISCO type 100DX 100 mL syringe pumps were coupled via a check valve assembly to allow operation in dual pump mode, to facilitate rapid filling and pressure equilibration of the reactor. The pump cylinders were cooled to facilitate rapid filling. A Rheodyne injection valve was incorporated in a sampling loop to allow for the introduction of liquid modifiers or reactants into the gas stream. A Parr high pressure stirred mini-reactor was fitted with two 2.5 cm dia. x 1.3 cm thick fused silica windows located near the bottom, 180° apart. Reactor vessels with internal volumes of 25 and 450 mL were used in the kinetic experiments. The reactor was fitted with a pressure transducer and a variable restrictor to provide a means for sampling during an experiment for analysis.

Kinetic measurements were obtained optically over the range of 180 to 650 nm. A xenon arc lamp was coupled to a fused silica fiber optic bundle which was focused through the reactor window onto another fiber optic bundle interfaced to an Oriel Multispec 1/8 meter spectrograph. A grating was used that provided a bandpass of 164 nm at a resolution of 0.4 nm with a 50 μ slit. An Oriel Instaspec II 1024 channel photodiode array (PDA) was operated with a personal computer, which allowed for data acquisition at a maximum rate of 62 kHz. Software routines were written to acquire background corrected PDA counts and absorbance measurements at predefined intervals.

Characterization of AIBN decomposition at sub-critical conditions was performed with a HP 6890 gas chromatograph equipped with a nitrogen specific detector. Product characterization was performed using an HP 5890 gas chromatograph with a Finnigan ion trap mass spectrometer detector.

**Kinetic Procedure.** The reactant was placed in the reactor and purged with argon for 5 - 10 minutes then with SFC grade CO<sub>2</sub> for one minute. The reactor was then pressurized to approximately 75.8 bar (1100 psi). After the reactor reached thermal equilibrium, the pressure was adjusted to the desired final pressure by addition of CO<sub>2</sub>. Optical measurements, in background corrected PDA counts, were obtained every 15 min for up to 8 hours. First-order rates were determined from photometric absorbance calculated from the acquired optical measurements.

## RESULTS AND DISCUSSION

In order to study the impact of supercritical solvents on the mechanism of hydrocarbon autoxidation, a model compound that constitutes a convenient source of free-radicals was first examined. The compound, 2,2'-azobis(isobutyronitrile) (AIBN) is commonly used as a free-radical polymerization initiator. The thermal decomposition of AIBN is well known and has been studied in supercritical CO<sub>2</sub> by DeSimone, et al (5). In the initial phase of this study, the kinetics of the thermal decomposition of AIBN were examined in the kinetic reactor described above in supercritical CO<sub>2</sub> at a pressure of 172 bar (2500 psi) and compared with their earlier work (5) performed at 276 bar (4000 psi).

As shown in Figure 2, thermolysis of AIBN generates free-radicals which have been proposed (6) to form in solvent cages. These radicals can either diffuse out of these cages or dimerize to form a transient keteimine adduct (II) that can, in turn dissociate

to regenerate the radicals. Solvent-solute interactions would exert an effect on the relative rates of diffusion out of the solvent cage and combination within the cage to form the adduct shown. Lower AIBN decomposition rates reported (5) in carbon dioxide compared with benzene illustrate the polar nature of the transition state and the impact of local changes in solvent dielectric properties. GC-MS analysis of AIBN in thermally stressed sub-critical benzene in the gas phase shows evidence of concurrent formation of compound II with a decrease in the abundance of the free radicals.

From absorbance measurements obtained during a typical kinetic experiment in supercritical CO<sub>2</sub> at 60°C and 172 bar, AIBN absorbance is shown (Figure 4) at 354.8nm and compound II at 290.1. The corresponding first-order plots of AIBN decomposition and the intermediate formation are shown in Figure 5. From the slopes of these plots, the rate constants ( $k_1$ ) were calculated at 172 bar to be  $7.4 \times 10^{-5} \text{ s}^{-1}$ ,  $1.5 \times 10^{-5} \text{ s}^{-1}$  and  $4.8 \times 10^{-5} \text{ s}^{-1}$  at 40, 50 and 60°C, respectively. The Arrhenius treatment of these data indicated the activation energy for thermal decomposition of AIBN in these experiments to be 80.9 kJ-mol<sup>-1</sup>.

The activation volume of species (x) is often expressed as  $\Delta v^\ddagger = -RT (\ln k_x / dp)_T$ . To examine the effect of pressure on the formation rate of II, kinetic measurements were obtained as a function of pressure at 50°C from 76 to 172 bar. The effect of pressure is clearly shown in Figure 6, where the first-order formation constants ( $k_2$ ) are plotted against pressure. While dielectric changes in carbon dioxide would be small at high pressures, in this region near the critical pressure of CO<sub>2</sub> (73.8 bar), the compressibility is high and local changes in dielectric properties can change by large amounts with small pressure changes. From a plot of the logarithm of  $k_2$  vs pressure, the activation volume for the intermediate product was estimated to be -143 cc/mole.

## SUMMARY

Real-time measurements of reaction kinetics in supercritical solvents has been demonstrated by examination of a model free radical source. However, while the kinetic rates measured in these experiments were self-consistent, they are higher by from 3 to 9 times than the values reported (5) for  $k_1$  at 276 bar. Moreover, the activation energy determined from these measurements was also lower than expected. Current efforts are underway to resolve these discrepancies before the work is extended to include radical trapping compounds and hydroperoxides.

## ACKNOWLEDGEMENTS

Funding for this work was provided by the Office of Naval Research.

## LITERATURE CITED

- (1) Randolph, T. W. and Carlier, C. *J. Phys. Chem.* **1992**, *96*, 5146.
- (2) Johnston, K. P. and Haynes, C. *AIChE J.* **1987**, *33* (12), 2017.
- (3) Martel, C. R. Air Force Aviation Fuel Thermal Oxidation Stability R&D. In *Jet Fuel Thermal Stability*, NASA TM 79231; Taylor, W. F., Ed.; NASA Lewis Research Center: Cleveland, OH, November 1978; pp 41-52.
- (4) Edwards, T and Zabarnick, S. *Ind. Eng. Chem. Res.* **1993**, *32* (12) 3117.
- (5) Guan, Z.; Combes, J. R.; Menciloglu, Y. Z. and DeSimone, J. M. *Macromolecules*, **1993**, *26*, 2663.
- (6) Wu, Chin-Hua S.; Hammond, G. S.; Wright, J. M. *J. Am. Chem. Soc.* **1960**, *82*, 5386.

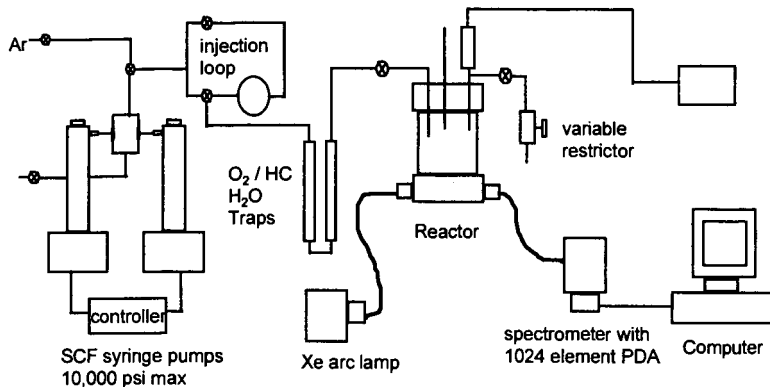


**Figure 1.** Schematic representation of apparatus for performing kinetic measurements in supercritical media.

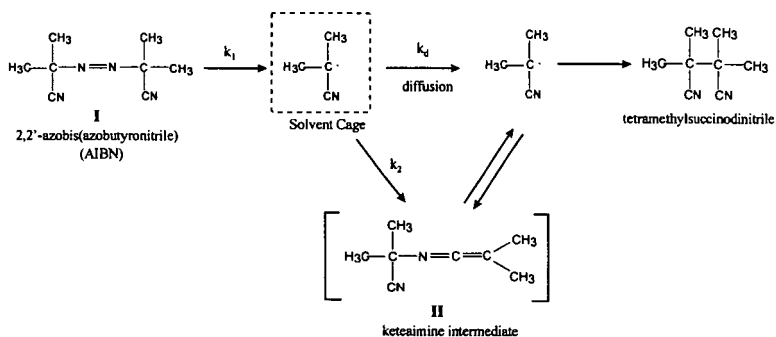


**Figure 2.** Thermal decomposition mechanism of AIBN (DeSimone, 1993)

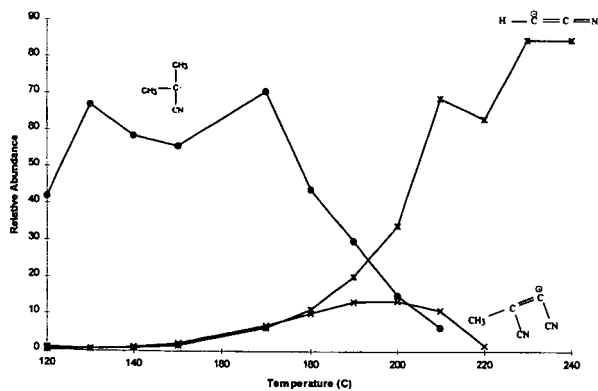


**Figure 3.** Major thermal decomposition products of AIBN in benzene at sub-critical conditions.

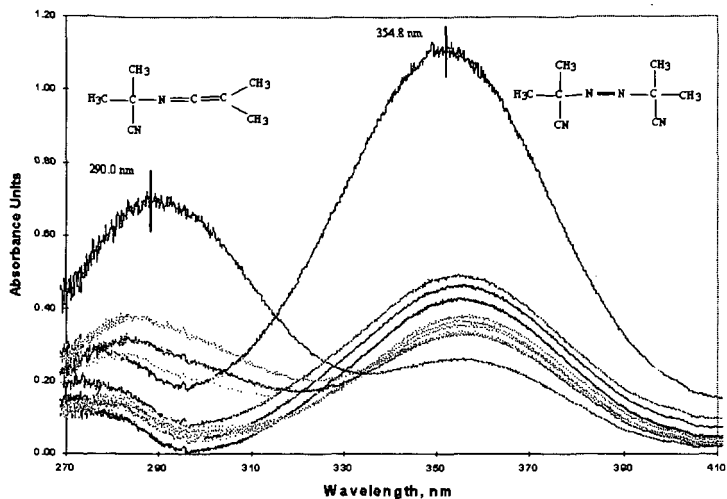


**Figure 4.** Absorption characteristics of AIBN thermal decomposition of AIBN in supercritical  $\text{CO}_2$  at  $60^\circ\text{C}$  and 172 bar (not all scans shown).

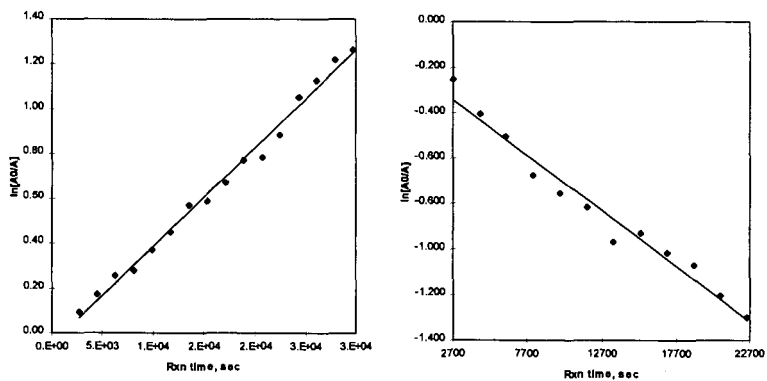


**Figure 5.** First order plots of AIBN thermal decomposition (left chart) and intermediate formation (right chart).

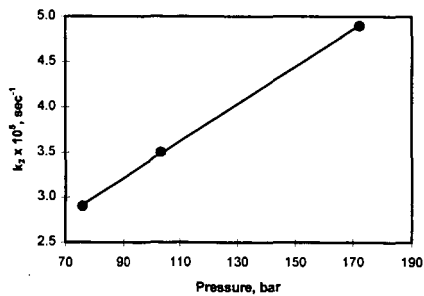


**Figure 6.** Variation of first order formation rate of ketamine intermediate with pressure.

# SUPERCritical-PHASE THERMAL DECOMPOSITION OF JET FUEL COMPONENTS: MODEL COMPOUND STUDIES

Jian Yu and Semih Eser  
Fuel Science Program  
Department of Materials Science and Engineering  
209 Academic Projects Building  
The Pennsylvania State University  
University Park, PA 16802

## INTRODUCTION

In an advanced aircraft, the fuel is the primary sink for the heat generated on board. With the development of high-speed aircraft, it is expected that the future fuel system will be operating at high-temperature supercritical conditions because of the increased thermal load (Edwards and Zabarnick, 1993). At high-temperature supercritical conditions, the fuel may decompose to form solid deposits. Solid deposition in various fuel system components, such as valves, filters, and fuel lines, could create serious problems in the operation and maintenance of aircraft. It is important to study supercritical fuel decomposition process in order to develop thermally stable jet fuels.

In this work, the thermal decomposition of *n*-decane (*n*-C<sub>10</sub>), *n*-dodecane (*n*-C<sub>12</sub>), *n*-tetradecane (*n*-C<sub>14</sub>), *n*-butylbenzene (BBZ), *n*-butylcyclohexane (BCH), decalin (DHN), and tetralin (THN) was studied under supercritical conditions. The results from thermal decomposition of C<sub>10</sub>-C<sub>14</sub> normal alkanes have been reported previously (Yu and Eser, 1997a, 1997b) and were presented here for completeness. These model compounds were selected because they are typical components found in jet fuels. It has been shown that both petroleum-derived and coal-derived fuels contain significant amounts of long-chain alkanes, alkylbenzenes, and alkylcycloalkanes (Lai and Song, 1995a, 1995b). The coal-derived fuels also contain significant amounts of decalins and tetralins.

## EXPERIMENTAL

Most of the model compounds used in this study were obtained from Aldrich. The *n*-butylbenzene and *n*-butylcyclohexane were obtained from TCI America. The purities of all compounds were higher than 99%. Decalin consisted of 47.90% of *cis*-decalin and 51.88% of *trans*-decalin as well as a small amount of tetralin and other impurities. All model compounds were used as received. Table I shows the critical properties of the model compounds.

Thermal reaction experiments were carried out at 400–475 °C and 10–100 atm (initial pressure) in a Pyrex glass tube reactor and, in some cases, in a 316 stainless steel tubing bomb reactor. A fluidized sand bath was used to heat the reactor. Before an experiment was started, the sand bath was preheated to the desired temperature. The reactor was then plunged into the bath. The heat-up period for the glass tube to reach 450 °C was less than two minutes and the corresponding value for the tubing bomb was about four to five minutes. It was found that the temperature of the sand bath was very uniform and was always within ±1 °C of the desired temperature after the heat-up period. After a given reaction time the reactor was removed from the bath and was cooled down using pressurized air (the glass tube) or quenched in cool water (the tubing bomb). The reaction products from the tubing bomb experiments were separated into gases and liquids for analysis. The gaseous products from glass tube experiments were not collected because of the extremely low gas yields.

The liquid products were analyzed quantitatively by a Perkin Elmer 8500 GC equipped with a DB-17 capillary column and a flame ionization detector (FID). The compounds in the liquid products were identified by gas chromatography-mass spectrometry (GC-MS) using a Hewlett Packard (HP) 5890 II GC connected with an HP 5971A mass selective detector. The identifications of the major compounds were also made by running standard mixtures. The gaseous products from the tubing bomb experiments were analyzed quantitatively using a Perkin Elmer AutoSystem gas chromatograph (GC) equipped with two different columns and detectors. One stainless steel column packed with 80/100 Chemipack C18 was used to determine the yields of C<sub>1</sub>-C<sub>6</sub> gases with an FID. The other stainless steel column packed with 60/80 Carboxen-1000 was used to determine the yields of H<sub>2</sub>, CO, CO<sub>2</sub>, CH<sub>4</sub>, C<sub>2</sub>H<sub>2</sub>, C<sub>2</sub>H<sub>4</sub>, and C<sub>2</sub>H<sub>6</sub> with a thermal conductivity detector (TCD). The gaseous products were identified and quantified by using standard gas mixtures.

## RESULTS AND DISCUSSION

**Kinetics.** Previous studies show that thermal decomposition of hydrocarbons usually follows a first-order rate law (Steacie, 1946; Fabuss et al., 1964). Therefore, the rate constants were determined by the following first-order expression:

$$k = \frac{1}{t} \ln \frac{1}{1-x} \quad (1)$$

where  $x$  is the fraction of the reactant converted (conversion),  $k$  is the rate constant ( $\text{h}^{-1}$ ), and  $t$  is the reaction time (h). The conversions were obtained from the thermal decomposition experiments in the glass tube reactor at different temperatures for different times. A fixed loading ratio, defined as the ratio of the initial sample volume to the reactor volume, of 0.36 was used in the experiments.

Figure 1 shows the relationship between  $\ln[1/(1-x)]$  and time for the thermal decomposition of *n*-butylbenzene. Similar linear relationships between  $\ln[1/(1-x)]$  and time were obtained for the decomposition of other model compounds. From the slopes of the lines in Figure 1, the first-order rate constants at different temperatures can be obtained. Table 2 shows the calculated first-order rate constants for the thermal decomposition of seven model compounds. From Table 2 one can see that for the three *n*-alkanes, the first-order rate constant increases with the increasing carbon number (at the same temperature). Among  $\text{C}_{10}$  hydrocarbons, the rate constant decreases in the order of  $\text{BBZ} > \text{n-C}_{10} > \text{BCH} > \text{DHN} > \text{THN}$ .

According to the first-order rate constants shown in Table 2, the apparent activation energies ( $E_a$ , kcal/mol) and preexponential factors ( $A$ ,  $\text{h}^{-1}$ ) can be determined using the following Arrhenius law:

$$k = A \exp(-E_a / RT) \quad (2)$$

Figure 2 shows the Arrhenius plots from the thermal decomposition of model compounds. The apparent activation energies and preexponential factors obtained from the Arrhenius plots are also shown in Table 2. The slight differences between the apparent activation energies for the three *n*-alkanes may arise from the experimental uncertainty.

**Product Distributions.** The reaction products from the thermal decomposition of  $\text{C}_{10}$ – $\text{C}_{14}$  *n*-alkanes under supercritical conditions can be divided into two categories: those from the primary reactions and those from the secondary reactions of the primary products. The primary products include *n*-alkanes from  $\text{C}_1$  to  $\text{C}_{m-2}$  ( $m$  = number of carbon atoms in the reactant) and 1-alkenes from  $\text{C}_2$  to  $\text{C}_{m-1}$ . The secondary products include *cis*- and *trans*-2-alkenes, *n*- $\text{C}_{m-1}$ , *n*- $\text{C}_{m+1}$ , and  $\text{C}_{m-2}$  to  $\text{C}_{2m-2}$  normal and branched alkanes. There are also small amounts of cyclopentanes and cyclohexanes. The yields of branched alkanes lighter than the reactant are not significant until high conversions are reached.

The liquid products from thermal decomposition of *n*-butylbenzene can also be divided into the primary products and the secondary products. The primary products include toluene, styrene, ethylbenzene, benzene, allylbenzene, and tetralin. The secondary products include *n*-pentane, 2-methylbutane, *n*-propylbenzene, isopropylbenzene, *sec*-butylbenzene, isobutylbenzene, *n*-pentylbenzene, 1-propylbutylbenzene, 1,3-diphenylpropane, 1,4-diphenylbutane, 1,3-diphenylhexane, and three other  $\text{C}_6$ -diphenyls. At higher conversions (> 30%), more than 150 liquid compounds were found. The gaseous products from thermal decomposition of *n*-butylbenzene include hydrogen, methane, ethane, ethylene, propane, and propylene.

The liquid products from *n*-butylcyclohexane thermal decomposition include the primary products cyclohexane, methylenecyclohexane, cyclohexene, methylcyclohexane, vinylcyclohexane, allylcyclohexane, ethylcyclohexane, some  $\text{C}_{10}$  alkenes and butylcyclohexenes, and the secondary products 1-methylcyclohexene, 3-methylcyclohexene, methylcyclopentane, 1-ethylcyclohexene, and *n*-propylcyclohexane. Some high-molecular-weight compounds, including *n*-pentylcyclohexane, *n*-hexylcyclohexane, several  $\text{C}_7$  and  $\text{C}_8$ -cyclohexanes, dicyclohexylmethane, dicyclohexylethane,  $\text{C}_7$ -dicyclohexyl, and  $\text{C}_8$ -dicyclohexyl, were also found. At the highest conversion obtained in this study (39%, 475 °C, 20 min), about 130 peaks were observed from the chromatogram of the liquid products. The gaseous products from thermal decomposition of *n*-butylcyclohexane include hydrogen, methane, ethane, ethylene, propane, propylene, butane, and butene.

The major liquid products from the thermal decomposition of decalin include spiro[4,5]decane, 1-methylcyclohexene, 1-butylcyclohexene, and 1-methylperhydroindan. Also appearing, but in slightly lower yields, are toluene, some C<sub>4</sub>-cyclohexenes, n-butylbenzene, and three unidentified compounds which eluted between trans-decalin and tetralin from the GC column. Some minor products include cyclohexane, cyclohexene, methylcyclopentane, methylcyclohexane, 3-methylcyclohexene, methylenecyclohexane, benzene, ethylbenzene, n-butylcyclohexane, tetralin, naphthalene, and some high molecular weight compounds. At 450 °C for 60 min, about 80 compounds were found in the liquid products. The gaseous products include hydrogen, methane, ethane, ethylene, propane, propylene, butane, and butene.

The most abundant liquid product from thermal decomposition of tetralin under supercritical conditions is 1-methylindan, followed by naphthalene, n-butylbenzene, and 2-methylindan. Also appearing, but in lower yields, are n-propylbenzene, ethylbenzene, and toluene. Hydrogen is dominant gaseous product. Other gases include methane, ethane, ethylene, propane, propylene, butane, and butene.

**Effects of Supercritical Conditions on Product Distributions.** Figure 3 shows the changes in overall molar yields of C<sub>6</sub>-C<sub>13</sub> n-alkanes, C<sub>6</sub>-C<sub>13</sub> 1-alkenes, C<sub>6</sub>-C<sub>12</sub> 2-alkenes, and C<sub>14</sub> normal and branched alkanes with the initial reduced pressure from the thermal decomposition of n-C<sub>14</sub> at 425 °C for 15 min. The initial reduced pressure ( $P_r = P/P_c$ ) was calculated at the given temperature and loading ratio using the Soave-Redlich-Kwong equation of state (Soave, 1972). It can be seen that the overall yield of C<sub>6</sub>-C<sub>13</sub> n-alkanes increases and that of C<sub>6</sub>-C<sub>13</sub> 1-alkenes decreases as pressure increases. The large changes in product distributions with pressure occur in the near-critical region. While the overall yields of C<sub>6</sub>-C<sub>12</sub> 2-alkenes and C<sub>14</sub> alkanes are low at low-pressure sub-critical conditions, their yields become significant at high-pressure supercritical conditions.

Figure 4 shows the effects of pressure on product distributions from the thermal decomposition of n-butylbenzene at 425 °C for 15 min. The major primary products are toluene and styrene. It can be seen that as pressure increases, the styrene yield decreases and the toluene yield increases. In contrast to a higher yield of styrene in the sub-critical region, a higher toluene yield is obtained in the far supercritical region. It is clear that high-pressure supercritical conditions suppress the formation of styrene. On the other hand, the yields of the high-molecular-weight products increase with the increasing pressure. Although not shown in Figure 4 because of low yields, the yields of some other high-molecular-weight products, such as 1-propylbutylbenzene and three other C<sub>6</sub>-diphenyls, also increase with the increasing pressure.

## CONCLUSIONS

Supercritical-phase thermal decomposition of jet fuel model compounds follows a first-order kinetics. Among the compounds studied, n-butylbenzene exhibited the highest reactivity, followed by n-C<sub>14</sub>, n-C<sub>12</sub>, n-C<sub>10</sub>, n-butylcyclohexane, decalin, and tetralin.

Thermal decomposition of C<sub>10</sub>-C<sub>14</sub> n-alkanes under supercritical conditions gave high yields of C<sub>3</sub> n-alkanes and significant amounts of heavy alkanes which are usually not observed under low-pressure sub-critical conditions. The pyrolyses of n-butylbenzene and n-butylcyclohexane were dominated by side-chain cracking. The formation of significant amounts of diphenylalkanes from pyrolysis of n-butylbenzene under supercritical conditions indicates that the reaction mechanism under these conditions is different from that under lower-pressure sub-critical conditions. The thermal decomposition of decalin and tetralin under high-pressure supercritical conditions was dominated by isomerization reactions. This is different from the results obtained under low-pressure and high-temperature conditions where cracking reactions (for decalin) or dehydrogenation reactions (for tetralin) dominate.

## ACKNOWLEDGMENT

This work was supported by the U.S. Department of Energy, Pittsburgh Energy Technology Center, and the Air Force Wright Laboratory/Aero Propulsion and Power Directorate, Wright-Patterson AFB. Funding was provided by the U.S. DOE under Contract DE-FG22-92PC92104. We would like to express our gratitude to Prof. Harold H. Schobert of Penn State for his support. We thank Mr. W. E. Harrison III and Dr. T. Edwards of AFWL/APPD and Dr. S. Rogers of PETC for many helpful discussions.

## REFERENCES

1. Daubert, T. E.; Danner, R. P. *Physical and Thermodynamic Properties of Pure Chemicals; Design Institute for Physical Property Data, AIChE: Washington, DC, 1992.*
2. Edwards, T.; Zabarnick, S. *Ind. Eng. Chem. Res.* **1993**, *32*, 3117.
3. Fabuss, B. M.; Smith, J. O.; Satterfield, C. N. *Adv. Petro. Chem. Refin.* **1964**, *9*, 157-201.
4. Lai, W.-C.; Song, C. *Fuel*, **1995a**, *74*, 1436.
5. Lai, W.-C.; Song, C. In *Advanced Thermally Stable Jet Fuels*, Technical Progress Report, April 1995 – June 1995, The Pennsylvania State University, August 1995b.
6. Soave, G. *Chem. Eng. Sci.* **1972**, *27*, 1197.
7. Steacie, E. W. R. *Atomic and Free Radical Reactions*; Reinhold: New York, 1946.
8. Teja, A. S.; Lee, R. J.; Rosenthal, D. J.; Anselme, M. *Fluid Phase Equil.* **1990**, *56*, 153.
9. Yu, J.; Eser, S. *Ind. Eng. Chem. Res.* **1997a**, *36*, 574.
10. Yu, J.; Eser, S. *Ind. Eng. Chem. Res.* **1997b**, *36*, 585.

Table 1. Critical Properties of Model Compounds

	$T_c$ , °F	$T_c$ , °C	$P_c$ , psia	$P_c$ , atm
n-C <sub>10</sub> <sup>a</sup>	652	345	304	20.7
n-C <sub>12</sub> <sup>a</sup>	725	385	262	17.9
n-C <sub>14</sub> <sup>a</sup>	786	419	228	15.5
n-butylbenzene <sup>b</sup>	729	387	419	28.5
n-butylcyclohexane <sup>b</sup>	741	394	373	25.4
cis-decalin <sup>b</sup>	804	429	470	32.0
trans-decalin <sup>b</sup>	777	414	411	28.0
tetralin <sup>b</sup>	837	447	525	35.7

<sup>a</sup> Teja et al. (1990). <sup>b</sup> Daubert and Danner (1992).

Table 2. Kinetic Parameters for Thermal Decomposition of Model Compounds

reactant	rate constant, h <sup>-1</sup>				$E_a^a$	log A <sup>b</sup>
	400 °C	425 °C	450 °C	475 °C		
n-C <sub>10</sub>	0.0341	0.174	0.758		60	18.0
n-C <sub>12</sub>	0.0453	0.231	1.13		62	18.8
n-C <sub>14</sub>	0.0640	0.364	1.67		63	19.3
BBZ	0.0891	0.422	1.72		57	17.6
BCH		0.0613	0.313	1.40	65	19.1
DHN		0.0238	0.132	0.669	69	20.1
THN		0.0090	0.0370	0.139	58	16.1

<sup>a</sup>  $E_a$ , apparent activation energy in kcal/mol. <sup>b</sup> A, preexponential factor in h<sup>-1</sup>.

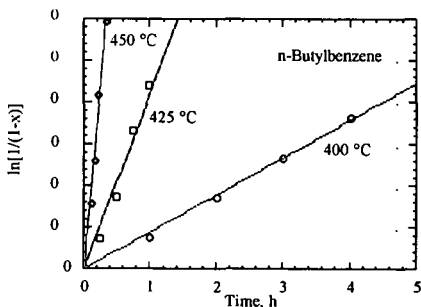


Figure 1.  $\ln[1/(1-x)]$  versus time from thermal decomposition of n-butylbenzene.

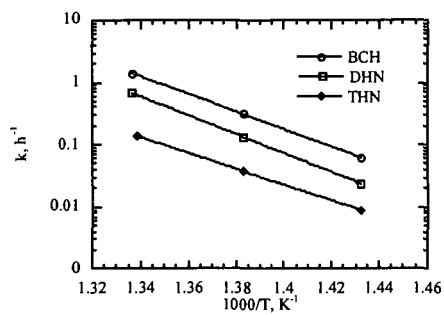
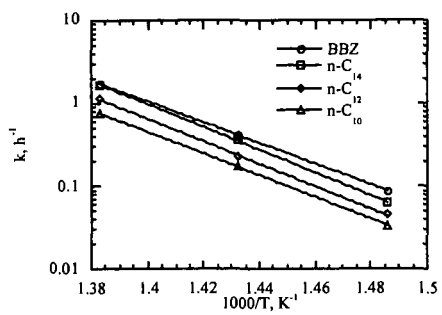


Figure 2. Arrhenius plots from thermal decomposition of jet fuel model compounds

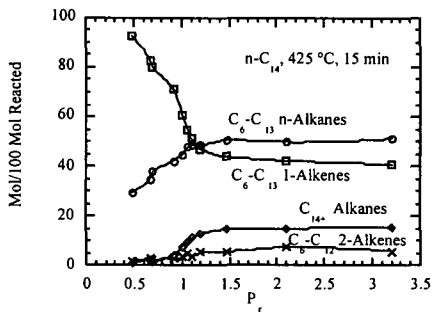


Figure 3. Product yields versus  $P_r$  from  $n\text{-C}_{14}$  at  $425\text{ }^\circ\text{C}$  for 15 min.

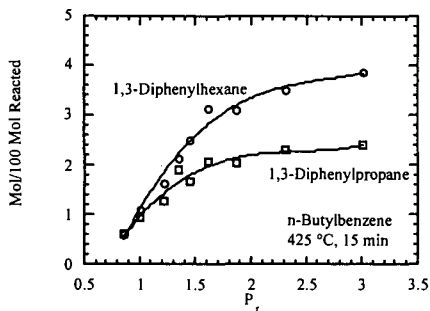
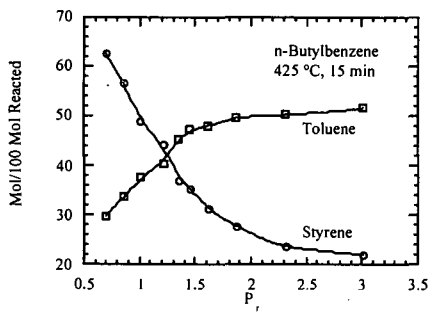


Figure 4. Product yields versus  $P_r$  from  $n\text{-butylbenzene}$  at  $425\text{ }^\circ\text{C}$  for 15 min.

# SUPERCritical-PHASE THERMAL DECOMPOSITION OF JET FUEL COMPONENTS: MIXTURE STUDIES

Jian Yu and Semih Eser  
Fuel Science Program  
Department of Materials Science and Engineering  
209 Academic Projects Building  
The Pennsylvania State University  
University Park, PA 16802

## INTRODUCTION

Jet fuels consist of hundreds of compounds, including long-chain alkanes, alkylbenzenes, and alkylcyclohexanes (Lai and Song, 1995). Coal-derived fuels also contain significant amounts of decalins and tetralins. In a previous paper (Yu and Eser, 1998), we have presented the results from the thermal decomposition of some typical jet fuel model compounds, including C<sub>10</sub>-C<sub>14</sub> n-alkanes, n-butylbenzene (BBZ), n-butylcyclohexane (BCH), decalin, and tetralin, under supercritical conditions. The studies on pure model compounds have provided valuable information on jet fuel thermal decomposition. However, these studies can not answer the question on how individual compounds interact with each other during the thermal reactions of jet fuels.

In this work, the thermal decomposition of some binary mixtures of jet fuel model compounds was studied under supercritical conditions. Five binary mixtures were used in this study, including n-C<sub>12</sub>/n-C<sub>10</sub>, n-C<sub>12</sub>/n-C<sub>14</sub>, n-C<sub>12</sub>/BBZ, n-C<sub>12</sub>/BCH, and BBZ/BCH. Every mixture consists roughly of 50 wt% of each component.

## EXPERIMENTAL

The n-C<sub>10</sub>, n-C<sub>12</sub>, and n-C<sub>14</sub> were obtained from Aldrich while BBZ and BCH were obtained from TCI America. All model compounds have 99+% purity and were used as received. Thermal reaction experiments were carried out in a Pyrex glass tube reactor with a strain point of 520 °C. In a typical experiment, the reactor was loaded, sealed, and then plunged into a fluidized sand bath preheated to the desired temperature. After a given reaction time, the reactor was removed from the bath and then was cooled down using pressurized air.

A Perkin Elmer 8500 gas chromatograph (GC) equipped with a DB-17 column and a flame ionization detector (FID) was used for the quantitative analysis of liquid products. The compounds in liquid products were identified by gas chromatography-mass spectrometry (GC-MS) using a Hewlett Packard (HP) 5890 II GC connected with an HP 5971A mass selective detector. The identifications of major compounds were also made by running standard mixtures. The gaseous products were not analyzed because of the extremely low yields.

## RESULTS AND DISCUSSION

**Reaction Rates.** The changes in conversions of individual model compounds with reaction time were obtained from the thermal decomposition of the mixture at 425 °C for 15-60 min with a loading ratio of 0.36. The loading ratio was defined as the ratio of the initial sample volume at room temperature to the reactor volume. Figure 1 shows the conversion of n-C<sub>12</sub> as a function of reaction time for the thermal decomposition of the pure compound, in n-C<sub>12</sub>/n-C<sub>10</sub> mixture, and in n-C<sub>12</sub>/n-C<sub>14</sub> mixture. One can see that the conversion of n-C<sub>12</sub> is affected by the presence of the second compound. While the conversions for the decomposition of n-C<sub>12</sub> in n-C<sub>12</sub>/n-C<sub>14</sub> mixture are higher than those for the decomposition of pure n-C<sub>12</sub>, the conversions of n-C<sub>12</sub> in n-C<sub>12</sub>/n-C<sub>10</sub> mixture are slightly lower than those for the decomposition of pure n-C<sub>12</sub>. These results suggest that the lighter alkane inhibits the decomposition of the heavier one while the heavier alkane accelerates the decomposition of the lighter one.

Figure 2 shows the conversion of n-C<sub>12</sub> as a function of reaction time for the thermal decomposition of the pure compound, in n-C<sub>12</sub>/BBZ mixture, and in n-C<sub>12</sub>/BCH mixture. It can be seen that the presence of BBZ accelerates the decomposition of n-C<sub>12</sub> and the presence of BCH inhibits the decomposition of n-C<sub>12</sub>. The increased decomposition rate of n-C<sub>12</sub> in the presence of BBZ can be explained by the increased radical concentration, resulting from the much faster initiation reaction of BBZ. The increase in radical concentration leads to an increase in the rates of hydrogen abstraction from n-C<sub>12</sub> and thus an increase in n-C<sub>12</sub> decomposition rates. On the other hand, the addition of BCH to n-C<sub>12</sub> reduces the radical concentration for the

decomposition of n-C<sub>12</sub> because some of the radicals produced from n-C<sub>12</sub> decomposition abstract hydrogen atoms from BCH instead of n-C<sub>12</sub>.

Figure 3 shows a comparison of BBZ conversions from the thermal decomposition of pure BBZ, in BBZ/n-C<sub>12</sub> mixture, and in BBZ/BCH mixture, under similar conditions. It seems that n-C<sub>12</sub> and BCH exhibit very similar inhibiting effect on the decomposition of BBZ. This is probably due to very comparable hydrogen abstraction rates from C<sub>12</sub> and BCH by free radicals. The decomposition of BBZ is inhibited by the addition of n-C<sub>12</sub> or BCH because some of the radicals, which would abstract hydrogen atoms from BBZ in the absence of n-C<sub>12</sub> or BCH, abstract hydrogen atoms from n-C<sub>12</sub> or BCH. Since the rates of hydrogen abstraction from n-C<sub>12</sub> and BCH are comparable, both compounds exhibit similar inhibiting effect on the decomposition of BBZ.

**Product Distributions.** The major components in liquid products from supercritical-phase thermal decomposition of n-C<sub>12</sub>/BBZ mixture were identified. Figure 4 shows the GC chromatogram of the liquid products from n-C<sub>12</sub>/BBZ mixture at 425 °C for 60 min with an initial reduced pressure ( $P_r = P/P_c$ ) of 2.04. The initial reduced pressure was calculated at the given temperature and loading ratio using the Soave-Redlich-Kwong equation of state (Soave, 1972). The products produced from the thermal decomposition of the binary mixture include those found in the decomposition of the pure compounds and those found only in the mixture reactions. The products formed from the decomposition of n-C<sub>12</sub> component include series of n-alkanes and 1-alkenes lighter than n-C<sub>12</sub> and some heavy normal and branched alkanes. The products produced from the decomposition of BBZ component include toluene, styrene, ethylbenzene, benzene, allylbenzene, tetralin, and some secondary products, including n-propylbenzene, isopropylbenzene, sec-butylbenzene, isobutylbenzene, n-pentylbenzene, 1-propylbutylbenzene, 1,3-diphenylpropane, 1,4-diphenylbutane, and four C<sub>6</sub>-diphenyls. Some products unique to the reaction of the mixture are also formed, including six C<sub>14</sub>-benzenes, a series of high n-alkylbenzenes up to n-dodecylbenzene, a series of 1-propylalkylbenzenes up to 1-propylundecylbenzene, and some other alkylbenzenes with branched side chains.

Figure 5 shows a comparison in product distributions between supercritical and sub-critical conditions. The reactions were carried out at 425 °C for 60 min. Two loading ratios were used: 0.36 (supercritical,  $P_r = 2.04$ ) and 0.08 (sub-critical,  $P_r = 0.77$ ). It can be seen that supercritical conditions favor the formation of n-alkanes, toluene, and high-molecular-weight compounds, and suppress the formation of 1-alkenes and styrene.

## CONCLUSIONS

Individual compounds interact with each other in the thermal reactions of binary mixtures. The compound with low reactivity inhibits the decomposition of the compound with high reactivity while the latter accelerates the decomposition of the former. Supercritical-phase thermal decomposition of n-C<sub>12</sub>/BBZ mixture produces not only the products found in the decomposition of pure compounds but also the products unique to the reaction of the mixture. High-pressure supercritical conditions result in the formation of significant amounts of high-molecular-weight compounds.

## ACKNOWLEDGMENT

This work was supported by the U.S. Department of Energy, Pittsburgh Energy Technology Center, and the Air Force Wright Laboratory/Aero Propulsion and Power Directorate, Wright-Patterson AFB. Funding was provided by the U.S. DOE under Contract DE-FG22-92PC92104. We would like to express our gratitude to Prof. Harold H. Schobert of Penn State for his support. We thank Mr. W. E. Harrison III and Dr. T. Edwards of AFWL/APPD and Dr. S. Rogers of PETC for many helpful discussions.

## REFERENCES

1. Lai, W.-C.; Song, C. *Fuel*, **1995**, *74*, 1436.
2. Soave, G. *Chem. Eng. Sci.* **1972**, *27*, 1197.
3. Yu, J.; Eser, S. This symposium.

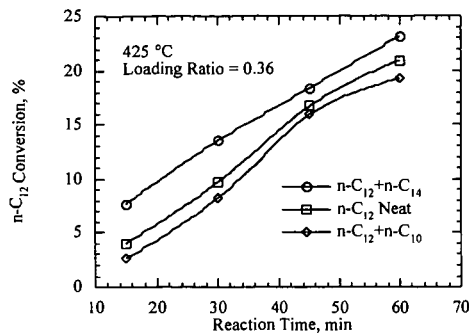


Figure 1. Conversion of n-C<sub>12</sub> versus reaction time from thermal decomposition of pure compound, in n-C<sub>12</sub>/n-C<sub>10</sub> mixture, and in n-C<sub>12</sub>/n-C<sub>14</sub> mixture.

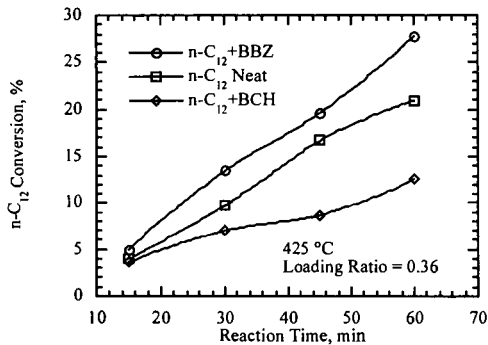


Figure 2. Conversion of n-C<sub>12</sub> versus reaction time from thermal decomposition of pure compound, in n-C<sub>12</sub>/BBZ mixture, and in n-C<sub>12</sub>/BCH mixture.

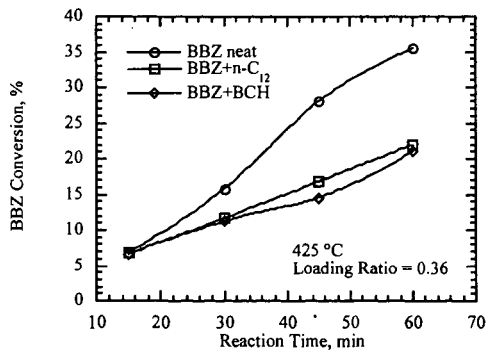


Figure 3. Conversion of BBZ versus reaction time from thermal decomposition of pure compound, in BBZ/n-C<sub>12</sub> mixture, and in BBZ/BCH mixture.

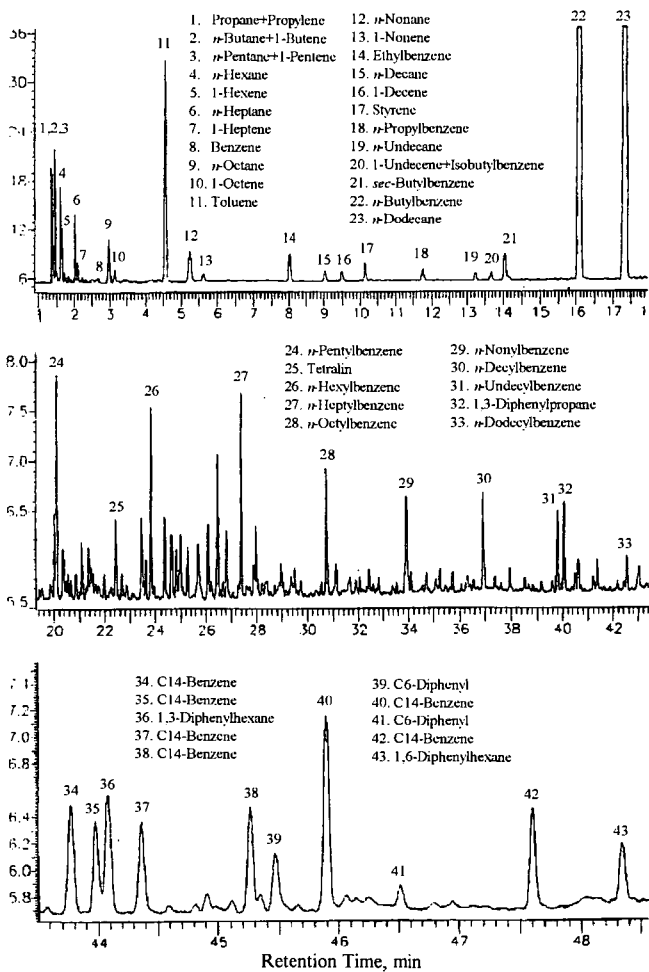


Figure 4. GC chromatogram of liquid products from thermal decomposition of *n*-C<sub>12</sub>/BBZ mixture at 425 °C for 60 min with a loading ratio of 0.36.

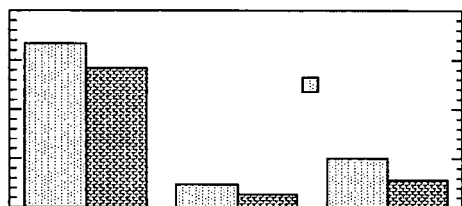
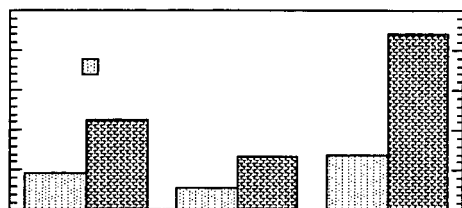
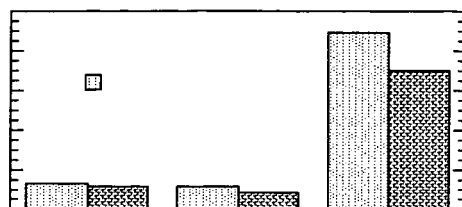


Figure 5. Comparison of product distributions between supercritical and sub-critical conditions.

## THE CHANGING NATURE OF DEPOSITS FORMED DURING THERMAL STRESSING OF JET FUELS

R. Malhotra  
SRI International, Menlo Park, CA 94025

and  
M. A. Serio  
Advanced Fuel Research, East Hartford, CT 06138

### ABSTRACT

A JP-5 fuel was subjected to thermal stress at various temperatures in a flow tube with a wire stretched along its length. The deposits formed on the wire, as well as those collected on a filter were examined by field ionization mass spectrometry. Two distinct kinds of spectra were observed. The first had a picket-fence like appearance and the masses corresponded to long chain alkanes. The spectrum spanned a mass range from about 300 to 500 Da. The alkanes in the fuel have molecular weights ranging from about 130 to 240. These waxy deposits were formed possibly by the coupling of alkyl radicals. The second class of deposits is characterized with a very rich spectrum spanning a mass range from 200 to 800 Da. Evidently, this deposit is formed by the reaction of many different fuel components and not just the alkanes. FT-IR examination of this deposit showed a strong peak due to aromatic C-H stretch. Implications of these two kinds of deposits to the overall thermal instability of jet fuels will be discussed.

### INTRODUCTION

The fuel in an aircraft is subjected to much thermal stress, and in advanced aircraft the degree of thermal stress is only expected to increase. This stress often results in the formation of insolubles that end up depositing on engine parts, fuel lines, and nozzles. In some instances, the deposits at critical points can completely block the flow of fuel to the engine with disastrous consequences. Not surprisingly, therefore, the thermal stability of jet fuels has been the subject of many studies, and jet fuels must pass the JFTOT test for thermal stability before they are deemed acceptable.

In pioneering work, Hazlett demonstrated the importance of autoxidation process in deposit formation during thermal stressing of fuels.<sup>1</sup> This process involves generation of radical species, which initiate a chain reaction with oxygen to give hydroperoxides, which are then considered to react with minor fuel components, that likely contain nitrogen and/or sulfur, to produce insoluble deposits. A substantial amount of work has been performed to elucidate the mechanisms of deposit formation, and many details have been added to this picture; however the essential aspects of this theory have been validated.<sup>2</sup>

A number of attempts have also been made to model the deposit formation. The models often treat all deposits as a lumped component, and proceed to describe the build up as a function of thermal stress (time, temperature).<sup>3</sup> Simple Arrhenius behavior is often assumed, although there is evidence that the observed activation energy in systems at low temperatures (long time) tends to be significantly lower than that observed at high temperatures (short time).<sup>4</sup> This behavior is clearly indicative of a change in the mechanism, and it should be reflected in the models, if they are to correctly describe the phenomena.

In this paper we show that the chemical nature of the deposits at lower and higher temperatures is markedly different. This finding is in concert with the varying activation energies, and might provide a basis for building a more accurate model.

## EXPERIMENTAL

A JP 5 fuel was flowed through a heated, glass-lined, stainless tube (1/8" OD, 0.7" ID, 44" long) at 0.5 mL/min. A stainless steel wire (0.008" dia) was stretched along the center of the tube, and some of the deposits were collected on this wire. The effluent passed through a stainless steel filter (0.2  $\mu\text{m}$ ) where the insolubles were collected. The effluent fuel cools before reaching the filter, and so the deposits on the wire represent materials that are insoluble in the hot fuel, whereas those on the filter are of materials insoluble in the fuel at the lower temperature of the filter. The wire deposits and the filtered deposits were analyzed by an Fourier transform infrared (FTIR) spectrometer and a field ionization mass spectrometer (FIMS).

## RESULTS AND DISCUSSION

FIMS analysis of the fuel showed the molecular weight of the component species ranged from about 120 to 230 Da, with an average value of about 170 Da. The spectrum also shows components with whole range of unsaturation indices, as would be expected of a typical fuel. The FIMS of the deposits collected on the wire and the filter at 150°C are shown in Figure 1. These spectra are characterized by a picket-fence like appearance. The prominent peaks are 14 Da apart and centered around 340 Da. The masses correspond to acyclic alkanes ( $14n + 2$ ), although they could also be due to acyclic ketones. These components are expected to arise from the autoxidation of alkanes. The long-chain waxy products are dimers resulting from the coupling of the alkyl and alkoxy radicals are not likely to be very soluble in the fuel and therefore it is not surprising that they drop out of the solution most readily. The filter deposits collected at 150°C show a very similar spectrum. The amount of the filter deposit was considerably larger, and consequently, the spectrum is less noisy. The filter deposit also shows peaks corresponding to dimers formed by the coupling of species other than acyclic alkanes.

Figure 2 shows the analogous spectra collected at 450°C. Although the amount of the wire deposit collected was larger at the higher temperature, its spectrum—and hence its nature—is essentially the same as that collected at 150°C. In contrast, the spectrum of the filter deposit is very rich, and shows a broad distribution of masses ranging from about 180 to over 800 Da. The waxes seen in the wire deposit are also present, but they are overshadowed by the other components.

FIMS analysis of the deposits clearly shows that the thermal deposits fall into two classes. The first are the alkane-rich waxes, which tend to be more insoluble, plate out even when the fuel is hot. These deposits do not contain much heteroatoms, except for some oxygen. The other class consists of a wide range of compounds, possibly with a much higher heteroatom content. This class of compounds forms later in the sequence, it is more soluble, and precipitates out when the fuel is somewhat cooler. The waxy deposits could also absorb the other fuel components and in effect increase their residence time in the hot zone. If that case, we would expect the rate of deposit formation to increase with time. Indeed, that was observed by Kamin and coworkers<sup>5</sup> when they monitored the deposit formation in a JFTOT with a fiber optic monitor. A preliminary model that incorporates the two different classes of deposits was able to mimic this time dependent variation in the rate of deposit formation.

## REFERENCES

- 1 Hazlett, R. N.; Hall, J. M.; Matson, M, *Ind. Eng. Chem., Prod. Res. Dev.* **1977**, *16*, 171.
- 2 Hazlett, R. N., "Thermal Oxidation Stability of Aviation Turbine Fuels," ASTM Monograph Series, ASTM, Philadelphia, 1991.
- 3 See for example, Heneghan, S. P.; Chin, L. P., *Proceedings of the 5th Intl. Conference on Stability and Handling of Liquid Fuels 1994*, p. 91.
- 4 Private communication from V. Reddy, cited by Heneghan, S. P., *Am. Chem. Soc., Div. Petr. Chem. Preprints* **1991**, *39(1)*, 14.
- 5 Kamin, R. A.; Nowack, C. J.; Darrah, S. ., *Proceedings of the 3rd Intl. Conference on Stability and Handling of Liquid Fuels 1988*, p. 240.

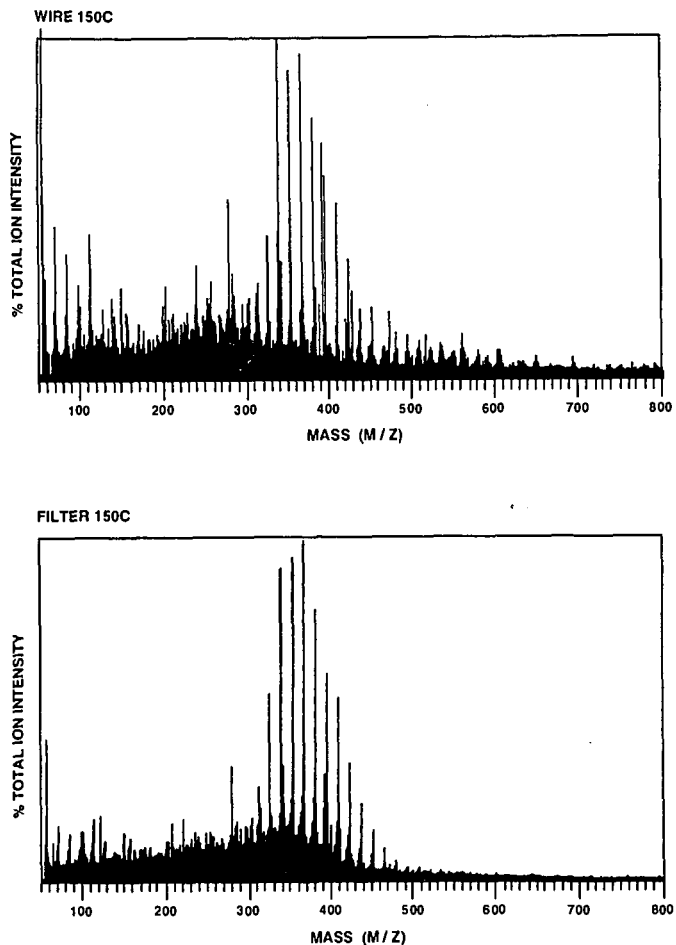


Figure 1. Field ionization mass spectrum of deposits collected on (a) wire and (b) filter from thermal stressing of aerated JP5 at 150°C.

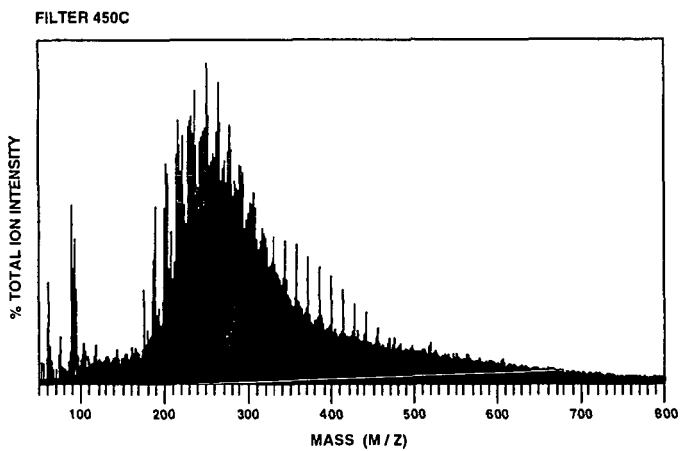
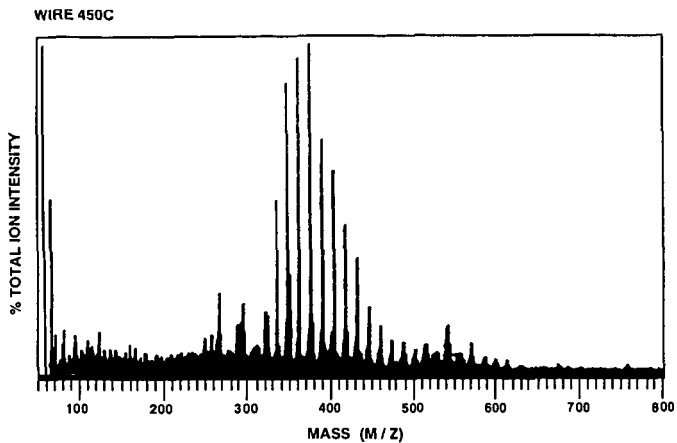


Figure 2. Field ionization mass spectrum of deposits collected on (a) wire and (b) filter from thermal stressing of aerated JP5 at 450°C.

# THERMAL STABILITY MEASUREMENT DEVICES REVISITED: GRAVIMETRIC JFTOT VERSUS SIMULATED TEST RIG

S.G. Pande<sup>1</sup> and D.R. Hardy

Code 6181, Naval Research Laboratory  
Washington, D.C. 20375.

<sup>1</sup>Geo-Centers, Inc. Lanham, MD 20706

**KEYWORDS:** jet fuel thermal stability, temperature, fuel velocity, MDA

## INTRODUCTION

Fuel thermal stability is one of the most critical fuel properties,<sup>1</sup> consequently, a reliable method for its measurement is desirable. The Jet Fuel Thermal Oxidation Tester (JFTOT: ASTM D3241) has been designated as the specification test method for measuring the aviation turbine thermal stabilities of commercial fuels (ASTM D1655), and military fuels (MIL-T-5624). However, JFTOT data have been reported to correlate poorly<sup>2,5</sup> with the thermal deposit results from test rigs that were designed to simulate the aircraft engine fuel system. Two examples of many such simulated test rigs include: (a) the injector feed arm rig (IFAR),<sup>2</sup> which measures burner stem fouling; and (b), the single tube heat transfer rig (STHTR),<sup>3,4</sup> which measures fuel degradation within an oil cooler. Reported disparities between the JFTOT and the IFAR/STHTR have been ascribed to:

(1) The short test duration of the JFTOT (2.5 hr).<sup>2,4</sup> This was the explanation given to account for the beneficial effect of MDA (the commonly used metal deactivator, N,N'-disalicylidene-1,2-propane diamine), observed in the JFTOT, and the innocuous effect of MDA on extended testing in the IFAR.<sup>2</sup>

(2) The differences in flow velocities. For example, in the JFTOT, the fuel flow is laminar (3 mL/min) whereas in aircraft operating systems, the flow is turbulent.<sup>3,5</sup>

To explore these differences, we used the gravimetric JFTOT (grav-JFTOT) since its operating conditions are not only similar to the JFTOT, but it has the added advantage of quantifying both the surface and bulk fuel deposits, based on weight.<sup>6</sup> Furthermore, the grav-JFTOT offers a more sensitive measure of the bulk fuel deposits than the JFTOT because the pore size of its effluent filter is considerably smaller, viz., 0.8 micron versus 17 microns for the JFTOT.

The effect of test duration was examined in a recent study, the results of which do not support the explanation that test duration is a factor. Specifically, we found<sup>7</sup> MDA to be beneficial in a non-copper doped Jet A and JP-5 type (Jet A + antioxidant) fuel, on extended duration testings which were conducted in the grav-JFTOT for approximately 150 hours.

Regarding the effect of fuel velocity on fuel thermal deposition, compared to laminar flow, turbulent flow has been suggested to increase thermal deposition by increasing both the mass transfer of oxygen to the heated surface and the quantity of reactants.<sup>3,8</sup> Nevertheless, on increasing test duration in the IFAR,<sup>2</sup> an underlying variable appears to be a temperature effect. In this paper we report the results of a grav-JFTOT study that was designed to investigate the effects of increasing temperature on thermal deposits, with and without the presence of MDA.

## EXPERIMENTAL

**Materials.** All materials were used as received. The test fuel was a typical, though aged, JP-5. The metal deactivator, N,N'-disalicylidene-1,2-propane diamine, commonly known as MDA, was obtained from Pfaltz and Bauer and used at 5.8 mg/L concentration.

**Procedure.** Thermal stability was determined using the grav-JFTOT. This laminar flow, bench test method gives the weight of total thermal deposits formed when the filtered fuel flowing at 3mL/min, under a back pressure of 500 psi, passes over a stainless strip (grade 302 and approximately 7 cm long, 0.5 cm wide, and 0.025 mm thick), contained in a strip

holder that is heated to 260°C, for 2.5 hours. These are the standard operating conditions of the grav-JFTOT.

However, for the studies conducted, the test temperatures ranged from 165° to 350°C for the neat fuel, and 220 to 350°C for the MDA additized fuel. The overall temperature range of 165° to 350°C was selected to mimic temperature increases in the IFAR, which include: the 165°C inlet fuel temperature and subsequent increases in the inner wall temperature. Specifically, in the IFAR, over a 70-h test duration and at a flow rate of 72 kg/h (approximately 1500 mL/min), the inner wall temperature increased from an initial 300°C to approximately 440°C.

The test duration per test temperature in the grav-JFTOT was 5 hours, and to simulate continuity, the same strip was used in the series of temperature-testings conducted per test fuel. The total deposit is the sum of the deposits formed on the stainless steel strip and the filterables contained in the effluent. The effluent was filtered using two Magna nylon membranes of 0.8 micron pore size. Further details of the method are described elsewhere.<sup>8,9</sup>

## RESULTS AND DISCUSSION

**Neat Fuel.** The effects of increasing wall temperature on thermal deposition in the grav-JFTOT, for the strip and filterable deposits are depicted in Figures 1 and 2, respectively. The overall results indicate a typical deposit distribution pattern for the grav-JFTOT, viz., higher deposition in the filterables than on the strip. Nevertheless, for both types of deposit, similar deposition profiles were observed with an increase in temperature. For example, in the case of the filterables, at 165° to 200°C, thermal deposition is apparently constant and likely simulates the "induction period" observed in the IFAR;<sup>2</sup> as the temperature is increased from approximately 200° to 300°C, deposition increases, but on further increase in temperature, i.e., from approximately 320°-350°C, deposition decreases.

For the temperature range, 200°-300°C, the rate of increase of the total thermal deposit with temperature is in accordance ( $R^2 = 0.99$ ) with the well known Arrhenius rate equation (rate = constant  $\times e^{-E/RT}$ ), where  $E$  is the activation energy,  $R$ , the gas constant, and  $T$ , the temperature in kelvin (see Figure 3). Moreover, calculation of the activation energy gives a value of approximately 83 kJ/mol. The corresponding value (65 kJ/mol) for the same fuel, obtained using a turbulent flow test rig, viz., the Naval Aviation Fuel Thermal Stability device (NAFTS), may be regarded as somewhat similar.

**Comparison with the IFAR.** The thermal deposition profile described above for the grav-JFTOT - wherein thermal deposition was plotted versus temperature - is similar to the IFAR's thermal deposition profile, wherein thermal deposition was plotted versus test duration. Specifically, in the case of the IFAR, with increasing test duration, an initial low rate of deposition, which was interpreted<sup>2</sup> to be an "induction period" is followed by an increase, then a decrease in thermal deposition.<sup>2</sup>

Furthermore, in the IFAR, the increase in deposition with test duration is concomitant with an increase in the inner wall temperature ( $\Delta TIW$ ), since  $\Delta TIW$  was the parameter used to measure thermal deposition. Use of the  $\Delta TIW$  parameter is based on the relationship<sup>2</sup> that the weight of carbon  $\propto [\Delta TIW]^2$ . Consequently, based on the above analyses, the operative variable between the two test devices is likely related to a temperature effect and not to a difference in flow velocity. In addition, the "induction period" that is reported to occur<sup>2</sup> can also be ascribed to a temperature effect as demonstrated in the profiles of the plots in Figures 1 and 2.

**MDA Additized Fuel.** For the MDA additized fuel, the strip and filterable thermal deposition profiles versus temperature show similar trends to that of the neat fuel, but the rate of deposition differed significantly with the type of deposit measured (Figures 1 and 2). For example, relative to the neat fuel, the rate of increase of the *strip* deposit was significantly lower in the MDA additized fuel. In contrast, the rate of increase of the *filterable* deposits of the MDA additized fuel was fairly similar to that of the neat fuel. These differences may well explain the beneficial effect of MDA observed in the JFTOT, where mainly the surface tube deposits are measured, versus the innocuous effect observed in the IFAR, on increasing test duration.<sup>2</sup> The diminished performance of MDA on increasing test duration in the IFAR,<sup>2</sup> may

will be due to a temperature effect, specifically, to the relative stability of MDA as the IFAR's initial inner wall temperature increases (see below). Possible breakdown of the MDA molecule at high temperatures (no numerical values given) has been suggested by Clark *et al.*<sup>10</sup>

**Realistic operating conditions/temperature effect.** Temperature is considered to be the most important physical factor in fuel thermal deposition.<sup>11</sup> The initial operating conditions in the IFAR (e.g., inner wall temperature of 300°C) were selected to represent a severe condition.<sup>2</sup> However, this severity is further exacerbated by subsequent temperature increases with increasing test duration. Such temperature increases likely exceed realistic operating conditions. Consequently, at inner wall temperatures above 300°C, the results obtained in the IFAR are flawed. Thus, the innocuous effect observed with MDA, on increasing test duration, is also likely flawed.

## CONCLUSIONS

The overall results suggest that the underlying variable between laminar and turbulent flow test devices for measuring thermal stabilities is a temperature effect and not their differences in flow velocities. Thus, the initial low rate of deposition observed in the turbulent flow test rigs, which was interpreted as an "induction period" is likewise a function of temperature.

At increasing test temperatures, the beneficial effect of MDA observed in the JFTOT (ASTM D3241) may well be related to the type of deposit measured, viz., surface deposit. In contrast, thermal deposition based on the corresponding filterable deposits, which comprise the bulk of the total deposits in the grav-JFTOT, is in agreement with the findings observed in turbulent test rigs for neat and MDA-doped jet fuels.

Consequently, the diminished performance of MDA/innocuous effect observed on increasing test duration in the IFAR, may be related to an increase in temperature effect. However, in the IFAR, the MDA results are likely flawed since its operating conditions, on increasing test duration, are not only severe but unrealistic. In conclusion, on the basis of test conditions, particularly, the very important parameter, temperature, the gravimetric JFTOT offers a more realistic measurement of fuel thermal stability than the IFAR.

**ACKNOWLEDGMENTS.** The authors thank the Office of Naval Research (Dr. M. Soto) for funding support.

## LITERATURE CITED

- (1) Lyon, T.F., Fuel Thermal Stability Outlook for GE Aircraft Engines in 1991; In *Aviation Fuel Thermal Stability Requirements*, ed Kirklin, P.W. and David, P., ASTM STP 1138, American Society for Testing and Materials: Philadelphia, PA., May 1992, p. 73.
- (2) Kendall, D.R.; Houlbrook, G.; Clark, R.H.; Bullock, S.P.; Lewis, C. The Thermal Degradation of Aviation Fuels in Jet Engine Injector Feed Arms. Part I. - Results from a Full Scale Rig. Presented at the Tokyo International Gas Turbine Congress, October, 26-31, Tokyo, Japan, 1987, Paper 87-IGTC-49.
- (3) Kendall, D.R. and Mills, J.S., SAE Technical Paper Series, 851871, Society of Automotive Engineers: Warrendale, PA, 1985.
- (4) Clark, R.H. The Role of a Metal Deactivator in Improving the Thermal Stability of Aviation Kerosines. Presented at the *3rd International Conference on the Stability and Handling of Liquid Fuels*: London, September 1988, Paper No. 47, p.283, Institute of Petroleum, 1989.
- (5) Clark, R.H.; Stevenson, P.A. *Prepr.-Am. Chem. Soc., Div. of Fuel Chem.* **1990**, 35, 1302.
- (6) Beal, E.J.; Hardy, D.R.; Burnett, J.C. In (a) *Proceedings of the 4th International Conference on Stability and Handling of Liquid Fuels*: Orlando, FL, Nov. 1991, pp. 245-259. (b) *Aviation Fuels Thermal Stability Requirements*, ASTM STP 1138; Kirklin, P.W.; David, P., Eds; American Society for Testing and Materials: Philadelphia, PA, 1992, pp. 138-150.

(7) Pande, S.G. and Hardy, D.R. accepted for publication in *Energy and Fuels*, **1998**.

(8) Clark, R.H. and Thomas, L. SAE Technical Paper Series, 881533, Society of Automotive Engineers: Warrendale, PA, 1988.

(9) Pande, S.G.; Hardy, D.R. *Energy and Fuels* **1995**, *9*, 177-182.

(10) Clark, R.H.; Delargy, K.M.; Heins, R.J. *Prepr.-Am.Chem. Soc., Div. Fuel Chem.* **1990**, *35*, (4), 1223.

(11) Hazlett, R.N. *Thermal Oxidation Stability of Aviation Turbine Fuels*; ASTM Mongraph 1, American Society of Testing and Materials: Philadelphia, 1991, page 51.

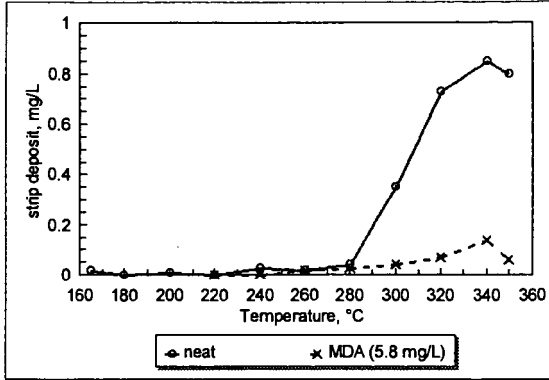


Figure 1. Effect of temperature on strip thermal deposit for a JP-5 fuel: with and without MDA.

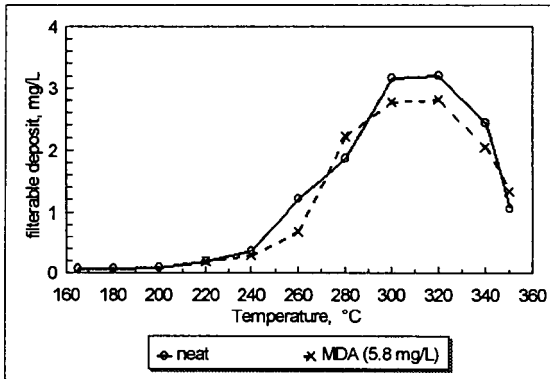


Figure 2. Effect of temperature on filterable thermal deposits for a JP-5 fuel: with and without MDA.

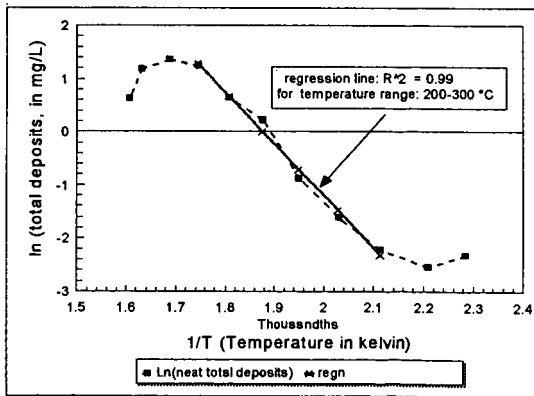


Figure 3. Arrhenius plot of total gravimetric JFTOT deposits formed at test temperatures, 165-350°C for a JP-5 fuel.

# ANALYTICAL SEPARATION AND QUANTITATION OF SPECIFICATION LEVELS OF MDA IN AVIATION FUELS

R.C. Striebich, R. R. Grinstead and S. Zabarnick  
Aerospace Mechanics Division, KL-463  
University of Dayton Research Institute  
300 College Park  
Dayton, Ohio 45469-0140

## INTRODUCTION

Metal deactivator additive (MDA) has been used for the past fifty years to chelate metals which accelerate oxidation reactions in distillate materials (1). Presently, MDA is added to aviation fuel in the concentration range of 0 - 5.8 mg/L. Because of its surface activity and adsorptive properties, MDA may be reduced in concentration as the fuel is handled. Also, as fuels are used to cool hotter aircraft engine components, metal concentrations may increase due to degradation of fuel system materials. Consequently, reduced concentrations of MDA may be insufficient to prevent accelerated autoxidation reactions. The ability to measure the concentration of MDA in storage stability tests, thermal stressing studies and additive addition in the field is important to the success of new thermal stability additives such as JP-8+100 (2).

This work describes a new technique for the determination of metal deactivator additive in aviation fuels and provides some examples of how this measurement can be used to understand the role and fate of MDA in thermally-stressed fuel systems. Several techniques are available in the literature which were not satisfactory for use with distillate fuels having high polars content, low levels of MDA, or for thermally stressed fuels (3,4,5). The technique described herein may be used for specification level analysis of small amounts of sample (200  $\mu$ L) without analyte concentration or significant sample preparation.

### Direct Analysis of MDA

Previous work has been performed in which gas chromatography - mass spectrometry (GC-MS) and similar chromatographic techniques were used to measure MDA concentration directly. However, the polarity and surface activity of MDA made direct detection impossible without specially deactivated chromatographic columns, split liners, and glass wool. Unfortunately, detection limits, detector linearity, and repeatability continued to be poor, even after the activities of these surfaces were reduced. Calibration curves for MDA in toluene indicated detection limits of 10 - 20 mg/L typically, with even higher detection limits for more complex solvent matrices. In order to lower the detection limits, silica gel solid-phase extraction (50:1 concentration) was performed for most aviation fuel samples, concentrating the polar fuel components and improving detectability. Although this technique was used to track MDA disappearance in thermally stressed systems, sample preparation time and reproducibility/repeatability were unacceptable.

### Chemical Derivatization

The analysis of MDA was performed by reacting this highly adsorptive polar compound with the silylating agent N,O-bis[trimethylsilyl]acetamide (BSA) to form the derivatized product as shown:



non-zero, indicating a lower detection limit of approximately 0.5 mg/L, possibly due to adsorption of the MDA on the glass vial before the BSA is added.

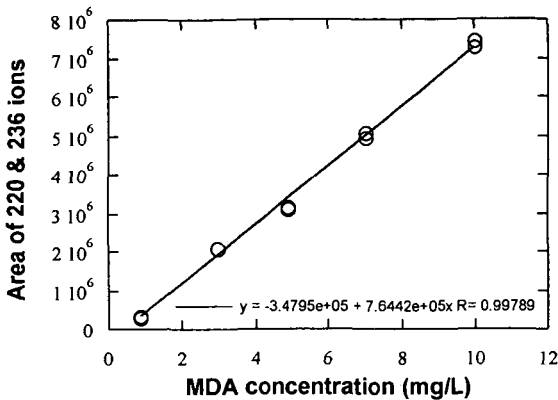


Figure 2. Typical calibration for derivatized MDA in a reference kerosene.

The lower detection limit (approximately 0.5 mg/L) of MDA as shown in figure 2 was affected by the adsorption of MDA to the glass insert and other surfaces to which the MDA is exposed. If BSA is added to a 10 mg/L MDA solution and the derivatized MDA serially diluted with kerosene to produce analytes between 0 and 1 mg/L, the minimum detectable level of MDA derivative is greatly decreased and linearity of detection greatly improved. This observation is consistent with MDA being adsorbed to active sites in the glass vial which have high surface to volume ratios, affecting the lower level standards more than higher level standards. The use of plastic inserts did not improve the amount of MDA adsorbed before it could be derivatized. Further studies may be conducted to see if surface deactivation (using an MDA wash solution) would enhance lower level detection of the additive.

#### Effect of Fuel Matrix on Measurement

A series of Jet A and JP-5 aviation fuels were spiked with a known amount of MDA. These samples were treated with BSA and duplicate measurements of each were used to quantitate the level of MDA (see Table 1). No history of the origin of the fuel was available; levels of MDA which may have already existed in the fuel were not available and could not be traced.

Table 1  
Results of Analysis of Samples Spiked with MDA

Sample ID	Fuel type	MDA added (mg/L)	MDA measured (mg/L)
POSF-2985	Jet A	2.0	2.0
POSF-2963	JP-5	2.0	2.2
POSF-2963	JP-5	6.0	5.0
POSF-3119	Jet A	2.0	2.7
POSF-3084	Jet A	2.0	2.8
POSF-2926	Jet A	2.0	2.4
POSF-2827	Jet A	2.0	2.8
POSF-3059	Jet A	2.0	2.5
POSF-2962	JP-5	6.0	6.0
POSF-2962	JP-5	2.0	2.5

All of the measurements obtained (POSF-2963 as an exception) were greater than or equal to the amount added to the original fuel. We suspect that these fuels may have been doped with MDA at the refinery (up to 5.8 mg/L is allowable). As the history of each fuel was unknown, all samples were reanalyzed with BSA alone to detect low levels of MDA. With the exception of POSF-2962, all samples showed small amounts of uncomplexed MDA present (less than 0.5 mg/L). Attempts were made to quantify the MDA, but the calibration curve was non-linear

between 0 and 1 mg/L due to adsorption of the small amounts of MDA on surfaces. Further work needs to be conducted to improve the low level accuracy (and precision) of this technique.

Samples POSF-2962 and POSF-2963 were of considerable interest because it is not known whether MDA that is chelated with a metal in solution can also be silylated. To examine this question, POSF-2962 was spiked with copper naphthenate (to 100 ppb copper) and renamed POSF-2963. This fuel (POSF-2963) was measured by ICP-AES to have a copper content of 98 parts-per-billion (ppb), with iron and zinc levels measured at 60 and 14 ppb, respectively. Because the mass spectrometer was used to detect a specific mass at a specific retention time, MDA complexed with copper and silylated should not be detected at the same retention time as MDA not complexed with copper. Therefore, POSF-2962 should have higher levels of MDA measured than its counterpart, POSF-2963, which was subjected to copper. This was indeed the case as shown in Table 1 for fuel spiked at the 2.0 and 6.0 mg/L levels of MDA: in each case, MDA concentration was higher in the POSF-2962 sample than the POSF-2963 sample. Further studies (using fuels with known processing histories) will be conducted to determine the chemistry of derivatization reactions for copper-containing MDA.

### Measurement of Field Samples for Additive Content

An additive package currently being investigated for Air Force fuels, JP-8+100, is comprised of several additives including a detergent/dispersant, antioxidant and the metal deactivator additive, MDA. Because the additive is introduced in the field at the user level, measurements of the level of MDA could provide an important check on the techniques used to deliver and mix the additive package. Four samples were obtained from active air bases currently using the JP8+100 additive and were received in undeactivated one gallon cans. Results from the four samples indicated that MDA concentrations were below the desired level of 2.0 mg/L with most measurements indicating less than 1 mg/L. Because field sampling cans have a low surface to volume ratio, one would probably suspect the glass containers used in the laboratory for the poor recovery of MDA. Additional work will address the possible deactivation of these surfaces so that field sampling of the additive package will predict or indicate problems in the field.

### Tracking Additive Concentration During Stressing Tests

Thermal stressing may decrease additive concentration in some fuels, so the ability to track additive concentration is of interest. Figure 3 shows that the MDA concentration decreases as a function of time with oxidative stressing at 180°C. MDA concentration decreases as a function of time due to its reaction with other species. As MDA reacts it may become less effective as a chelation additive, and therefore unable to complex metals which may increase in concentration during stressing due to materials degradation (7).

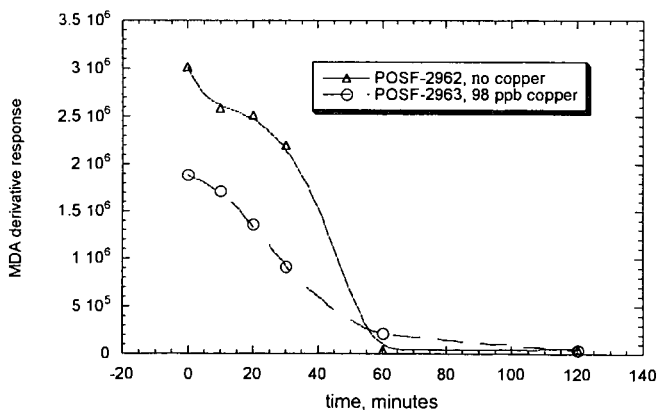


Figure 3. MDA reaction during thermal stressing of neat and copper-doped fuel in the Isothermal Corrosion Oxidation Tester.

## CONCLUSIONS

Metal deactivator additive (and potentially, other phenolic additives) can be successfully analyzed using chemical derivatization followed by GC-MS detection. Because of the surface active nature of MDA, conventional chromatographic techniques are prone to poor accuracy and precision, as well as high detection limits. Derivatization with BSA can be conducted at room temperature using extremely small samples (200  $\mu$ L) with sensitivity sufficient to cover the specification range of the additive. Analysis time due to selected ion monitoring on the GC-MS can be as short as 13 minutes. Consequently, this technique can be used to evaluate additive concentrations in the field, track additive usage in stressing studies and to understand the relationship between metal deactivator additive and surfaces or metals in the fuel.

## ACKNOWLEDGMENTS

This work was sponsored by the US Air Force, AFRL/PRSF, at Wright-Patterson AFB, Ohio under contract number F33615-97-C-2719. Mr. Charles Frayne was the technical monitor.

## REFERENCES

1. Pederson, C. J., *Ind. Eng. Chem. Res.*, **48**, pp. 1881-1884, 1936.
2. Heneghan, S.P., Zabarnick S., Ballal, D. R., Harrison III, W. E., *J. Energy Res. Tech.*, **118**, pp. 170-179, September 1996.
3. Kauffman, R.E., ASME Publication 97-GT-77, ASME: Orlando, FL, June 1997.
4. Henry, C., Octel America analytical method, November 1995.
5. Schulz, W.D., *ACS Petroleum Preprints*, **37**, 2, San Francisco, CA, March 1992.
6. Zabarnick, S., ASME Paper No.: 97-GT-219, ASME: Orlando, FL, June 1997.
7. Pierce, A.E., Silylation of Organic Compounds, Pierce Chemical Co., Rockford, IL, 1968.